HYDROGEL DEVICES FOR CONTROLLED DRUG RELEASE

by

Suk-Zu Song

A dissertation submitted to the faculty of The University of Utah in partial fulfillment of the requirements for the degree of

Doctor of Philosophy

Department of Pharmaceutics

The University of Utah

June 1980

THE UNIVERSITY OF UTAH GRADUATE SCHOOL

SUPERVISORY COMMITTEE APPROVAL

of a dissertation submitted by

Suk-Zu Song

I have read this dissertation and have found it to be of satisfactory quality for a doctoral degree.

John R. Cardinal
Chairman, Supervisory Committee

I have read this dissertation and have found it to be of satisfactory quality for a doctoral degree.

Date

Kim
Member, Supervisory Committee

I have read this dissertation and have found it to be of satisfactory quality for a doctoral degree.

Date

Joseph D. Andrade
Member, Supervisory Committee

I have read this dissertation and
doctoral degree.

Date

Member, Supervisory Committee

I have read this dissertation and have found it to be of satisfactory quality for a doctoral degree.

Date

Dónald E. is
Member, Supervisory Committee

THE UNIVERSITY OF UTAH GRADUATE SCHOOL

FINAL READING APPROVAL

To the Graduate Council of The University of Utah:

I have read the dissertation of Suk-Zu in its final form and have found that (1) its format, citations, and bibliographic style are consistent and acceptable; (2) its illustrative materials including figures, tables, and charts are in place; and (3) the final manuscript is satisfactory to the Supervisory Committee and is ready for submission to the Graduate School.

Cardinal
Member, Supervisory Committee

Approved for the Major Department

Robert V. Petersen
Chairman Dean

Approved for the Graduate Council

James L. Clayton
Dean of The Graduate School

ABSTRACT

Controlled release drug delivery systems are polymeric devices which are implanted at or near the intended site of action for the purpose of drug delivery at controlled rates for extended periods. In this thesis, various types of drug delivery devices including monolithic, reservoir, and combined monolithic-reservoir devices were prepared and the release kinetics evaluated as a function of device design and composition. Emphasis is placed on progesterone as a model hydrophobic drug. The hydrogel devices were prepared from hydroxyethyl methacrylate (HEMA) and copolymers of HEMA with methoxyethyl methacrylate (MEMA), methoxyethoxyethyl methacrylate (MEEMA), or methyl methacrylate (MMA). Hydrogels prepared from chitosan were investigated also.

Initial work emphasized drug transport studies in hydrogel films. For these studies, an equation was developed to describe the special case of solute transport under the condition of a high membrane-water partition coefficient and low solubility in the permeation solvent. Several solute-membrane combinations were investigated which may be summarized as follows: (i) an increase in the initiator content leads to a small decrease in progesterone permeability coefficients probably due to increased crosslinking of the polymers; (ii) estriol permeability coefficients in pHEMA crosslinked with ethylene glycol dimethacrylate were smaller than progesterone

due to a decrease in the solute membrane partition coefficient; (iii) progesterone and estriol permeability coefficients decrease with increases in weight percent of MMA in copolymers of HEMA and MMA due to a decrease in the water content. At high mole fractions of MMA, the permeability coefficients are relatively constant suggesting that a solution-diffusion mechanism is operative; (iv) partition coefficients for both estriol and progesterone produce a maximum when plotted as function of weight percent MMA. This was interpreted in terms of a domain structure for the HEMA-MMA copolymers; and (v) hydrogels prepared from chitosan are, in general, more permeable than pHEMA for the same solutes, however, chitosan permeabilities were found to be sensitive to the charge of the solute due to charge-charge interactions in the film.

Existing equations which describe solute release rates from cylindrical monolithic devices were evaluated and a new equation developed which includes the effects of drug released from the planer ends of the device. The conditions under which the release from the planer ends can be neglected were developed from the release data.

Drug release from cylindrical monolithic hydrogel devices containing progesterone were evaluated. It was found that the rate of water influx strongly influences the initial release rates. It was postulated that the initial release rates should decrease due to a crossflow of solute and solvent within the water-filled channels or pores of the film. It was found, also that the permeability

coefficients were dependent upon the initial drug load. This effect was probably due to changes in polymer structure which arise during precipitation of the solute. That this effect was not an artifact of the release studies was confirmed from transport studies on drug depleted films.

The release of drugs from reservoir and the combined reservoir-monolithic devices were, in general, consistent with those expected based on the transport studies. However, when the swelling of the monolithic core material was strongly affected by the barrier layer, the release rates were significantly lower than predicted values.

The final portion of this thesis deals with the mechanisms of solute permeation in pHEMA-based hydrogels using the methods of irreversible thermodynamics. From this study, it was found that hydrogels are highly selective membranes. The selectivity is increased by crosslinking. The results of the study emphasize the porous nature of solute transport in the films. However, for certain solutes, transport within and through the polymer segments contributes to the total solute permeability.

TABLE OF CONTENTS

LIST OF TABLES

LIST OF FIGURES

ACKNOWLEDGMENTS

The author wishes to express his appreciation to Drs. J. R. Cardinal and S. W. Kim for their encouragement and helpful discussions during the course of this research. He also wishes to thank the members of his Supervisory Committee for their helpful suggestions and discussions.

The author would like to thank the following people for their friendship and assistance during his work: G. M. Zentner, S. Wisniewski, J. C. McRea, S. H. Kim, E. S. Lee, C. Ebert, C. G. Anderson and L. A. Nelson.

This work was supported by the National Institute of Health Grant HD 09791.

Finally, the author gives thanks to his wife and family for their silent help.

Chapter 1

INTRODUCTION

Recently, the use of polymeric materials for medical purposes has been an intense area of research. Rapid progress in polymer chemistry and modern medical technology has made it possible to use polymeric materials for implant devices that would reinforce or replace the function and structure of weakened organs and tissues. Some examples of such devices are sutures, catheters, blood expanders, synthetic cartilages, artificial joints, artificial organs, dental devices, contact lenses, and drug delivery systems.

A great variety of polymers have been studied as candidate materials for implant devices. Although the proporties required by the polymer will depend upon the specific application, certain general properties must be met by all materials. Included among these are: (i) the appropriate physical-mechanical properties to achieve the desired structural function of the device; (ii) the necessary chemical stability to ensure the maintainance of the mechanical properties over time; and (iii) the desirable, biocompatability of the material. The physical and chemical properties should be retained during prolonged implantation in the rather severe environment of the body. Hydrolytic stability of the material is required since enzymes and body fluids may cause degradation of susceptible chemical bonds. Adsorption and absorption of biological fluids,

which will inevitably occur, should not alter or adversely affect the properties of the implanted polymer. Finally, the implanted device in contact with the biological system must not contribute to deleterious toxicity, tissue reaction, blood clotting, infection, allergy, irritation, or carcinogensis.

Polymers frequently used in medicine include: silicones (1-4), acrylic resins (5-7), poly(vinyl chloride), polytetrafloroethylene, polyethylene, polypropylene, epoxyresins, polyurethanes(8), polyesters (9), polycarbonates, and hydrogels. Of these, the hydrogels have attracted attention for applications which require blood and tissue biocompatability.

A hydrogel is defined as a polymeric material capable of imbibing large quantities of water (e.g., greater than 20 percent by weight) without dissolving. Many polymers of synthetic and natural origin satisfy this definition. For example, synthetic hydrogels include poly(hydroxyalkyl methacrylates), poly(vinyl alcohol), and crosslinked poly(N-vinyl pyrrolidone). Natural biopolymers such as chitosans, dextans, and collagens are also hydrogels.

Hydrogels have many advantages relative to other synthetic polymers for certain biomaterial applications. Some of the advantages are: (i) the soft and rubbery character of a hydrogel, (ii) the high permeability to small molecules, and (iii) a good biocompatability. The soft and rubbery character affords greater compatability with surrounding tissue by minimizing mechanical irritation. Small molecules such as polymerization initiators, decomposition products, and unreacted monomer are thought to be the cause of toxic

inflammation and eventual rejection of implanted biomaterials (10). These undesired small molecules can be eliminated from the gel by soaking in proper solvents for an appropriate period prior to the implantation of the hydrogel in the body. According to the minimum interfacial free energy hypothesis developed by Andrade et al. (11, 12, 13), hydrogels may exhibit a high degree of blood and tissue biocompatability due to low water-polymer interaction energy. If protein absorption is assumed to decrease as the interfacial free energy decreases, a good biomaterial should exhibit the lowest interfacial free energy when in contact with biological fluid. For hydrogels this value is close to zero whereas most other polymers exhibit much larger values in interfacial free energy (e.g., > 20 ergs/cm^2). With respect to this property the hydrogel can be considered a good candidate biomaterial. More recently, work by Ratner (14) has suggested that an adequate amount of water present in the polymer is necessary rather than merely a high water content in the polymer. The basis of this hypothesis resides in a consideration of the proper "balance of polar and apolar sites" present at the surface of the polymer. Ratner found that approximately equal amounts of polar and a polar sites on polymer surface enhanced blood compatability.

Hydrogels can be synthesized from various monomers such as hydroxyalkyl methacrylate, acrylamide derivatives, N-vinylpyrrolidone, acrylic acid derivatives, and aminoethyl methacrylate. Hydrogels also can be formed by the conversion of functional groups from other polymers (e.g., poly(vinylalcohol) from poly(vinylacetate)).

The properties of various hydrogels change depending on the nature of the functional groups attached to the polymeric backbone. This wide number of possible hydrogel structures results in a correspondingly large number of possible applications of the hydrogels in the biomedical field (15-47). Some examples of biomedically important hydrogels are:

1. Poly(acrylamide), poly(methacrylamide), and derivatives (48);
2. Polyelectrolyte complexes (49-51);
3. Poly(vinylalcohol) (52-56);
4. Anionic and cationic hydrogels (18, 20, 22, 57, 58);
5. Poly(N-vinyl-2-pyrrolidone); and
6. Poly(hydroxyethyl methacrylate), (pHEMA).

Among these, pHEMA has received special emphasis because this polymer is hydrolytically stable, and is generally biocompatible. In addition, the water content of this polymer can be controlled easily by copolymerization and to some extent by crosslinking.

Water content is one of the most important properties of a hydrogel. As discussed above, much of the rationale for the biocompatability of hydrogels revolves around the presence and the water content of the polymer. Water content also affect mechanical properties. It is generally found that as the water content increases the mechanical strength decreases while the "softness" of the hydrogel increases. Water content is important also in the control of the solute transport characteristics of hydrogel

membranes. Generally, a higher water content leads to an increased rate of solute transport (59).

pHEMA is a hydrogel with a water content of about 40 percent by weight. Copolymerization of pHEMA with poly(methoxyethoxyethyl methacrylate), (pMEEMA), will increase the final water content of the copolymer whereas copolymerization of pHEMA with either poly-(methoxyethyl methacrylate), (pMEMA), or poly(methyl methacrylate), (pMMA), will reduce the water content of the copolymer from that of pure pHEMA.

It is, therefore, natural to expect that pHEMA and its various copolymerized methacrylate derivatives will exhibit a broad range of transport properties which may provide a wider variety of potential application such as, soft contact lenses (60), kidney dialysis mebranes (45, 61-65), reverse osmosis membranes (61, 66-69), and controlled release drug delivery systems.

In this study, applications of hydrogel for controlled release drug delivery systems will be specifically discussed.

Conventional methods of drug delivery such as tablets and capsules require periodic administration. As a result of this method of administration, 'peaks' and 'valleys' in the drug plasma concentration will be produced (Figure 1.1). These fluctuations in the plasma concentration of a drug can result in near toxic or sub-therapeutic drug levels. On the other hand, frequent application of smaller doses, which is thought to 'smooth-out' these fluctuations in plasma concentration, will cause inconvenience and a greater chance of the patient's failure to comply with the prescribed drug

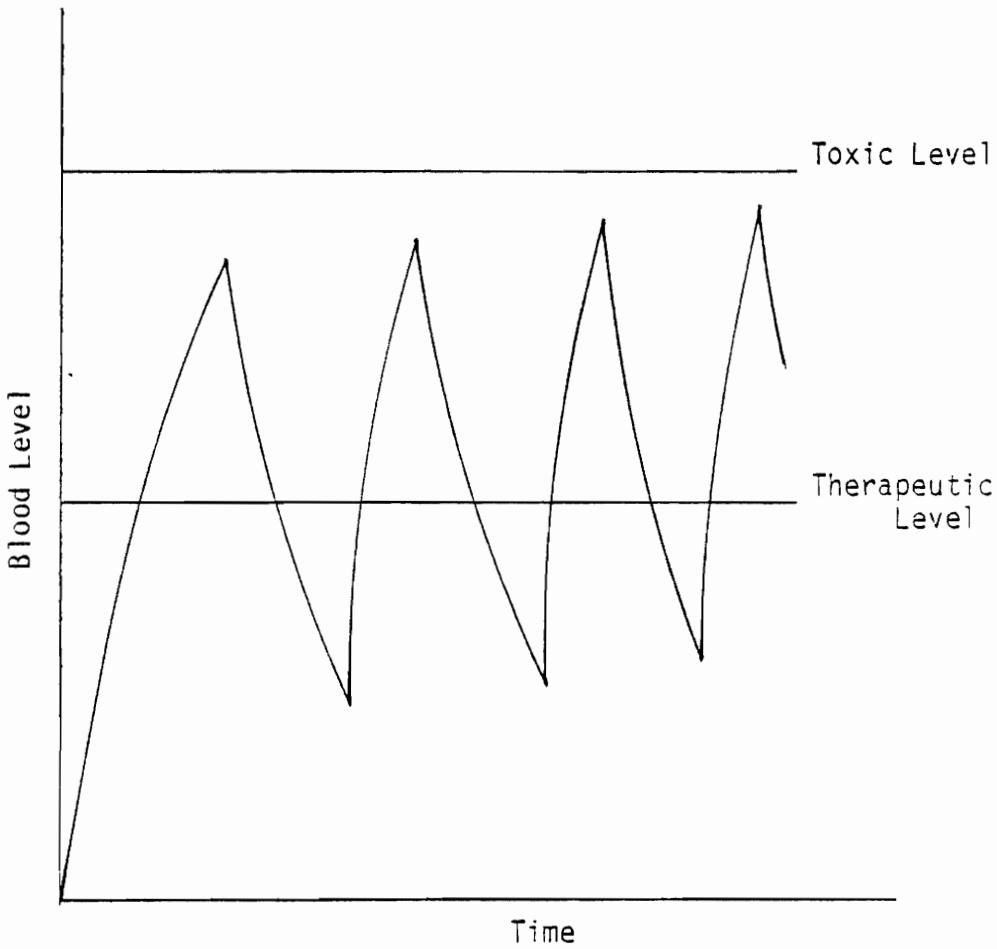

Figure 1.1. Schematic plot of drug blood level versus time for conventional drug dosage regimen.

therapy. Such a failure may result in the lack of effectiveness of the drug.

Because of these problems, related to conventional drug administration, recent efforts have been made at new drug administration techniques which can provide both sustained and controlled release of pharmacological agents at the desired site of action. Such methods of drug delivery are especially suited to drugs which must be delivered at constant rates over long periods. Examples of such drugs include contraceptive steroids, narcotic antagonists, antihypertensives, and anticonvulsants.

Polymeric devices can be used to deliver drugs to a specific site by implantation at or near the intended site of action. Polymeric devices containing a certain amount of drug may be implanted at the specific site on or in the body. Because a drug can permeate through a polymer membrane, the drug may be delivered directly to the site. Providing that the release rate of drug can be controlled, a properly designed device could deliver precise amounts of drug to the implantation site for extended periods. Some of the examples of localized polymeric drug delivery systems are PROGESTASERT (70) and OCUSERT (70). The PROGESTASERT delivers progesterone to the uterus for one year while the OCUSERT delivers pilocarpine to the eye of the patient for seven days.

Controlled release drug delivery systems are formulated by the combination of the drug and polymer. The polymer membrane controls the release rate of the drug at an optimal level by acting as a diffusional barrier for the release of the drug.

Many design variations for controlled release drug delivery systems have been studied or proposed. Although the shapes or geometries can vary widely, the basic design can be classified as monolithic, reservoir, or combined monolithic-reservoir type devices.

Monolithic devices are composed of a drug dispersed within a polymer matrix. The polymer may be either biodegradable or non-biodegradable. The polymer matrix controls the release by controlling the diffusion rate of solutes through the matrix or by erosion of the matrix. In the latter case it is likely that both erosion and diffusion contribute to the total release rate. For the case of monolithic hydrogel devices containing highly water soluble solutes dispensed in the matrix, an additional release mechanism is possible (71). In such systems, large osmotic pressures can be generated which act as the major driving force for drug release. Release occurs through channels created by osmotic rupture of drug containing capsules within the polymer.

Reservoir type devices consist of a polymeric capsule which is filled with an active agent or with a suspension of the drug in a fluid medium. In this device, drug release is controlled by diffusion through the polymer wall.

Combined type devices are composed of a core polymer containing dispersed drug as in the monolithic device. This core is surrounded by a second polymer of lower permeability than the core polymer. Drug release is controlled mainly by diffusion through the second polymer.

In order to design a controlled release system, many factors should be considered. Some of them are as follows: (i) optimum therapeutic level of the active agent, (ii) membrane biocompatability with the biological environment, (iii) physiochemical stability of a membrane in the environment, (iv) reactivity of active agents with the polymer, (v) kinetics and transport mechanisms of the active agent from the polymeric system, and (vi) influence of the biological environment on the transport mechanism and kinetics.

In this research, the potential of hydrogels as biomedically applied materials for controlled release drug delivery systems is evaluated. The kinetics and mechanisms of drug permeation through hydrogel films are studied. Drug release from three types of drug delivery systems are presented. In Vitro release data from such devices can be interpreted based on the data obtained in this study together with data reported in the literature. Chapter 2 describes experimental procedures. In Chapter 3, transport phenomena for steroids through various hydrogels is described to obtain diffusion data needed for the design of contraceptive drug delivery systems. Permeation studies of nonsteroidal solutes such as urea, glucose, and sucrose are studied also to better understand general solute permeation phenomena. Poly (hydroxyethyl methacrylate) containing various amounts of ethylene glycol dimethacrylate as a crosslinking agent is used in the hydrogel membranes. Copolymers of hydroxyethyl methacrylate and methyl methacrylate are also used to regulate permeability. Chitosan is used as a membrane material to further study solute-polymer interactions. Progesterone release from

monolithic, reservoir, and combined devices is described in Chapters 4 and 5. The experimental release rates from these devices are compared with predicted values based on theories found in the literature. Dependence of the drug release rate on device geometry is studied. An irreversible thermodynamic approach of analyzing diffusion phenomena is presented in Chapter 6 to obtain more detailed information concerning solute diffusion which cannot be obtained by classical methods of analysis. Chapter 7 provides a summary and conclusions of all work.

Chapter 2

EXPERIMENTAL

2.1. Materials

Silastic elastomer (Medical grade 382) and DOW CORNING Catalyst M. (Dow Corning Corporation, Monrovia, California) were used as received. The elastomer has a filler of unknown concentration.

Hydroxyethyl methacrylate (HEMA; courtesy of Hydron Laboratories, New Brunswick, New Jersey), was a highly purified sample and was used as received. A typical analysis of impurities as determined by Hydron Laboratories is

Methacrylic acid	0.04%
Ethyleneglycol dimethacrylate (EGDMA)	0.013%
Diethyleneglycol methacrylate	0.216%
Water	0.08%
Hydroquinone	28 ppm

Methoxyethoxyethyl methacrylate (MEEMA) was prepared by the following method: To a 2 l round bottom flask equipped with thermometer, Dean-Stark trap, magnetic stirrer and heating mantle were added methacrylic acid (225 ml, 260 g), methoxyethoxyethanol (427 ml), 10 g hydroquinone monomethylether, 2 g p-toluenesulfonic acid, and 400 ml benzene. The flask was heated to reflux and water was removed as a benzene azeotrope using a Dean-Stark trap. After no more water

was collected, approximately 75 percent theoretical, the reaction mixture was allowed to cool. The reaction mixture was extracted with 5 percent NaOH solution to remove unreacted methacrylic acid, p-toluenesulfonic acid and hydroquinone monomethyl ether. After three extractions the organic phase was dried over anhydrous magnesium sulfate and the solvent was removed under reduced pressure. The resulting material was then vacuum distilled to yield MEEMA. The center cut of the distillate (B.P 65-70°C at 1 mm Hp) was used for further study.

MEMA was synthesized in the same manner. (The above procedure for the preparation was kindly provided by Dr. D. E. Gregonis of the Department of Materials, Science and Engineering, The University of Utah.)

Ethyleneglycol dimethacrylate (EGDMA, Monomer Polymer Laboratories, Philadelphia, Pennsylvania), was purified by base extraction to remove inhibitor followed by distillation. Azobis (methylisobutyrate), prepared by the method of Mortimer (72), was used as initiator.

Chitosan was prepared by the method of Brossignac (73) where a deacetylation reaction using base treatment of chitin (poly-N-acetyl glucoasamine; practical grade, SIGMA Chemical Company, St. Louis, Missouri), was used. Specifically, 20 gms of chitin was refluxed under a nitrogen atmosphere in 150 ml of 3.5% NaOH solution for one hour. The mixture was filtered hot and was washed until neutral with distilled water, then with 95 percent ethyl alcohol, and finally, diethyl ether. The solid was dried in vacuuo for one hour at 45°C.

The deproteinized chitin was then refluxed under nitrogen atmosphere in mixed solution system which contains 67 g ethyleneglycol, 67 g 95 percent ethyl alcohol, 5 ml distilled water, and 134 g KOH. After 20 hours the yellow mixture was diluted with 200 ml ethyl alcohol and filtered hot. The filtrate was washed with distilled water until neutral and then with ethyl alcohol and diethyl ether. The filtrate was dried in vacuuo for 90 minutes at 45 - 50°C. The final product was approximately 13 g of white solid

Progesterone, estriol (Steraloids, Inc., Wilton, New Hampshire), sodium methotrexate (Lederle Parenterals, Inc., Carolina, Puerto Rico 00630), cocaine hydrochloride (USP grade Merck & Co., Inc., Rahway, New Jersey), [1,2 - ^{3}H] progesterone, [benzoyl - 3,4 - ^{3}H] cocaine hydrochloride, [^{14}C] urea, [^{14}C] sucrose, [^{3}H] water (New England Nuclear, Boston, Massachusetts), sodium [3', 5', 7 - ^{3}H] methotrexate and [2,4,6,9 - ^{3}H] estriol (Amersham, Arlington Heights, Illinois) were used as received. Thin layer chromatographic analysis of the steroids showed that these of compounds are pure. Urea, glucose, and sucrose were reagent grade purity and recrystallized either from ethyl alcohol or water.

2.2 Methods

2.2.1 Membrane Transport Experiments

Hydrogel membranes from methacrylate derivatives were synthesized by free radical polymerization. Azobis (methylisobutylate) was used to initate polymerization at a concentration of 7.8 m mole/liter monomer. The mixture of monomer and initiator was polymerized

between two high density polyethylene plates at 60°C for 24 hours. After polymerization, the membrane was soaked in deionized distilled water for at least seven days. Water was replaced every day to eliminate impurities such as unreacted monomer.

Chitosan membranes were prepared by a solvent casting method. Chitosan was converted to the perchlorate salt. The salt formation procedure is as follows: 2.5 g of chitosan was added to 80 ml of distilled water which was stirred by magnetic stirring bar. Seventy percent $HClO_4$ was added dropwise until most of the solid was dissolved. The pH of the solution was maintained at approximately 5.0 to avoid hydrolysis. The viscous solution was centrifuged for 15 minutes at 5,000 rpm and then decanted. The solution was freeze dried to give a white solid of chitosan perchlorate.

To prepare chitosan membranes the perchlorate salt was dissolved in distilled water. This solution was cast in a plastic petri dish and evaporated to give a thin membrane. This membrane was soaked in 10 percent ammonium hydroxide solution to convert the perchlorate salt to the neutral chitosan. This membrane was placed in water for at least seven days. Water was replaced every day to eliminate impurities. (The above procedure for the preparation of chitosan film was kindly provided by Dr. C. G. Anderson of this laboratory.)

A glass diffusion cell, which contains two compartments of equal volume (175 ml), Figure 2.1, was utilized in diffusion experiments. The membrane was clamped between two compartments of equal volume. In order to minimize boundary layer effects each compartment was stirred continuously at 1600 rpm by glass stirrers which were

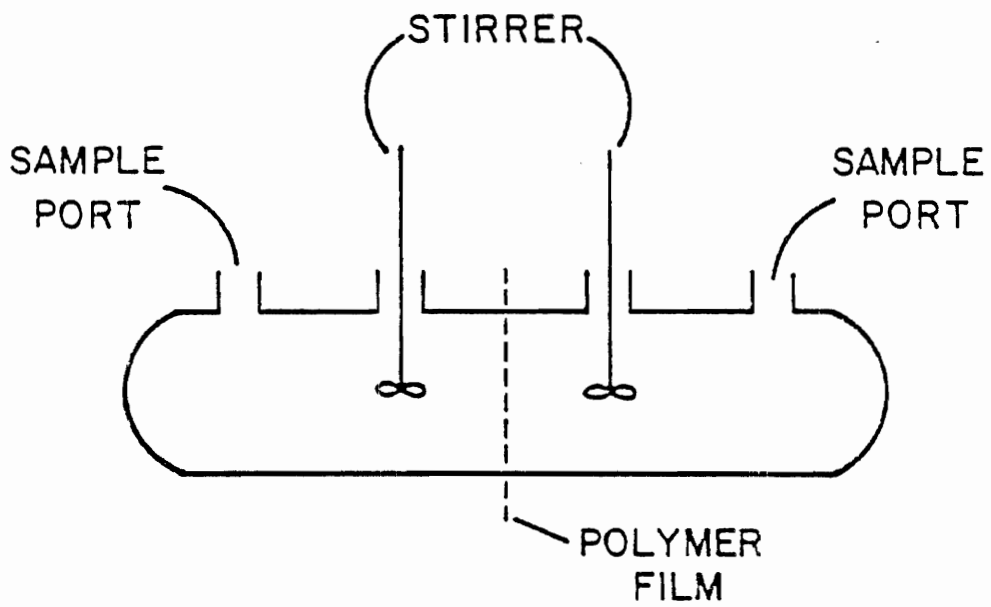

Figure 2.1. Schematic diagram of diffusion cell used in membrane transport studies.

externally mounted to a constant speed synchronous motor.

At the beginning of each experiment, one compartment was filled with a solution containing both labeled and unlabeled solute. The other was filled with nonradioactive solution of the same solute or with distilled water. The concentrations of solute in both chambers were measured by withdrawing approximately 150 μl of sample in duplicate at various times. The samples were weighed in tared vials, 10 ml of scintillation fluid (Formula 950A, New England Nuclear, Boston, Massachusetts) was added and the sample was counted in a Packard Scintillation Counter. In some experiments solute concentrations were measured by both UV spectroscopy and scintilation counting. Both methods gave the same result in the limit of experimental error (usually plus minus 10 percent error). The thickness of the wet membrane was measured using a light micrometer (Van Keuren Company).

The water content of the hydrogel membrane (Wf) was determined using the following equation:

$$Wf = (Wo - Wd)/Wo \qquad (2\text{-}1)$$

where Wo and Wd are the weight of the hydrated gel and weight of the nonhydrated membrane, respectively.

Partition coefficients (Kd), defined as the ratio of the concentrations in the gel and in the aqueous phase, were determined by a solution depletion technique (74) in which the aqueous solution was allowed to equilibrate with a hydrogel membrane. The following equation was used:

$$Kd = \frac{Vw}{Vm} \quad \frac{Co - Ce}{Ce} \qquad (2\text{-}2)$$

Where Vw is the volume of water, Vm is the volume of membrane, and Co and Ce are the initial and equilibrium solute concentrations, respectively.

2.2.2 Release from Monolithic Devices

2.2.2.1 Progesterone release from silastic devices. A mixture of labeled and unlabeled progesterone was made by dissolving the steroids in ethanol and evaporating the solvent. This mixed drug together with 0.125% of catalyst by weight was added to the silicone polymer. A mortar and pestle was utilized to achieve a good dispersion of these constituents. The mixture thus obtained was placed in a high density polyethylene mold and allowed to cure. These rods were cut to give three different values of the ratio of radius to height of the device. Each of these rod shaped devices was immersed in a 1 l beaker containing 900 ml of distilled deionized water. The devices were supported in the cell via metallic holders made from nickel-chrome wire. The aqueous phase was constantly agitated by a stirrer at 1600 rpm. The eluting fluid was totally replaced at each sampling period, which was usually every hour in root time for three days and every day thereafter. All experiments were performed at room temperature (23 $\pm$ 1°C). Sampling was continued until more than 90% of drug was released. The concentrations of the solutions were measured by scintillation counting. A sample volume of 0.5 ml was used.

In order to evaluate the release rate from these devices, the aqueous solubility of progesterone is required. This value was determined using three methods. In the first, a rod-shaped hydrogel matrix device containing labeled and unlabeled drug was placed in an aqueous solution in a covered beaker. The aqueous phase was stirred continuously and the concentration was checked until a constant value was reached. The second method was similar to the first, except that several rod shaped hydrogel devices containing both labeled and unlabeled drug were placed in an open beaker. The aqueous phase was stirred continuously. Over time, the volume of the aqueous phase decreased. The aqueous phase concentration was monitored until a steady state value was reached. At this time, the aqueous phase was passed through a glass membrane filter until successive portions produced the same value. In the third method, excess solid progesterone was added to a beaker containing approximately one liter of water. This solution was sonified for approximately six hours. The solution was allowed to cool and was then left undisturbed for two days. The supernatant was filtered through a glass filter, and the concentration was determined by UV spectroscopy.

2.2.2.2 Progesterone release from monolithic hydrogel devices. Rod shaped monolithic hydrogel devices were prepared in a polyethylene mold by polymerization at 60°C for 24 hours. Azobis (methylisbutyrate) at a concentration of 7.84 m moles/liter of monomer was used as the initiator. Prior to polymerization, a mixture of labeled and unlabeled progesterone was dissolved in the

monomer to obtain a homogeneous solution. The maximum concentrations utilized approximate the saturation solubility of drug in monomer. The dimensions of the dried devices used in the experiments were approximately 4 cm (height) by approximately 0.5 cm (diameter). Planer monolithic hydrogel devices were prepared using similar techniques except only unlabeled drug was utilized. The thickness of these dried films was approximately 0.03 cm.

Progesterone release studies on the rod shaped devices were performed by the same method as in silastic device case.

The amount of water taken up was determined over time on rod shaped devices prepared in an analogous fashion (without labeled drug). Excess surface water was removed with tissue paper prior to weighing. Percent of water uptake (Wp) was defined as:

$$Wp = \frac{Wh - Wo}{Wo} \times 100 \qquad (2\text{-}3)$$

Where Wh and Wo are the weight of hydrated device and the weight of initial dry device.

Permeability coefficients were determined on the planner devices using the diffusion cell (Figure 2.1) by the same method described in Section 2.2.2.1. In this case, the films were depleted of the initial drug load by placing the films in a large volume of water prior to this experiment. The aqueous phase was stirred continuously and exchanged every day till the drug is completely depleted. The release of drug was followed by UV spectroscopy. Film thicknesses, partition coefficients, and water contents of the hydrated films were determined as described previously.

2.2.3 Release of Progesterone from Reservoir and Combined Type Devices

2.2.3.1 Drug release from reservoir devices. Rod-shaped hydrogel devices which did not contain progesterone were prepared in a polyethylene mold by polymerization of monomers by the method described previously. The dimensions of these hydrogel rods were approximately 4 cm (height) by 0.5 cm (diameter). A reservoir was created by drilling out the central portion of these rods with a drill and a 1/8" bit. The central reservoir was filled with approximately 100 mg of a mixture of labeled and unlabeled progesterone in silicone oil. The tops of these devices were sealed by layering monomer over the silicone oil and polymerizing.

Progesterone release studies on the rod-shaped devices were performed by the method described in Section 2.2.2.1. The thickness of the membrane barriers of the devices together with the diameters were determined subsequent to the release studies by light microscopy.

2.2.3.2 Drug release from combined type devices. Hydrogel capsules were prepared as described in the previous section. The central hole was filled with a monomer solution containing a mixture of labeled and unlabeled steroid. This central mixture was polymerized and the top of the device was then sealed as described.

Progesterone release from this combined type device was performed in the manner described in Section 2.2.2.1.

2.2.4 Membrane Characteristics by Irreversible Thermodynamic Method

pHEMA films with and without one mole percent crosslinker (EGDMA) were obtained as described in Section 2.2.2.1. Permeability coefficients of solutes in these membranes were taken from the work of Wisniewski (59). The water contents in terms of volume fractions were obtained from

$$W_{vf} = d \cdot Wf \qquad (2\text{-}4)$$

Where d is density (obtained from the weight of a disk-shaped membrane of known volume which had been equilibrated with an aqueous solution of the solute at a concentration of 0.15 M) and Wf is the water content (by weight). Water content (Wf), permeability, and partition coefficients were obtained as described in Section 2.2.2.1. The partial molal volumes for aqueous urea were evaluated from the data of Gucker et al. (75). The values for glucose and sucrose were taken from Fritzinger et al. (76).

Volume flow was determined in cell (Figure 2.2) similar to that described by Fritzinger et al. (76) suitably modified to permit temperature control via an external circulatory water bath. It was constructed from two No. 25 O-ring joints, 2.5 cm ID. The left compartment has a volume of 65 ml while the right has a volume of 60 ml. The membrane surface area was 7.54 cm^2. Vigorous stirring was induced by externally driven magnetic stirring bars. Volume flow was determined by measuring the change in liquid height in the capillary with a cathetometer as a function of time.

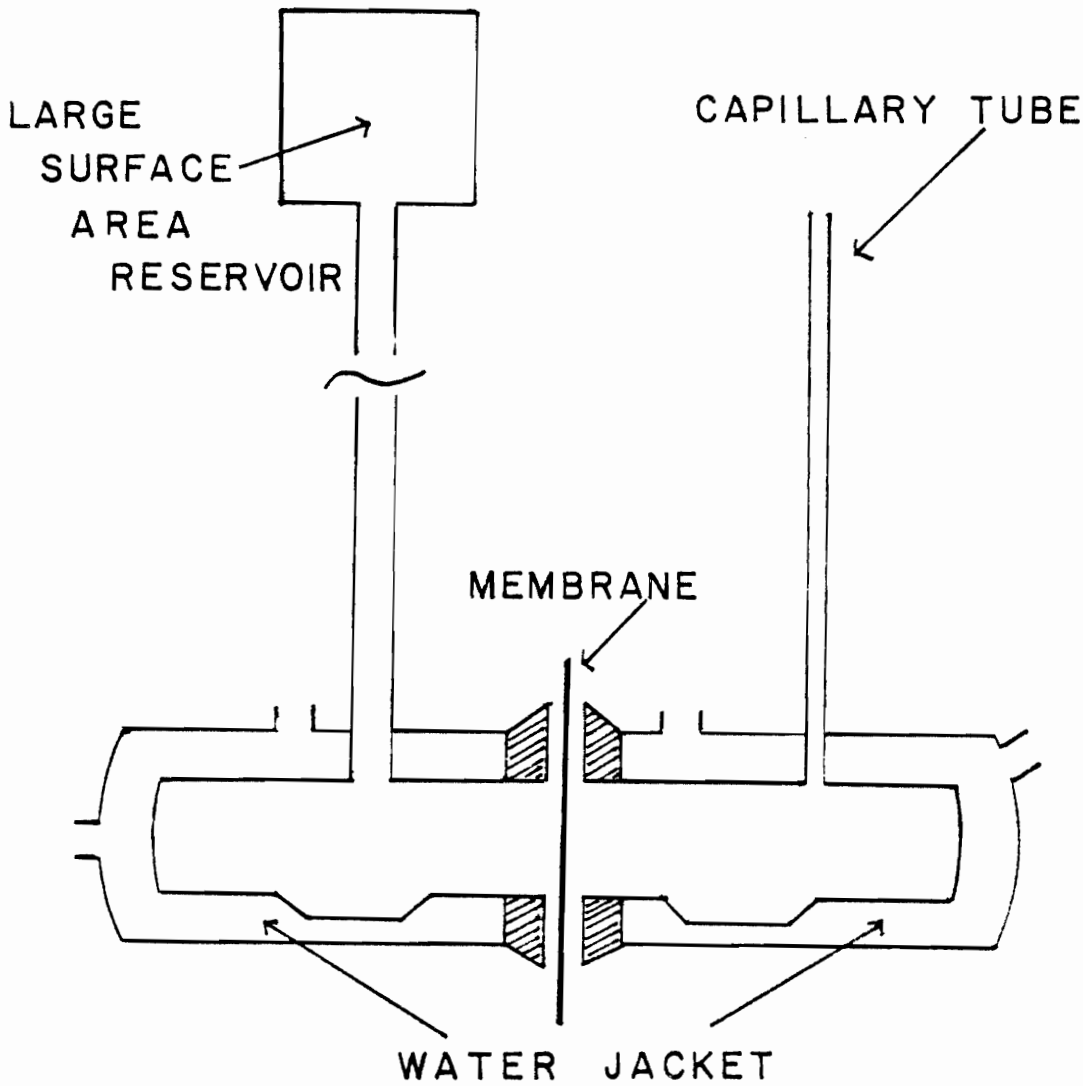

Figure 2.2. Cell for determining total volume flow.

In the determination of the filtration coefficients, the volume flow was measured at zero osmotic pressure difference, i.e., solute concentrations were the same in both chambers (0.15M). A constant hydrostatic pressure was maintained across the membrane by the large reservoir of solution.

In the determination of the reflection coefficients, the volume flow as measured with an osmotic pressure gradient and a constant hydrostatic pressure (150 cm Hg). Initially, a 0.15 M solution was present in right chamber and distilled water was present in left chamber and reservoir.

Chapter 3

SOLUTE DIFFUSION ACROSS HYDROGEL MEMBRANES

3.1. Introduction

Determination of permeability parameters of drugs in polymer membranes is essential information for the design of controlled release drug delivery systems. In addition, valuable insight into the transport process can be gained based upon mechanistic interpretations of drug permeation data. In this chapter, permeation data on several solutes in various hydrogels are discussed. The effects of initiator, crosslinker, and functional groups are studied. A new equation for transport studies in polymeric films, where partition coefficients are large, is derived and compared with results obtained from previous equations. A mechanistic interpretation of the permeation data is provided for the transport of solutes in pHEMA.

3.2.1 Derivation of Equations

Diffusion is mass transport which occurs if a concentration gradient is present. This transport occurs as a result of the random thermal motions of molecules. In the presence of other molecules, an individual molecule will take a random step through the container owing to collisions with other molecules or with the walls of the container. As time passes, it would be expected intuitively that a net flow of molecules from concentrated solution to more dilute

solution will occur. The rate of transport should be proportional to the concentration gradient, the distance between points of observation, and the area through which transport occurs. The relationship between these variables is know as Fick's Law:

$$\text{Flux} = J = \frac{dm}{dt} = - DA \frac{dc}{dl} \qquad (3\text{-}1)$$

Where m is the mass of material transfered, t is the time, l is the distance in the direction in which diffusion occurs, A is the area of the plane through which the transfer is made, and D is a proportionality coefficient known as the diffusion coefficient.

Usually, the diffisuion coefficient is a function of concentration because molecular thermal motion is dependent upon frictional forces which are a function of concentration. However, in dilute solution, the frictional force between solute and solvent can be assumed constant since most collisons of a solute molecule are with surrounding solvent molecules. Therefore, the diffusion coefficient should be independent of concentration when the concentration of solute is low.

In the case of a solution/membrane/solution type of diffusion system, the concept of partition is important. When there is a solvent, a membrane, and one kind of solute, the solute will distribute between membrane and solvent until its activity is the same in both phases. Because of differing interactions with the phases, the solute concentration in the phases at the same activity may be different. The ratio of solute concentration at equilibrium is called

the partition coefficient. The partition coefficient, Kd, is defined as:

$$Kd = \frac{\text{Solute Concentration Within the Polymer Membrane}}{\text{Solute Concentration in the External Aqueous Phase}} \quad (3\text{-}2)$$

The partition coefficient is, in general, dependent on solute concentration (77). However, for the present study, it is assumed that Kd is constant in the range of experimental concentration. This assumption will be verified in Section 3.2.2.

Figure 3.1 is a diagram showing the distribution of a solute in a solution/membrane/solution system in which a concentration gradient exists. In such systems, it is generally assumed that the concentration gradient in the membrane is linear.

In order to determine a diffusion coefficient for a solute in such a system, it is necessary to develop appropriate solutions to Fick's Law. The final equations developed are dependent upon the specific conditions under which the experiment is carried out. In the present work, equations will be developed for the condition of very low aqueous phase concentrations and high membrane-water partition coefficients. Fick's Law can be applied in a membrane.

$$J = - DA \left(\frac{dCm}{dl}\right) \quad (3\text{-}3)$$

where Cm is the solute concentration in the membrane. During steady state, it is assumed that a linear concentration gradient exists in the membrane so that:

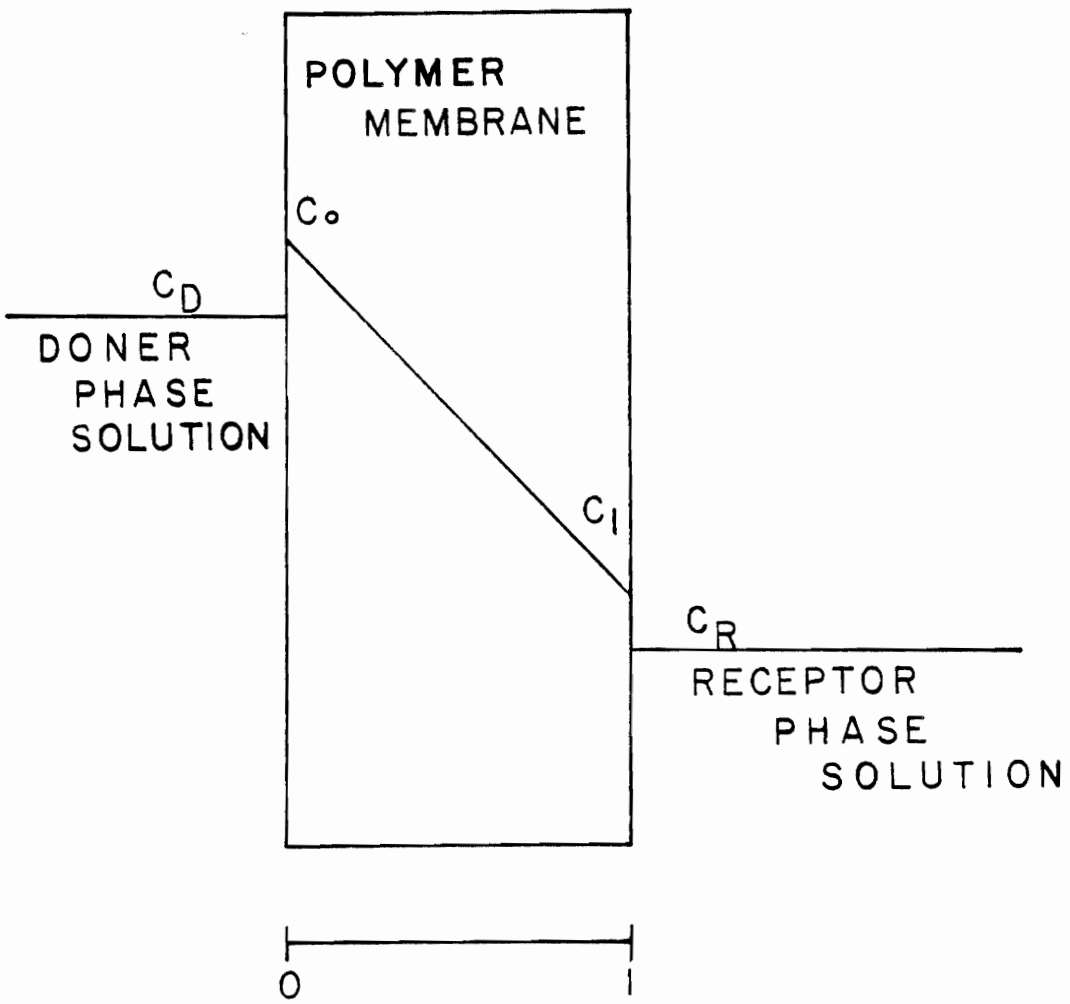

Figure 3.1. Schematic representation of the concentration gradient across a membrane.

$$-\frac{dCm}{dx} = \frac{Co - C_1}{l} \qquad (3\text{-}4)$$

where Co and C_1 are the respective surface concentrations of the membrane. Substitution of Equation 3-4 into Equation 3-3 gives:

$$J = DA \frac{Co - C_1}{l} \qquad (3\text{-}5)$$

If the partition coefficient, Kd, is constant in the range of experimental concentration, Equation 3.1 can be expressed as:

$$J = DA \frac{Kd\ (C_D - C_R)}{l} \qquad (3\text{-}6)$$

where C_D and D_R are the respective solute concentrations of donor phase and receptor phase, and Kd is defined as:

$$Kd = \frac{C_o}{C_D} = \frac{C_1}{C_R} \qquad (3\text{-}7)$$

Mass balance between the donor and receptor phases during steady state gives:

$$J = \frac{V_D dC_D}{dt} \qquad (3\text{-}8)$$

and

$$J = \frac{V_R dC_R}{dt} \qquad (3\text{-}9)$$

Where V_D and V_R are the volume of doner phase and receptor phase, respectively. Rearrangement and addition of Equations 3-8 and 3-9 gives:

$$dC_D - dC_R = d(C_D - C_R) = -\left(\frac{1}{V_D} + \frac{1}{V_R}\right) J\, dt \qquad (3\text{-}10)$$

Equation 3-10 and Equation 3-6 can be combined to give the following:

$$\frac{d(C_D - C_R)}{C_D - C_R} = -\frac{DAKd}{1}\left(\frac{1}{V_D} + \frac{1}{V_R}\right) dt \qquad (3\text{-}11)$$

Integration of Equation 3-11 gives:

$$\ln(C_D - C_R) = -\left(\frac{1}{V_D} + \frac{1}{V_R}\right) \frac{DAKd}{1} t + C_1 \qquad (3\text{-}12)$$

where C_1 is integration constant. C_1 can be obtained using the boundary conditions. If C_{D1} and C_{R1} are the respective concentrations of doner and receptor phases at the time (t_1) during steady state, then C_1 can be expressed as:

$$C_1 = \ln(C_{D1} - C_{R1}) + \left(\frac{1}{V_D} + \frac{1}{V_R}\right) \frac{DAKd}{1} t_1 \qquad (3\text{-}13)$$

Equation 3-13 can be substituted into Equation 3-12 to give:

$$\ln\left(\frac{C_D - C_R}{C_{D1} - C_{R1}}\right) = -\left(\frac{1}{V_D} + \frac{1}{V_R}\right) \frac{DAKd}{1} (t - t_1) \qquad (3\text{-}14)$$

When the phase volumes are equal, Equation 3-14 can be expressed as follows:

$$\ln \left(\frac{C_D - C_R}{C_{D1} - C_{R1}}\right) = - \frac{2DAKd}{Vl} \quad (t - t_l) \qquad (3\text{-}15)$$

Where V is the volume of either phase. Equations 3-14 and 3-15 are valid under the condition of steady state and constant partition coefficient in the range of experimental concentrations.

These equations can be simplified further under the special conditions which follow:

1. The amount of solute in the membrane is negligible compared with total solute amount.

2. Steady state is reached essentially at the onset of the experiment.

3. Initially, no solute is present in the receptor phase.

Under the above conditions, t_l can be taken as zero when the doner phase concentration is zero. Therefore, Equation 3-14 can be written as:

$$\ln \frac{C_D - C_R}{Co} = - \frac{2DAKd}{Vl} \quad t \qquad (3\text{-}16)$$

where Co is the initial solute concentration in doner phase. The amount of solute in the receptor phase, $C_R V$, should be the amount of solute leaving the doner phase, $C_o V - C_D V$. This gives the following equation:

$$C_D = C_o - C_R \tag{3-17}$$

Equation 3-17 can be substituted to Equation 3-16 to give

$$\ln \frac{C_o - 2C_R}{C_o} = - \frac{2DAKd}{Vl} t \tag{3-18}$$

This equation is valid under the conditions of a steady-state flux in the membrane and a low membrane-water partition coefficient (78).

Equation 3-15 can be modified to more clearly demonstrate the role of solute partitioning in the membrane in controlling the transport process.

Mass balance at steady state gives

$$(C_{Do} + C_{Ro})\, V = (C_{Dl} + C_{Rl})\, V + C_m V_m \tag{3-19}$$

$$(C_{Do} + C_{Ro})\, V = (C_D + C_R)\, V + C_m V_m \tag{3-20}$$

Where C_{Do} and C_{Ro} are the initial concentrations of solute in donor and receptor compartment and C_m is the average solute concentration within the membrane whose volume is V_m.

Provided that the concentration gradient in the membrane is linear, the average solute concentration in the membrane, C_m, can be expressed as:

$$C_m = \frac{Kd\,(C_{Dl} + C_{Rl})}{2} = \frac{Kd\,(C_D + C_R)}{2} \tag{3-21}$$

Substitution of Equation 3-21 into Equations 3-19 and 3-20 gives, after rearrangement:

$$C_{D1} = \frac{2V}{2V + KdV_m} \left(C_{Do} + C_{Ro} - C_{R1} - \frac{KdC_{R1}V_m}{2V}\right) \qquad (3\text{-}22)$$

and

$$C_D = \frac{2V}{2V + V_m} \left(C_{Do} + C_{Ro} - C_R - \frac{K_d C_R V_m}{2U}\right) \qquad (3\text{-}23)$$

Equations 3-22 and 3-23 can be substituted into Equation 3-15 to eliminate C_{D1} and C_D terms as:

$$\ln \left(\frac{C_{Do} + C_{Ro} - (2 + KdVm/V)\, C_R}{C_{Do} + C_{Ro} - (2 + KdVm/V)\, C_{R1}}\right)$$

$$= - \frac{2ADKd}{lV} (t - t_1) \qquad (3\text{-}24)$$

Equation 3-24 reduces to Equation 3-18 in the limit that Kd is small. When the term KdVm/V, is not negligible, it is apparent that D values calculated by Equation 3-18 will be in error.

Diffusion coefficients can be obtained either by Equation 3-15 or Equation 3-24. The use of Equation 3-24 is relatively simple because it requires that the concentration variation with time in only one compartment must be determined. However, this equation demands an accurate knowledge of total membrane volume. In the present study, it is difficult to obtain this value accurately due to the lateral diffusion of solute in the membrane. Because of this,

the membrane volume is not a simple function of the diffusion cell geometry. For this reason, Equation 3-15 is preferred for the determination of membrance diffusion coefficients.

In studies of membrane diffusion phenomena, the permeability coefficient is frequently utilized to describe the flux of solute from the donor solution to the receptor solution. The permeability coefficient (P) can be defined as the product of membrane diffusion coefficient and membrane-water partition coefficient.

$$P = Kd \times D \tag{3-25}$$

Equation 3-25 can be substituted into Equation 3-15 to give the following equation:

$$\ln \left(\frac{C_D - C_R}{C_{D1} - C_{R1}}\right) = - \frac{2AP}{Vl} (t - t_1) \tag{3-26}$$

P is obtained from a plot of $\ln \left(\frac{C_D - C_R}{C_{D1} - C_{R1}}\right)$ versus $(t - t_1)$. From the known values of A, V, l, and the slope which is $- \frac{2AP}{Vl}$, permeability is calculated.

3.2.2 The Nature of Diffusion and the Validity of the Derived Equations

As previously stated, the driving force of diffusion is a concentration gradient. Flow arises from the random thermal motions of individual molecules. This random thermal motion produces a net flow of molecules from areas of high concentration to areas of low

concentration. However, if we could view this phenomena on the microscopic scale and follow the motion of any given molecule, there would be an equal chance that this molecule would move from areas of low concentration to high concentration. This result is a consequence of the fundamental nature of diffusion. This point was verified by the following experiments:

The size and chemical properties of the radiolabeled progesterone is almost identical to those of unlabeled progesterone. Therefore, the transport properties of radiolabeled progesterone is expected to be almost the same as those of unlabeled progesterone. The permeating properties of labeled and unlabeled progesterone were initially confirmed. In one experiment, a progesterone solution of 10 µgm/ml was present on the left side of the membrane, while pure water was present on the right side. A small amount of radiolabeled progesterone was added to the left side. The transport of both radiolabled and unlabeled progesterone were measured by radioactivity and by UV, respectively. As shown by the data in Table 3.1, both experiments yield the same permeation coefficient. This implies that radiolabeled progesterone permeates with same rate as unlabeled progesterone. Based on this finding, labeled progesterone was treated identical to unlabeled progesterone for the permeation study.

The movement of molecules from a lower concentration to a higher concentration was also confirmed. In the next experiment, a progesterone solution of 10 µgm/ml was present on the left side of a membrane. On the right side, a progesterone solution of 1µgm/ml containing a trace amount of radiolabeled progesterone was present

Table 3.1. Solute Permeation Coefficients in pHEMA: Concentration Effects on Diffusion Coefficients

Solute	Concentration On Left Chamber	Concentration On Right Chamber	$P \times 10^7$ (cm^2/sec)
Proges-terone	10µg/ml*	0	10.3
	10µg/ml	0 (by uv)	10.1
	1.1 µg/ml*	0	10.5
	10µg/ml	1µg/ml*	9.96
Urea	0.15M*	0	7.87
	0.15M	0 (by refracto-meter)	7.88
	0.05M*	0	7.93
	0.15M	0.01M*	7.47
Sucrose	0.15M	0 (by refracto-meter)	0.114
	0.05M*	0	0.112
	0.15M	0.01M*	0.118

*Small amount of radiactive material is added.

initially. The concentration changes of both radiolabeled and unlabeled progesterone over time were measured by the use of scintillation counter and UV spectroscopy, respectively. It was found that the concentration of radiolabeled progesterone in left chamber increases, while that of unlabeled progesterone in same chamber decreases. Moreover, the calculated value of the permeation coefficient of a radioactive isotope, whose net flow is from right to left, was close to a nonradioactive isotope provided net flow is from left to right. If only concentration gradient cause solute transport, there should be no drug permeation from right side to left side.

Data shown in Table 3.1 also justifies the assumption of a constant partition coefficient during an experiment for the systems used in this study. The concentration of a nonradiactive solute, which moves from left to right, is tens of thousands of times greater than that of the radioactive solute which moves from right to left. If the partition coefficient were to have changed with respect to the solute concentration in this experiment, the permeation coefficients of both isotopes would have been found to be quite different. The results of this experiment indicate that at the low concentration used (< 12 μgm/ml for steroids and $\leq .15$ M for urea and sucrose) there was a constant partition coefficient in the solute-hydrogel system during the course of the experiment. Since steady state conditions and a constant partition coefficient were assumed in Equation 3-15. the use of this equation is quite reasonable using the diffusion cells shown in Figure 2.1.

3.3.1 Mechanisms of Solute Transport Through Hydrogel Membranes

In order to explain various phenomena of solute transport through a polymer membrane, two mechanisms have been suggested. These are: The pore mechanism in which the solute molecules are transported through aqueous (solvent filled) micro channels (pores) within the membrane; and, the partition mechanism which involves solute dissolution within the polymer membrane and consequent diffusion of the solute along and among the polymer chains.

Good examples of these two mechanisms were found in the work of Lyman (79). This author has shown that solute permeation through cellophane, which is thought devoid of any charge or absorption properties, follows the pore mechanism. This conclusion was based on the observation that linear relationship existed between solute molecular weight and half-time rate of transfer of many different types of solutes. Craig's work (80) has shown the more basic nature of the pore mechanism. When a cellophane membrane was stretched in a biaxial manner, the pore size of membrane increased and the permeability of ribonuclease increased. However, if the membrane was stretched in one direction only, the pores change from a circular to an eliptical shape, and thus, reduces the effective diameter of the passage, reducing the permeability of the solute. Thus, in the pore mechanism, the solute passes through micro holes or channels and the permeability is directly related to the molecular volume of the diffusing solute.

In contrast, Lyman (79) has shown that the permeabilities of

various solutes through block copolymers, based on polyoxyethylene glycol and polyethylene terephthalate, demonstrate no clear cut relationship between molecular weight and half-time rates of transfer. This author also studied the effect of temperature on the dialysis of urea through the copolymer-ester membrane and concluded that the membranes did not act as sieves. This phenomenon may be explained by the partition mechanism where the solute dissolves in the membrane and diffuses through it. In the partition mechanism, membrane solubility is one of the factors which controls solute permeability. Because of differences in membrane solubility, solute transport cannot be explained by solute size alone.

For solute transport in hydrogel films, Yasuda et al. (61, 81-83) developed a model for transport based on the free volume approach. It was proposed that a homogeneous polymer membrane, in the nonhydrated state, is packed uniformly with randomly coiled macromolecules leaving unoccupied space as free volume. In the hydrated state, an additional contribution to the total free volume of the polymer will arise from the free volume within this water phase. It was proposed that solute transport within these films is restricted to diffusion within the total free volume of the polymer. Based on this model, these authors developed the following equations which describe the transport of a solute in a hydrated polymer membrane.

The diffusion coefficient for the solute in the membrane can be described by:

$$D = \nu\phi(q) \exp(- Bq/V_f) \exp(- E/kT) \qquad (3\text{-}27)$$

Where D is the diffusion coefficient, ν is the translational oscillating frequency of the diffusing molecule, $\phi(q)$ is the probability that a solute will find at its location a hole of cross-sectional radius q which is sufficiently large for the passage of the solute, B is a proportionality constant, V_f is the total free volume of the polymer, E, k, and T have their usual meanings. In an analogous fashion, the solute diffusion coefficient in water, Do, can be described by:

$$D_o = \nu \exp (- Bq/V_{f,o}) \exp (- E/kT) \qquad (3\text{-}28)$$

where V_f, is the free volume in the water. The total free volume of the polymer can be defined by:

$$V_f = HV_{f,o} + (1\text{-}H)V_{f,1} \qquad (3\text{-}29)$$

where H is the volume fraction of water in the polymer (i.e., the partition coefficient of water between the membrane and water) and $V_{f,1}$, is the free volume of the polymer in the dry state. If it is assumed that solute transport occurs only within the aqueous filled channels, then $V_f = HV_{f,o}$ and Equations 3-28 and 3-29 can be combined to provide that:

$$\frac{D}{D_o} = \phi(q) \exp \left[- B(q/V_{v,o}) \left(\frac{1}{H} - 1\right)\right] \qquad (3\text{-}30)$$

According to this equation, a plot of ln(D/Do) versus (1/H-1) should be linear. Agreement of experimental data with such a plot would suggest that solute transport occurs primarily within the aqueous filled channels or pores of the polymer film.

For the case of water transport in hydrated polymers, Yasuda,

Lamaze, and Peterlin (82) developed a similar theory based on the free volume approach. For water, these authors assumed that transport can occur within the total free volume of the polymer, that is, transport is not restricted to the water plase. For this case, the final equation may be expressed by:

$$\left(\ln \frac{D}{Do}\right)^{-1} = -\frac{1}{\beta(1-\alpha)} X^{-1} - \frac{\alpha}{\beta(1-\alpha)} \qquad (3\text{-}31)$$

where $X = (1 - H)/H$, $\alpha = V_{f,1}/V_{f,o}$, and $\beta = V^*/V_{f,o}$. V^* is a characteristic volume parameter which can be considered to be the product of the cross-sectional radius of the diffusing molecule and the diffusional jump distance. Equation 3-31 should be applicable to any solute which transports the membrane by diffusion within the total free volume of the polymer.

In principle, it should be possible to discuss the mechanism of solute transport in hydrated polymer films by an application of both Equations 3-30 and 3-31 to the solute permation data. It is expected that all solutes which permeate by diffusion within the free volume of both the water and the polymer will follow the behavior dictated by Equation 3-31. However, when diffusional data are plotted according to Equation 3-30, and the solute permeation mechanism is such that transport occurs in regions other than the water filled channels, agreement between theory and experiment should not exist and linear behavior of the data should not be found. Any deviations from this plot could then be interpreted in terms of a mechanism other than transport within the water filled channels or pores.

Yasuda et al. (81-83) have studied the permeation of various

solutes including water through various hydrogel membranes. They found good agreement between theory and experiment for all solutions investigated. The water soluble solutes considered including urea and sodium chloride produced good agreements with the model when the diffusional data were plotted according to Equation 3-30. For water, good agreement was found with Equation 3-31 for hydrogels in which H varied over a wide range.

Wisniewski and Kim (84) studied the transport of water and water soluble solutes in pHEMA based hydrogels. These authors showed that water transport data in pHEMA and copolymers of HEMA with MEEMA or MEMA were in good agreement with Equation 3-31. For water soluble solutes in pHEMA it was found that plots of ln D/Do versus r^2, where r is the cross-sectional radius of the solute, were linear. This result is also in agreement with the treatment of Yasuda et al. (81). Such behavior is implicit in Equation 3-30 in that D is related to the cross-sectional radius of the permeating solute.

Several authors have considered the effects of crosslinking of pHEMA on the solute transport mechanism (84-85). Wisniewski et al. (84) showed that both the pore and the partition mechanism contribute to the transport of water depending upon the crosslinker concentration. A similar conclusion was reached by Zentner et al. (85) for the transport mechanism of progesterone in pHEMA films crosslinked with EGDMA. Upon a more detailed analysis of the data (86), they were able to define an approximate contribution of each mechanism (pore and partition), to the total transport in pHEMA.

Based on the above it may be concluded that water and water

soluble solutes appear to transport pHEMA and copolymers of HEMA with MEEMA or MEMA primarily by the pore mechanism except at high concentrations of EGDMA whereas the partition mechanism dominates at high concentrations of this crosslinking.

3.3.2 Effect of Initiator Concentration on Progesterone Permeation Through pHEMA

It is well know that changes in polymerization conditions can affect the structure of the polymer formed (87). Since solute transport in polymer films is strongly dependent on structural properties, such studies should provide information about polymer structure with variations in the polymerization conditions. For example, Kapur and Rogers (88) investigated the transport properties of inert gases to determine the effects of aging on polyethylene film. In this laboratory, Zentner et al. (89) utilized studies on progesterone permeability in hydrogel films to determine the effects of the polymerization solvent on the properties of these films. Quite surprisingly, they found that variations in the solvents (water, ethanol, and tert-butanol), and solvent concentration produced no significant change in the transport properties of the films.

In the present study, the effects of the concentration of the initiator azobis(methylisobutyrate) on the transport properties of hydrogel films was investigated. The initiator concentration was varied from 7.84 to 31.36 mmoles initiator per liter of monomer. In all previous work from this laboratory (85, 88, 89, 90), the initiator concentration was held constant at 7.84 moles per liter of of monomer. Thus, the highest concentration used in the present

study was four times greater than the concentration routinely utilized in previous studies. Attempts to polymerize films at one-half this value failed. At a concentration of 3.92 mmole initiator per liter of monomer, polymerization was not complete.

In Table 3.2, the permeability coefficients for progesterone in pHEMA films are listed as a function of the initiator concentration. It is apparent that the permeability coefficients decrease as the initiator concentration increases. This effect is rather small, i.e., a four-fold increase in the initiator contribution produces only a twenty percent decrease in P. This small effect is most likely due to an increase in the crosslink density as the initiator content increases.

3.3.3 Effect of Crosslinker Concentration on Estriol Permeation Through pHEMA

Most previous work in this laboratory (85, 86, 88, 90) on solute transport in hydrogels has utilized progesterone as the model drug. This drug and the devices developed may have possible applications in the development of controlled release devices for contraceptive applications. It has been shown recently (91) that estriol may also be useful in such applications. The drug appears to be effective in utero at much lower concentrations than progesterone. With respect to the development of hydrogel devices for such applications, this could be of potential benefit since much smaller devices could be designed which would still be effective for at least one year. In view of this, a study of the permeation parameters for estriol in the hydrogel was initiated.

Table 3.2. Effect of Initiator Concentration on the Permeation Coefficients of Progesterone in pHEMA.

Concentration of Initiator (m Moles/Liter of Monomer)	P x 10^8 (cm^2/sec)
7.84 m moles/liter monomer	10.3
15.68 m moles/liter	8.88
31.36 m moles/liter	8.26

Permeation parameters for estriol in pHEMA crosslinked with EGDMA are shown in Table 3.3. As expected, the permeability coefficients decrease as the crosslinker content increases. In comparison with progesterone in the same membranes, these P values are smaller by a factor of about two (85). This is probably due at least, in part, to a decrease in the partition coefficients of estriol in these films relative to progesterone. Kd values for estriol are about a factor of two lower than progesterone in the same membranes.

A direct comparison of the diffusion coefficients for progesterone and estriol in pHEMA membranes crosslinked with EGDMA is shown in Figure 3.2. In general, the diffusion coefficients for estriol are somewhat larger than for progesterone at the same crosslinker content. Also, the variation of D with mole percent crosslinker follows a pattern somewhat different from that of progesterone. In particular, a limiting value of D for estriol at high concentrations of the crosslinker is not apparent. Based on this, it must be concluded that the mechanisms of transport of this steroid may be somewhat different. This could be related to the role of membrane partitioning in governing the mechanisms of solute transport. From the Kd values it was pointed out that estriol partitions somewhat less into these hydrogel membranes than does progesterone. This suggests that the pore mechanism of solute transport could be somewhat more important in estriol permeation through the range of crosslinker concentrations.

The effective dose of estriol for contraceptive purposes is about 12 μgm/day delivered <u>in utero</u>. This is about a factor of five less than that of progesterone (65 μgm/day). Unfortunately, this

Table 3.3 Permeation, Partition, and Diffusion Coefficients for Estriol Through EGDMA Crosslinked pHEMA.

Weigh Percent of EGDMA	P x 10^7(m^2/Sec)	Kd	D x 10^9 (m^2/Sec)
0	3.80	56.1	6.78
1	2.68	61.0	4.39
3	1.53	67.1	2.28
5	0.834	73.3	1.14
7	0.359	87.7	0.409

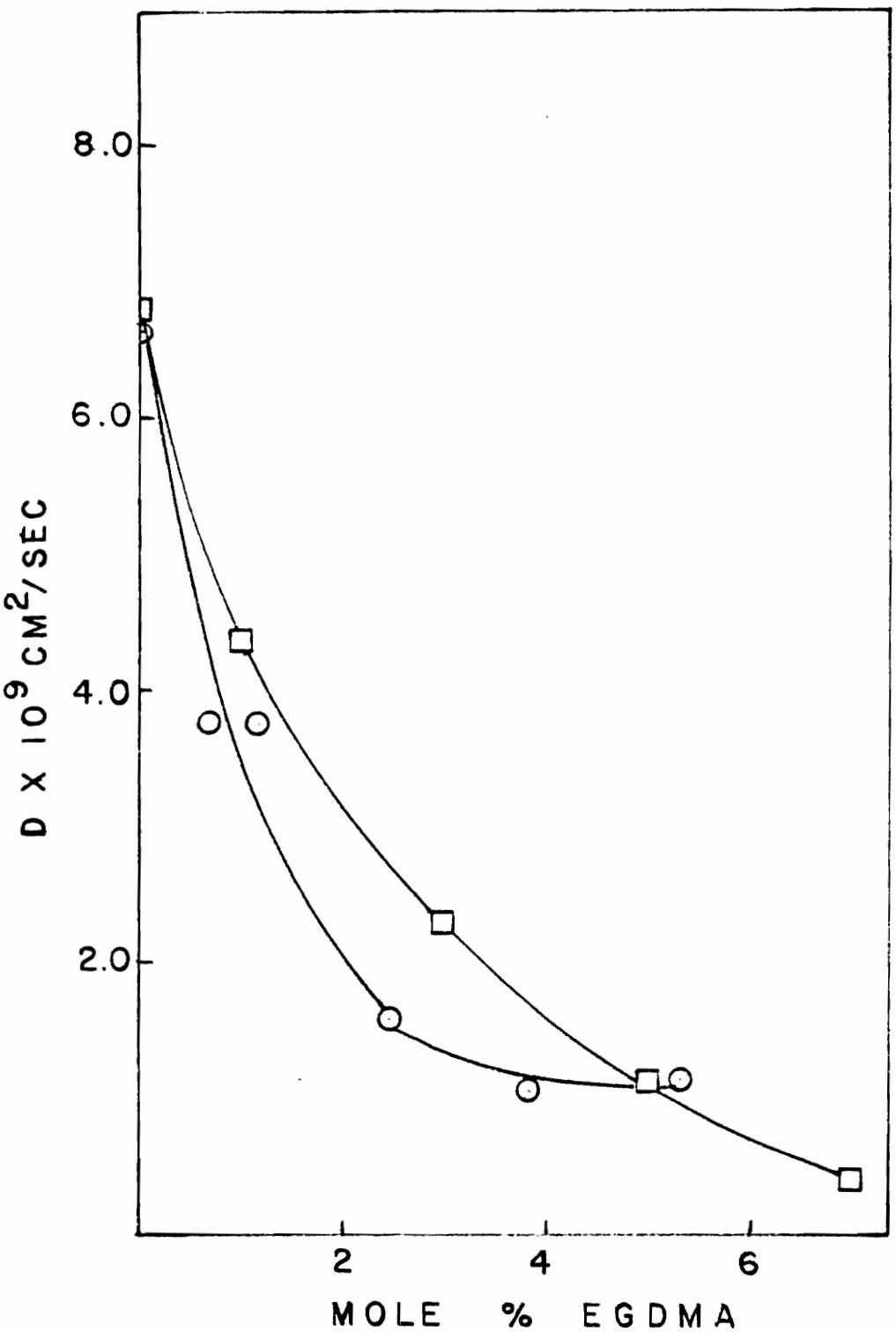

Figure 3.2 A plot of diffusion coefficient versus mole percent of crosslinker. EGDMA crosslinker in pHEMA: (□) estriol; (○) progesterone.

advantage of a reduced dosage in terms of hydrogel contraceptive devices is reduced somewhat by the decrease in the permeability coefficient of estriol relative to progesterone. Nevertheless, it would appear that hydrogel devices prepared with estriol could be somewhat smaller than progesterone devices. In the ultimate application of the devices discussed in this thesis, such differences could be significant.

3.3.4 Solute Permeation Through Chitosan Membrane (Effect of Functional Group on Solute Permeation Through Hydrogel)

Chitosan is a polymer of glucosamine Figure 3.3. It is found in plant cell walls (92) and is the most abundant component of the cell wall of filamentous and yeast-like forms of the mucor rouxii group grown under air and carbon dioxide atmospheres respectively (93). Chitosan is usually prepared by a deacetylation reaction of chitin which is a polymer of acetylated glucosamine (Figure 3.3). This polymer can be obtained in large amounts from crab shells.

Chitosan is a hydrogel whose equilibrium water content can be controlled by the method of preparation. Chitosan can be converted into a membrane by first making a water soluble salt of the polymer which is cast into films and then converted into free chitosan by treatment with a basic solution. The soft, yet tough, mechanical property of swollen chitosan makes this hydrogel a good candidate material for implant devices.

In this study, solute permeation through chitosan membranes was investigated in order to test the potential of this polymer for

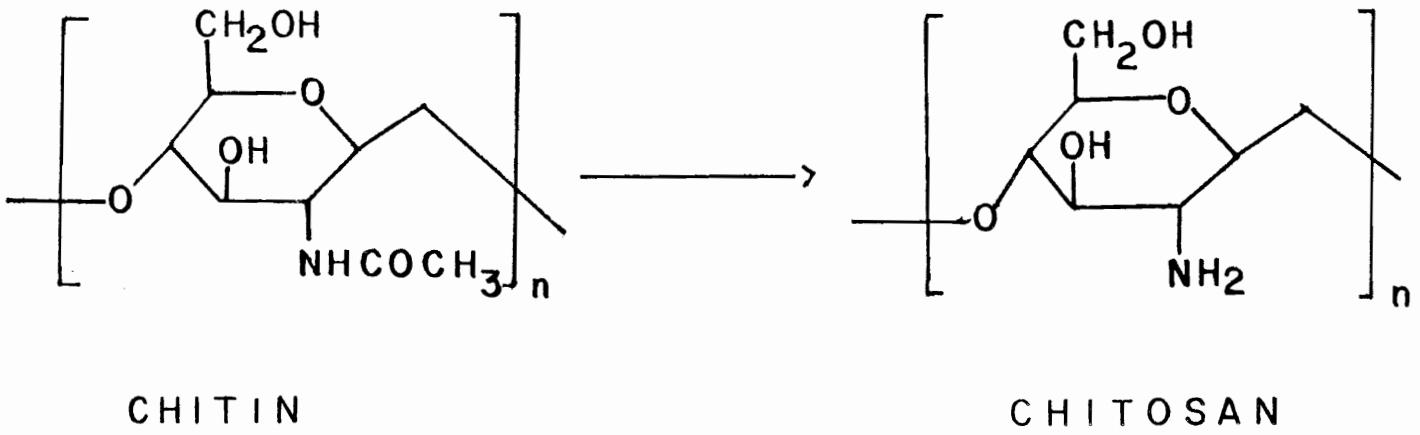

Figure 3.3. The structures of chitin and chitosan.

use in drug delivery systems. Because of the free amino group present in chitosan, information concerning the interactions of solute functional groups with this amino group during permeation can be obtained.

The equilibrium water content of chitosan (46 percent) is greater than that of pHEMA (41 percent). Based on this high water content and the theories of Yasuda et al. (61, 81-83), it is expected that solute transport in chitosan will occur primarily in the water filled pores or channels of the membrane. The data given in Table 3-4 seem to be consistent with this hypothesis.

Previous work from this laboratory (59) and others has demonstrated that solute transport in hydrogels by the pore mechanism is strongly dependent upon solute size. This is evident from the data shown in Table 3.4 for both the pHEMA and the chitosan membranes. For example, by comparison of the P values for sucrose and water in the same membrane it is seen that sucrose is much less permeable than is water. However, the relative decrease in the permeability coefficient is much greater in pHEMA than in chitosan. This result suggests that the relative pore size in pHEMA is smaller than in chitosan.

Na methotrexate and cocaine HCl are solutes which have larger cross-sectional areas than sucrose and, therefore, it is expected that both solutes would have permeability coefficients which are smaller than sucrose. From Table 3.4 it is seen that the permeability coefficient for methotrexate in chitosan is larger than sucrose by about a factor of three. In contrast, the permeability coefficient for cocaine HCl is lower than sucrose by about a factor of ten. These

Table 3.4. Permeability Parameters for Solutes in Chitosan and pHEMA.

Solute	P* x 10^7 (cm^2/sec)	P x 10^7 (cm^2/sec)	Kd	KJ	D* x 10^8 (cm^2/sec)	D x 10^8 (cm^2/sec)
Tritiated water	17.7	31.6				
Sucrose	0.114	0.514				
Na Methotrexate	1.09	1.63				
Cocaine HCl	--	0.0547				
Progesterone	8.44	1.64	139	4.8	7.41	33.8
Estriol	3.80	4.33	51	15.1	7.39	28.8

*Data for pHEMA membrane (59).

results can best be interpreted in terms of specific charge effects between the solutes and the membrane. Due to the amino group in chitosan, the membrane carries a net positive charge. This positive charge should retard the passage of cocaine due to like charge repulsion. For methotrexate, which has a negative charge, ionic charge attraction between drug and the membrane could account for the enhanced permeability of this solute relative to sucrose.

Based on the above, it can be concluded that chitosan appears to behave as a pore type membrane in terms of the solute transport mechanism. However, the permeability coefficients can be strongly influenced by specific interactions, especially charge-charge interactions, between the membrane and solute.

Such specific interactions also appear to be important with the two hydrophobic solutes investigated, namely, progesterone and estriol. For example, again by comparison with the sucrose data and the solute size argument, it would be expected that the permeability coefficients for these solutes in the same membrane would be similar and that the P values in chitosan would be about four times greater in chitosan than in pHEMA. Based on Table 3.4, it is apparent that this predicted behavior is not found in the permeability coefficients. Such differences could arise from specific interactions between the solute and the membrane which are best explained via the membrane partition coefficients. These values are listed in Table 3.4 for progesterone and estriol in both membranes.

By comparison of the Kd values, it is apparent that chitosan and pHEMA differ substantially with respect to their solute

partitioning behavior. Progesterone, which has a very high partition coefficient in pHEMA, produces a very low Kd value in chitosan. In contrast, the estriol Kd values differ by much less between the two membranes and do not show the same order. Such differences emphasize the difficulty in predicting the effects of functional groups on the solubilities of drugs in various media.

Given Kd values, solute diffusion coefficients can be calculated from the relationship P = DKd. The diffusion coefficients for estriol and progesterone are given in Table 3.4. The diffusion coefficients follow the behavior predicted previously for the P values for thse solutes. In both films, the diffusion coefficients are very nearly the same. This is expected based on the similar cross-sectional radii. Also, the D values in chitosan are about four times greater compared to pHEMA. This is consistent with the argument presented earlier, that is, pHEMA is a membrane with a much smaller average pore size than chitosan.

3.4 Solute Permeation Through Copolymer of HEMA and MMA

Though the minimum interfacial free energy hypothesis developed by Andrade et al. (11-13) may predict biocompatability of polymers, other studies (19, 21, 22, 94) have shown that an adequate amount of water is necessary for biocompatability rather than just high water content alone. Quite recently, Ratner et al. (14) found that a copolymer of HEMA and EMA (ethyl methacrylate) whose water content is around fifteen percent has better blood compatability as measured by platelet consumption than a polymer with higher water content.

According to this "hypothesis of a balance of polar and a polar sites" at the polymer surface (14), it may be possible that some of the copolymers composed of HEMA and MMA will show better biocompatability than pHEMA membrane.

It is also probable that some of these copolymers of HEMA and MMA have stronger mechanical properties than pHEMA due to decreased water content. In case of reservoir type device of contraceptive drug delivery system the required thickness of the device is less than 1 mm. Therefore enhanced mechanical property is quite important. Because of the possibility of better biocompatability and strong mechanical property, steroid transport through these copolymer of HEMA and MMA is studied to test these polymers for contraceptive drug delivery systems. Water transport in these copolymers was studied first to know better understanding of the mechanism of transport.

Table 3.5 shows permeation parameters of tritiated water through copolymer of HEMA and MEMA. Figure 3.4 are plots of volume and weight fraction of water versus weight percent of MMA. Both weight and volume fraction decrease somewhat linearly as the fraction of MMA increases.

A plot of the diffusion coefficient of water versus weight percent of MMA is shown in Figure 3.5. The diffusion coeffificents decrease as the MMA content increases in a nonlinear relationship. However, the leveling of diffusion coefficient at high concentration of MMA is not observed. If water permeates by the partition mechanism, the diffusion coefficients are expected to reach certain value

Table 3.5. Permeation, Partition, and Diffusion Coefficient for Tritiated Water Through HEMA-MMA Copolymer and Fraction of Water in the Copolymer.

Weight Percent of MMA	P x 10^7(cm^2/sec)	Kd	Wf	D x 10^6(cm^2/sec)
0	17.9	0.523	0.410	3.42
2.6	--	0.516	0.385	--
5.1	13.42	0.474	0.363	2.83
9.2	9.82	0.457	0.354	2.15
18.3	4.83	0.350	0.274	1.38
32.7	--	0.285	0.230	--
37.3	1.17	0.229	0.184	0.51
47.3	0.69	0.195	0.160	0.353

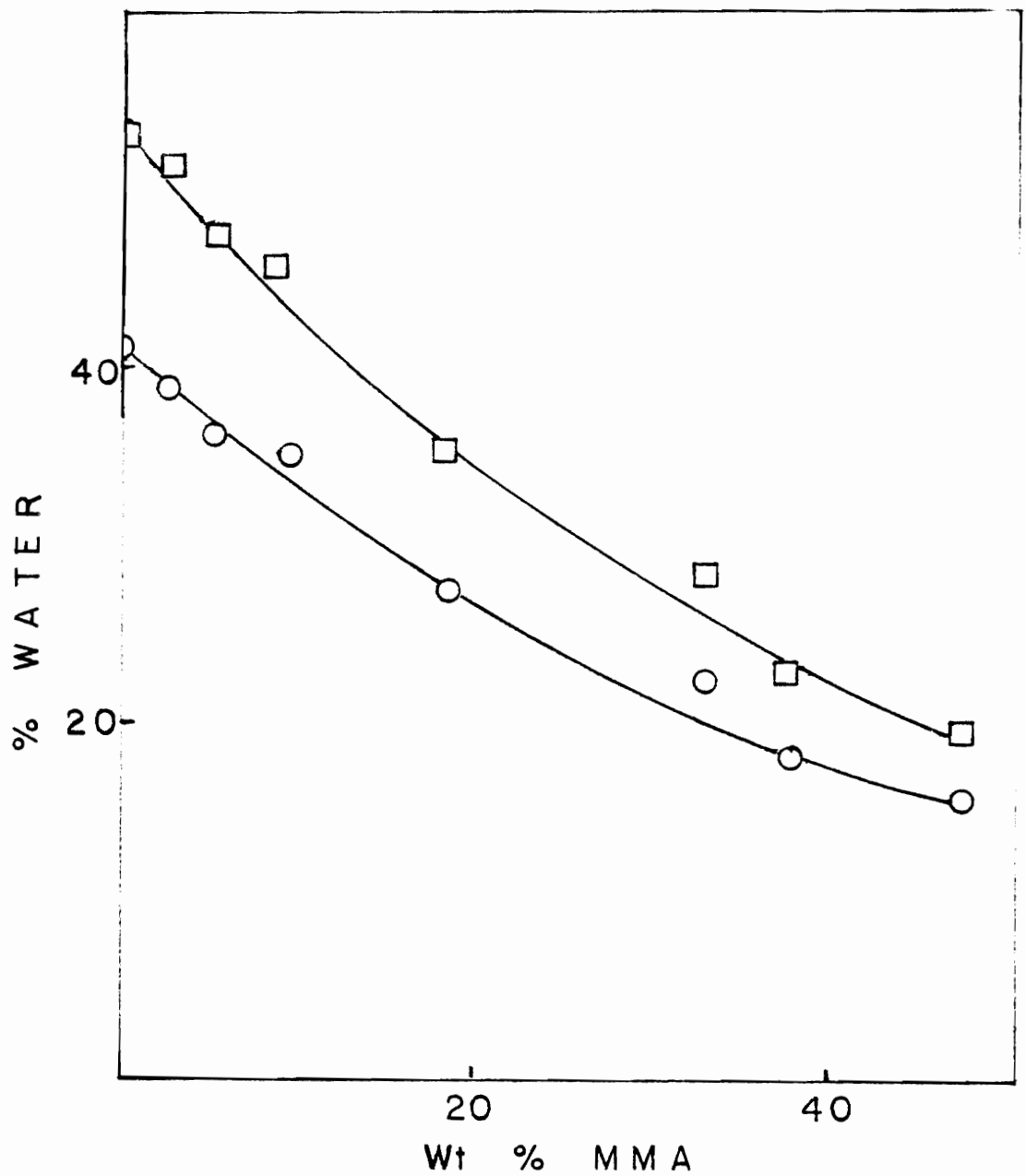

Figure 3.4. A plot of water content versus weight percent MMA in copolymers of HEMA and MMA. (□) = volume; (○) = weight.

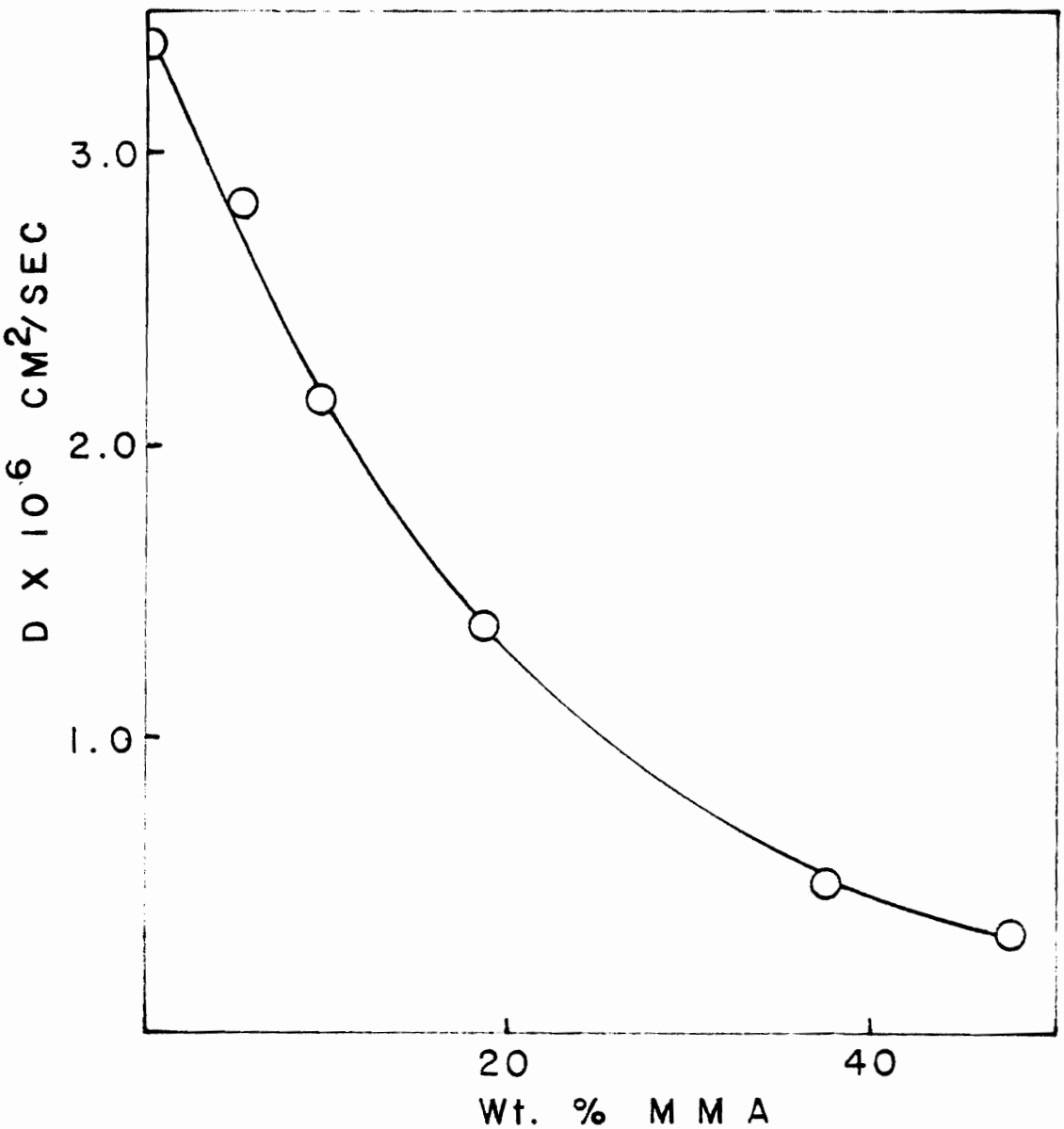

Figure 3.5. A plot of diffusion coefficients of water versus percent MMA in copolymers of HEMA and MMA.

at high concentration of MMA. The above findings may indicate that the pore mechanism is dominant throughout the range of MMA concentration used.

Table 3.6 shows the values of $(\ln D/Do)^{-1}$ and X^{-1} for various MMA concentrations. Figure 3.6 is a plot of $(\ln D/Do)^{-1}$ versus X^{-1}. A good linear relationship (a correlation coefficient of 0.99) indicates that Yasuda's free volume theory applies well to this system.

Permeation parameters of progesterone and estriol through copolymers of HEMA and MMA are shown in Table 3.7 and Table 3.8 respectively. In Figure 3.7 the diffusion coefficients of estriol and progesterone are plotted against percent MMA. The diffusion coefficients of estriol decrease quite rapidly as the MMA content reaches approximately twenty percent and then decreases somewhat slowly after that. This may be interpreted to mean that for this solute, a pore mechanism is dominant at MMA contents of twenty percent or less and that a partition mechanism is dominant after that.

In Figure 3.8, plots of the partition coefficients of two steroids versus percent of MMA are shown. It is interesting to note that the partition coefficients can have maximum values. In the general case there is a correspondingly continuous increases or decrease in the partition coefficient of the solute for a copolymer series where the fraction of one of the components increases. The partition coefficient is related to the interaction between solute and membrane. The intensity of the interaction should increase or decrease continuously as the fraction of one component of copolymer increases and if the membrane can be thought of as being

Table 3.6. Values of $(\ln D/D_o)^{-1}$ and X^{-1} for Tritiated Water in HEMA-MMA Copolymers.

Weight Percent Of MMA	$\ln(D/D_o)^{-1}$	$X^{-1} = K_D/(1-K_D)$
0	- 0.527	1.098
5.1	- 0.479	0.900
9.2	- 0.423	0.842
18.3	- 0.356	0.539
37.3	- 0.263	0.296
47.3	- 0.240	0.243

$D_o = 2.28 \times 10^{-5} cm^2/sec$

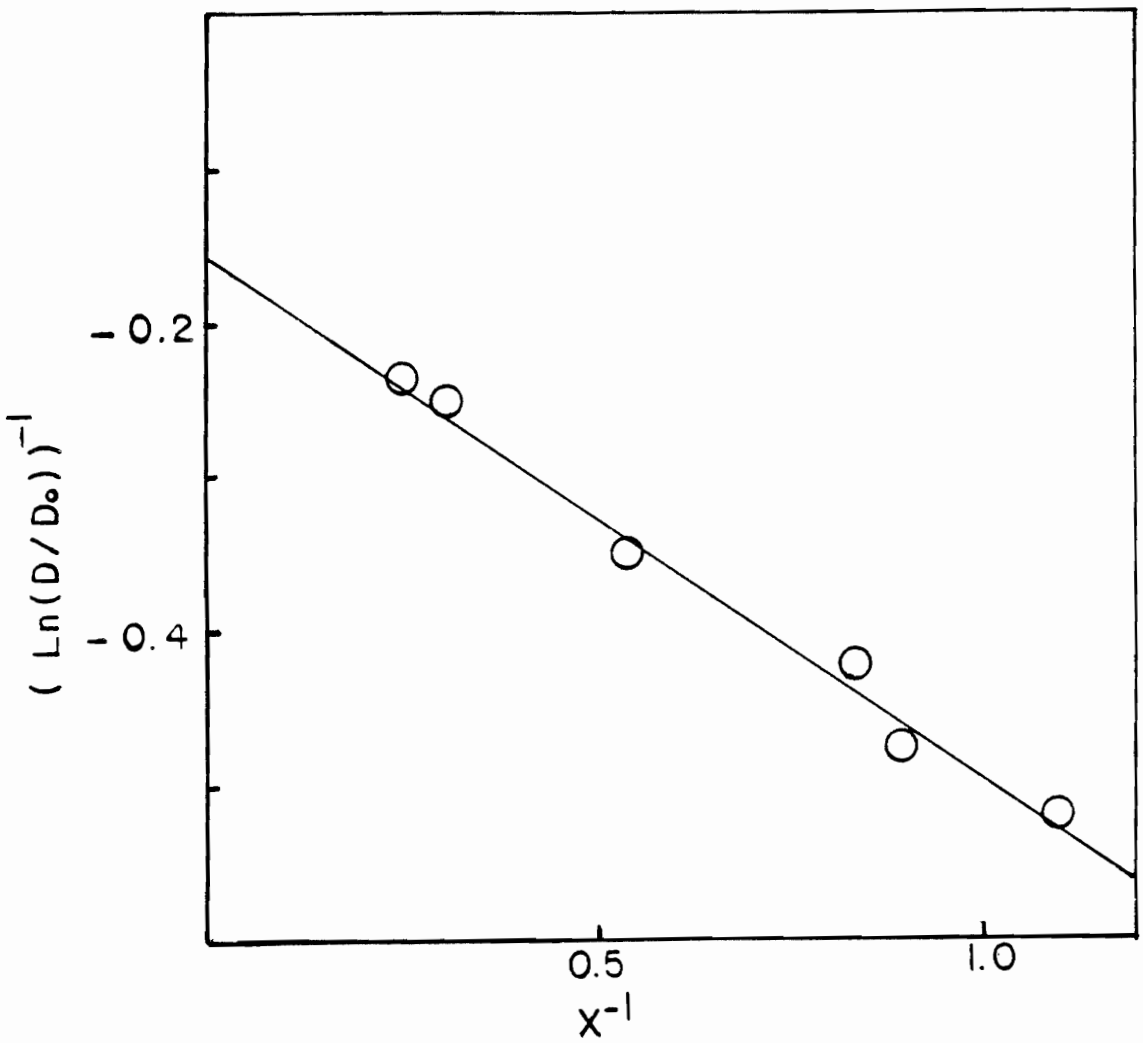

Figure 3.6. Plot of $(\ln D/Do)^{-1}$ versus X^{-1} for tritiated water in HEMA-MMA copolymers.

Table 3.7. Permeation, Partition, and Diffusion Coefficients for Estriol Through HEMA-MMA Copolymers

Weight Percent of MMA	P x 10^8(cm^2/sec)	K_d	D x 10^{10}(cm^2/sec)
0	38.0	51.26	74.1
5.1	26.7	70.03	38.1
9.2	14.8	74.17	20.0
18.3	4.84	84.38	5.74
32.7	0.575	55.46	1.04
37.3	0.319	25.91	1.23
47.3	0.182	24.21	0.751

D_o = 6.8 x 10^{-6} cm^2/sec (78)

Table 3.8. Permeation, Partition, and Diffusion Coefficients for Progesterone Through HEMA-MMA Copolymer.

Weight Percent of MMA	P x 10^7 (cm^2/sec)	K_d	D x 10^9 (cm^2/sec)
0	10.3	139.34	7.39
2.6	7.79	180.25	4.32
5.1	5.82	218.51	2.66
9.2	3.51	237.69	1.48
18.3	0.667	279.11	.239

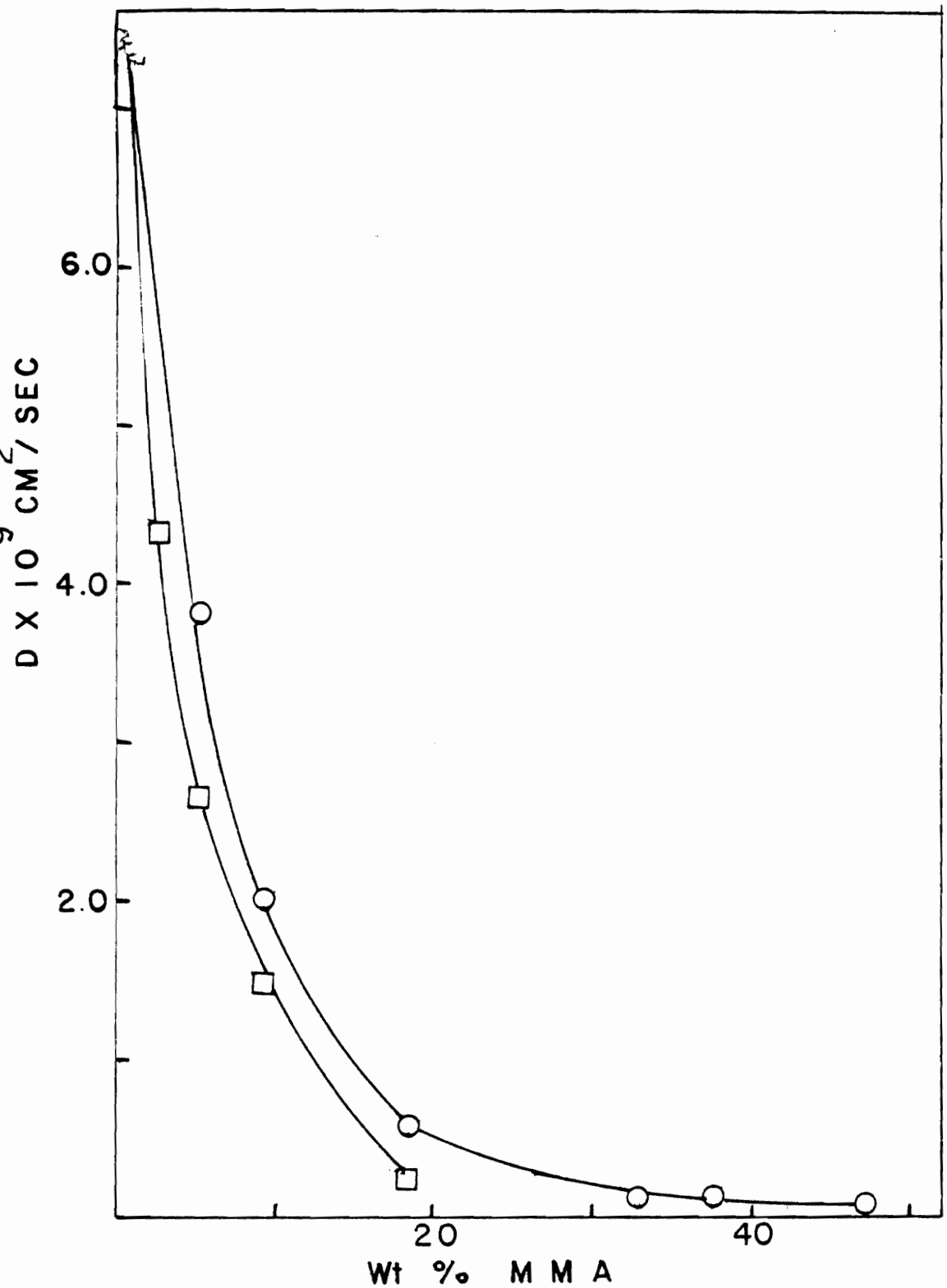

Figure 3.7. Diffusion coefficients of progesterone and estriol as a function of weight percent MMA in copolymers of HEMA and MMA. (○) = estriol; (□) = progesterone.

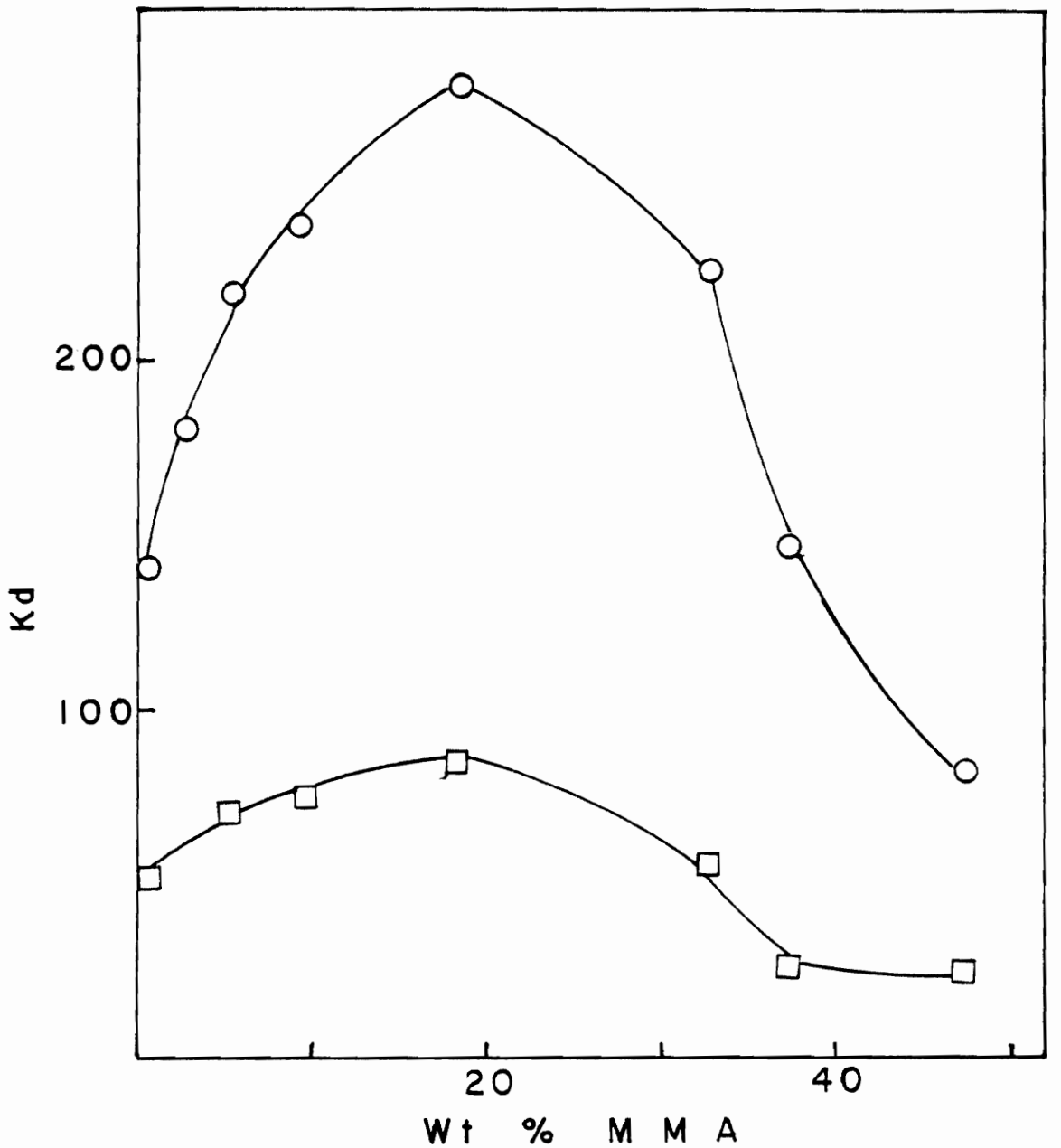

Figure 3.8. Partition coefficients of progesterone and estriol as a function of weight percent MMA in copolymers of HEMA and MMA. (○) = progesterone; (□) = estriol.

homogeneous. The appearance of a maximum partition coefficient may be explained by the following assumptions. The membrane is composed of hydrophilic domains scattered through a hydrophobic matrix and hydrogen bonding is possible between steroid and hydrophilic domain. The size of domain and distance from one domain to another domain is determined by the ratio of hydrophilic monomer to hydrophobic monomer. A maximum interaction occurs when the hydrophobic portion of the steroid molecule faces the matrix and the functional groups of the steroid faces the hydrophilic domain. In the case of a copolymer of HEMA and MMA, optimal matching of hydrophobic and hydrophilic portion takes place when the fraction of MMA is around twenty percent.

In the course of this work it became of interest to investigate the applicability of the theories of Yasuda et al. (61, 77-83) to the transport of water and hydrophobic solutes in the pHEMA based hydrogels. In section 3.3.1 the basic equations of the Yasuda theory were outlined. For transport of water soluble solutes in which transport occurs only within the free volume of the water, Equation 3-30 is valid. For transport within the total free volume of the polymer, Equation 3-31 should be valid provided that the activation energy for transport is the same irrespective of the region of solute transport.

When solute transport occurs through the total free volume of the polymer, a plot of $(\ln D/Do)^{-1}$ versus X^{-1} should be linear with an intercept of $-\alpha/\beta(1-\alpha)$ and a slope of $-1/\beta(1-\alpha)$ where $\alpha = V_{f,o}/V_{f,1}$ and $\beta = V^*/V_{f,1}$. In general, such plots are linear. This has been shown by Wisniewski et al. (84) for water transport in copolymers of HEMA with MEMA or MEEMA. Zentner et al. (85) found the

same result with progesterone in these copolymers. As mentioned previously the plot in Figure 3.6 also is linear for the permeation of water in copolymers of HEMA and MMA. These results suggest that, in general, the Yasuda theory is valid for the case where the total free volume (polymer plus water) is considered.

As an adidtional test of the theory, it was of interest to consider the relative consistency of the results for different solutes in the same polymers. For example, for water and progesterone transport in the HEMA copolymers, the value of α should be independent of solute size whereas β should be size dependent. The latter conclusion is based upon the fact that V* should be size dependent. In order to investigate these points, all available data from these laboratories (59, 77) were plotted according to Equation 3-31. The slopes and the intercepts of these plots were determined by linear regression analysis. For all systems considered except HEMA-TEGDMA, the correlation coefficients were greater than 0.90 and, in most cases, greater than 0.95. From the slopes and the intercepts of these plots, values of α and β were determined for each system considered.

Based on the discussion above, all values of α in the same polymer system should be a constant, or nearly so. Also, the differences in α should be dependent only upon the free volume of the anhydrous polymer. It is expected that these values should be some function of monomer geometry. From the data in Table 3.9 no apparent trend in the values of α is discernable. For example, in HEMA-MMA copolymers, water and progesterone yield the same value of α. However, α for estriol is much higher. The consistency of the

Table 3.9. Comparison of the Parameters α and β for Water, Progesterone, and Estriol in Various HEMA Polymers.

	Solute = Water		Solute = Progesterone		Solute = Estriol	
Polymers	α	β	α	β	α	β
HEMA-MMA Copolymers	0.5268	6.510	0.5311	23.87	0.9543	306.7
HEMA-MEMA or MEEMA Copolymers	0.6885*	11.14*	3.354*	- 13.87*	--	--
HEMA + EGDMA	1.767*	-7.663*	0.8530*	95.69*	0.6659	36.15
MEMA + TEGMA	2.387*	-5.160*	3.171*	- 14.14*	--	--

*Calculated from data in references (59, 77).

calculated value of α would not be improved significantly by excluding those copolymers which appear to have a different mechanism of solute transport based on Figure 3.9. For copolymers of HEMA with MEMA or MEEMA, the value of α obtained from water transport is somewhat larger than that of the HEMA-MMA copolymers. However, the value for α obtained from the progesterone study in this copolymer is very high and seems to be inconsistent with any plausible model for the copolymer free volume. The same can be said for most values of α obtained in the crosslinked polymers.

The values of β shown in Table 3.9 show even greater scatter than the α values just discussed. In many systems negative values of β result. This is not physically possible since β is the ratio of two volume terms.

Based on this discussion, it is apparent that even though all systems studied provide good linear correlations when plotted according to Equation 3-31, the expected behavior of these systems with respect to α and β is very far from the expected behavior. Some of this inconsistency would be due to experimental error, especially in the H value. It is unlikely, however, that this is the total source of the error. It is more likely that some of the inconsistency lies in the fact that the theory may not be applicable to hydrophobic solutes and/or to those systems in which solute transport occurs in regions other than the aqueous channels or pores.

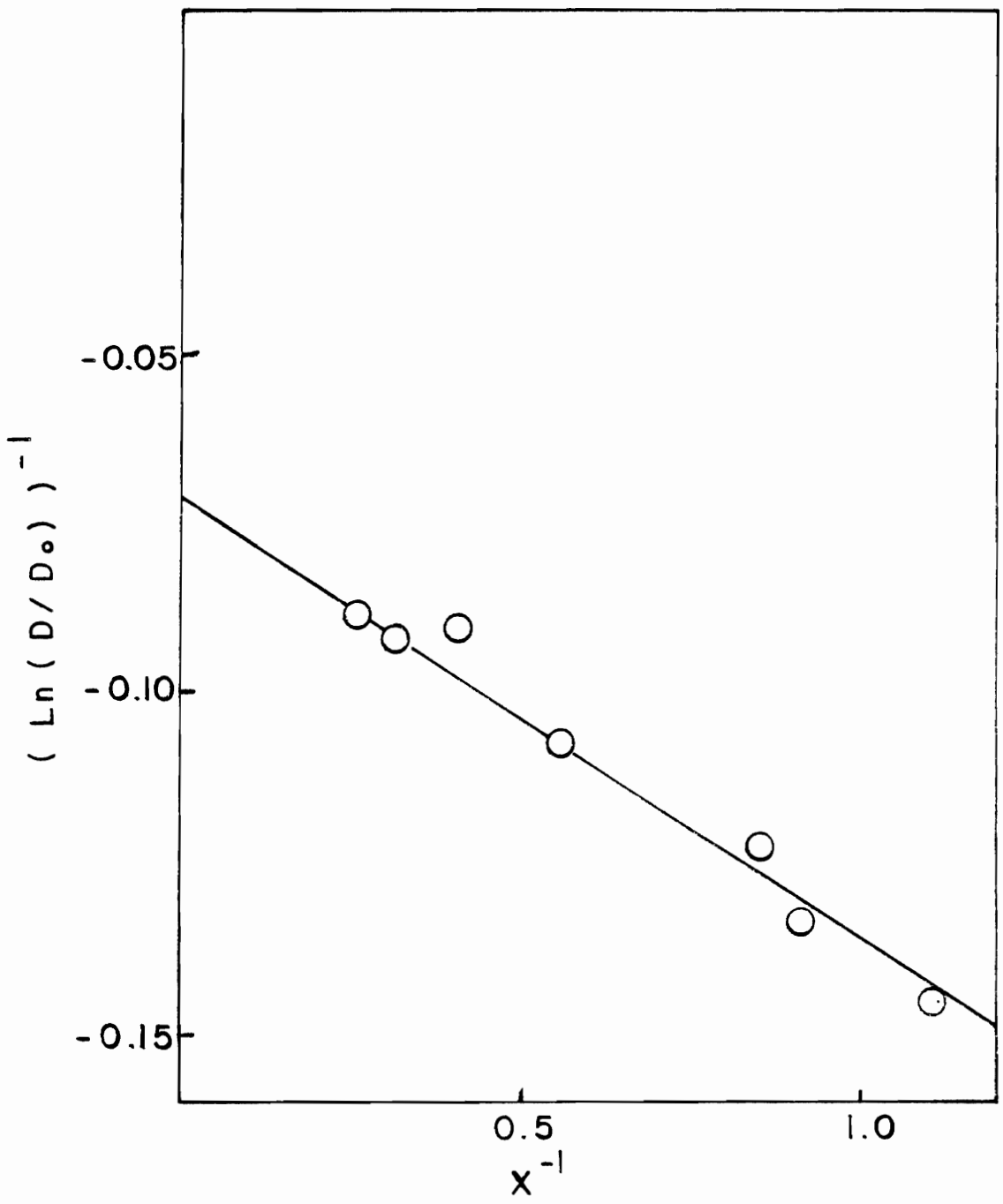

Figure 3.9. Plot of $(\ln D/Do)^{-1}$ versus X^{-1} for estriol in HEMA-MMA copolymers.

Chapter 4

PROGESTERONE RELEASE FROM MONOLITHIC DEVICES

4.1. Introduction

Monolithic devices have been extensively studied for the purpose of controlled drug delivery. A monolithic device consists of drug molecules either physically dispersed or chemically dissolved (in a thermodynamic sense) within a polymeric matrix. Monolithic devices are advantageous in that fabrication methods are easily modified to produce a wide variety of device designs; however, the inherent first-order release kinetics cannot provide stable blood and tissue drug levels as a function of time. As a result, such devices are not ideally suited for pharmaceutical application, but rather, are powerful tools for evaluating drug permeation factors and release kinetics from polymer matrices. In this chapter, two aspects of the release of solutes from monolithic devices containing dispersed drugs are evaluated. In the first section, a new equation will be developed which describes the release of drug from such devices. In the next section, it will be shown that this equation adequately describes the release pattern for all cylindrical geometries irrespective of the length of the cylinder. In the last section of this chapter, the release of progesterone from monolithic hydrogel devices will be evaluated. Particular attention is devoted to the role of water uptake by the devices on the observed release rates.

4.2.1 Derivation of Equation for Drug Release from Cylindrical Geometry

It is well known that drug release from monolithic devices is dependent upon the matrix geometry. Although the configurations of the systems may vary greatly, the systems may be geometrically categorized into three types. These are: (i) slabs, (ii) cylinders or rods, and (iii) spheres. Of these configurational types, cylinders are the most frequently used for practical purposes.

Models for the release of drug from slabs and spheres have been well developed by Higuchi (95, 96). Diffusion models from cylinders are more complex and two cases may exist. For long cylinders, in which the relative contribution of drug release from the ends of the cylinder (end effect) is negligible compared to the amount of drug release that takes place along the longitudinal axis of the cylinder, Roseman and Higuchi (97) developed a kinetic model to describe the release rate from such devices. For finite cylinders in which end effects cannot be neglected, Cobby et al. (98-100) and Fu et al. (101) have developed appropriate kinetic models and derived the corresponding release rate equations. Cobby's treatment can be fitted to experimental data and readily converts to the slab case when the longitudinal axis becomes exceedingly small. However, his equation cannot be converted to a long cylinder where end effects are negligible. The incompleteness of Cobby's equation comes from the incorrect assumption that the drug boundary retreat distance is proportional to square root time regardless of matrix geometry. In general, this proportionality does not apply (96, 97), except in the case of slab

geometry. Fu's treatment fits well with experimental data and converts to slab and long cylinder cases when appropriate approximations are made for certain terms in the finite series comprising the final equations describing drug release. A further disadvantage of both of these treatments, relative to that of Roseman and Higuchi, is that computer analysis of the data is required.

It is the purpose of the following development to derive an equation for the release rate from cylindrical monolithic devices based on the assumption that drug diffusion at the longitudinal surfaces follows Roseman's Equation (97) and that drug release at the end surfaces occurs as described by Higuchi (95). The validity of the new equation will be tested using progesterone disperced in a silicone matrix as a model system, where the radius to height ratio will be varied over a wide range.

Under the condition where the total amount of drug in the matrix per unit volume, Co, is much greater than the drug's matrix solubility, Cs, a quasi-steady state exists and diffusion is controlled by the matrix. The following equations were derived for the planar (95), and the long cylinder cases (97), adhering to the above conditions, with drug release into a perfect sink. For the planar case

$$X^2 = \frac{2DC_s}{Co} t \qquad (4\text{-}1)$$

and

$$Mt = A \ (2 \ Co \ DCs \ t)^{1/2} \qquad (4\text{-}2)$$

Where X is the boundary retreat distance, D is the diffusion coefficient in the matrix, A is the surface area, and Mt is the amount of drug released at the time t.

For the long cylinder case,

$$\frac{r^2}{2} \ln \frac{r}{r_o} + \frac{1}{4}(r_o^2 - r^2) = \frac{C_s Dt}{C_o} \qquad (4\text{-}3)$$

and

$$F + (1 - F) \ln (1 - F) = \frac{4C_s Dt}{C_o r_o^2} \qquad (4\text{-}4)$$

where r is the radius at the boundary retreat distance, r_o is radius of the cylinder, and F is the fraction of drug released.

As time progresses, the release boundary, the area where dissolution of solid drug occurs, retreats from the polymer surface as shown in Figure 4.1. The height (h) of the cylinder will change following Higuchi's equation.

$$h = h_o - 2\sqrt{\frac{2DC_s}{C_o} t} \qquad (4\text{-}5)$$

where h_o is the initial height of the cylinder. The radius of the cylinder will change according to Equation 4-3.

$$\frac{r^2}{2} \ln \frac{r}{r_o} + \frac{1}{4}(r_o^2 - r^2) = \frac{C_s D}{C_o} t \qquad (4\text{-}3)$$

The total amount of drug in the matrix (M_∞) can be expressed as:

$$M_\infty = \pi r_o^2 h_o C_o \tag{4-6}$$

Because of the assumption that $C_o >> C_s$, the amount, Mt, of drug released at time t will correspond to the difference between M_∞ and the amount of drug in the shaded volume in Figure 4.1. The drug remaining at the time t is equal to $\pi r^2 h C_o$. Therefore,

$$Mt = \pi r_o^2 h_o C_o - \pi r^2 h C_o \tag{4-7}$$

The fraction of drug release can be obtained from Equations 4-6 and 4-7.

$$F = \frac{Mt}{M_\infty}$$

$$= \frac{\pi r_o^2 h_o C_o - \pi r^2 h C_o}{\pi r_o^2 h_o C_o}$$

$$= 1 - \frac{r^2 h}{r_o^2 h_o} \tag{4-8}$$

Equation 4-4 can be introduced into Equation 4-8 to give the following equation:

$$F = 1 - \frac{r^2}{r_o^2}\left(1 - 2\sqrt{\frac{2DC_s}{C_o h_o^2}}\right) \tag{4-9}$$

which can be rearranged to give

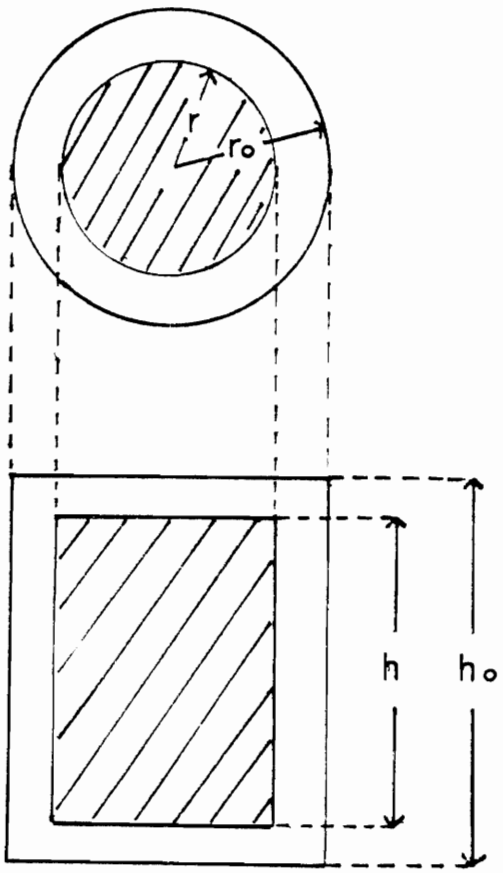

Figure 4.1. Release profile of drug from cylindrical monolithic devices.

$$\frac{r^2}{r_o^2} = (1 - F)/(1 - \sqrt{at}) \qquad (4\text{-}10)$$

where

$$a = \frac{8DC_s}{C_o h_o^2}$$

Equation 4-10 can be combined with Equation 4-3 to give the following equations:

$$\frac{1 - F}{1 - \sqrt{at}} \ln \frac{1 - F}{1 - \sqrt{at}} + 1 - \frac{1 - F}{1 - \sqrt{at}} = \frac{4DC_s}{C_o r_o^2} t \qquad (4\text{-}11)$$

or

$$\frac{1 - F}{1 - b\sqrt{kt}} \ln \frac{1 - F}{1 - b\sqrt{kt}} + 1 - \frac{1 - F}{1 - b\sqrt{kt}} = \frac{k}{2} t \qquad (4\text{-}12)$$

where b is the ratio of radius to height of the device (r_o/h_o) and

$$k = \frac{8DC_s}{r_o^2 C_o} \qquad (4\text{-}12a)$$

Equation 4-12 is the final equation which describes drug release from a polymer matrix device of cylindrical geometry. This equation is simlar, though more elaborate than Equation 4-4, which was derived for a long cylinder where end effects are neglected. In practical application, k values are determined so that the equation can be made to 'fit' the experimental data. Diffusion coefficients can

be obtained from k values using the following equation:

$$D = \frac{k\, r_o^2\, C_o}{8 C_s} \tag{4-13}$$

Permeability coefficient, P, can be obtained from the diffusion coefficient, D, by the following relationship:

$$P = DKd \tag{4-14}$$

where Kd is the partition coefficient for the drug between polymer and water phases.

To be valid, an equation which describes a release mechanism should predict release kinetics in special cases such as long cylinders and slabs. In the case of long cylinders, the value of b, which is the ratio of radius to height of the cylinder, is very small. When b approaches zero, $1 - b\sqrt{kt}$ becomes 1, and Equation 4-12 reduces to

$$(1 - F) \ln (1 - F) + F = \frac{1}{2} kt \tag{4-15}$$

which is the equation for long cylinders where end effect are neglected.

The slab can be represented by another extreme case for cylinders where the height of cylinder is insiginificant compared to the radius of the cylinder (i.e., $r_o >> h_o$). If r_o is very large,

the right side of Equations 4-11 or 4-12 will approach zero.

$$\frac{1}{2} kt = \frac{4DC_s}{r_o^2 A} t \rightarrow 0 \quad \text{as } r_o \rightarrow \infty \tag{4-16}$$

Under this condition, both equations convert to Equation 4-17.

$$\frac{1 - F}{1 - \sqrt{at}} \ln \frac{1 - F}{1 - \sqrt{at}} + 1 - \frac{1 - F}{1 - \sqrt{at}} = 0 \tag{4-17}$$

The solution of Equation 4-17 is as follows:

$$F = \sqrt{at} \tag{4-18}$$

where

$$a = \frac{8DC_s}{C_o h_o}$$

which is the equation for the slab case.

4.2.2 Progesterone Release from Cylindrical Monolithic Devices: Comparison of Experimental Release Rates with Various Mathematical Models

In Section 4.2.1, various mathematical models for drug release from cylindrical monolithic devices containing drug dispersed in the matrix were presented. It was argued that previous models adequately describe the release rate from long cylinders. However, for devices in which the ratio of the radius to the height is relatively large, it was suggested that extensions of previous equations

were required to provide an adequate description of the release rate from these devices. A new equation was developed to meet this need.

In this section, the release of progesterone from cylindrical monolithic devices will be examined in terms of the previous model and the equation developed in this thesis.

Cylindrical devices containing two percent progesterone by weight were prepared. The radii and heights of the devices varied so that the ratio b varied from 0.05 to 0.28. The release of progesterone from these devices was followed over time until the fraction released, F, was at least 0.90. These release curves are shown in Figures 4.2 thru 4.4.

Permeability coefficients for progesterone in each device were developed via Equation 4-12. In essence, this was done by picking values of k (Equation 4-12), and comparing the predicted versus experimental values. The value of k was adjusted to give the best fit to the experimental release curve. For each time, the value of F was calculated from k using the Newtonian iterative technique.

Because diffusion coefficients as well as permeabilities of devices are unique properties of a given matrix polymer composition, these values should be independent of device geometry. Values of permeability and diffusion coefficients for each sytem which have a different b value are shown in Table 4.1. Each experiment gives the same value of permeability and diffusion coefficients. Furthermore, the rlease rate calculated according to Equation 4-12 are in excellent agreement with the experimental values throughout the

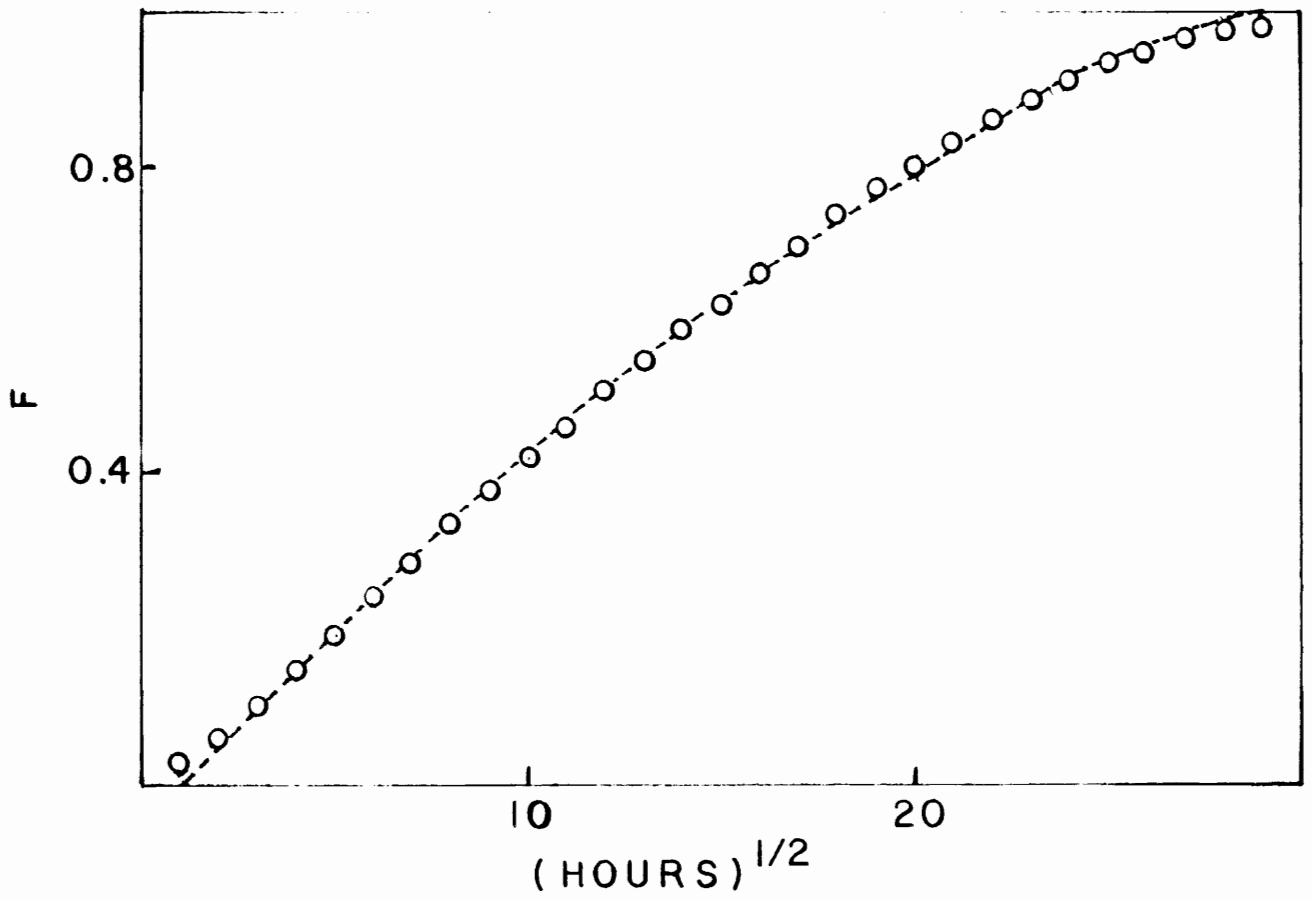

Figure 4.2. Plot of F versus $(\text{hours})^{1/2}$ when b is 0.04. O = experimental; --- = theoretical.

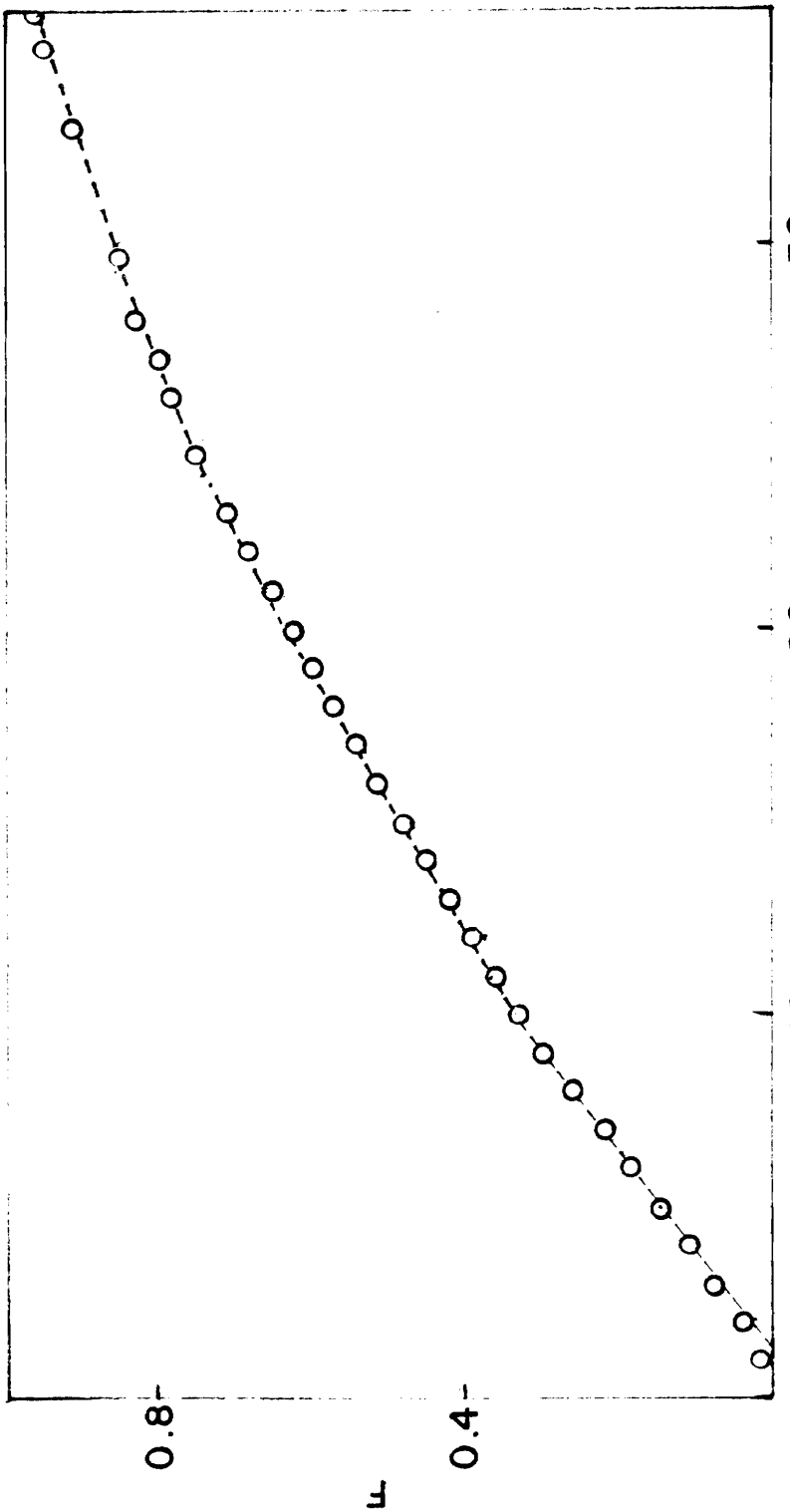

Figure 4.3. Plot of F versus (hours)$^{1/2}$ when b is 0.14. O = experimental; --- = theoretical.

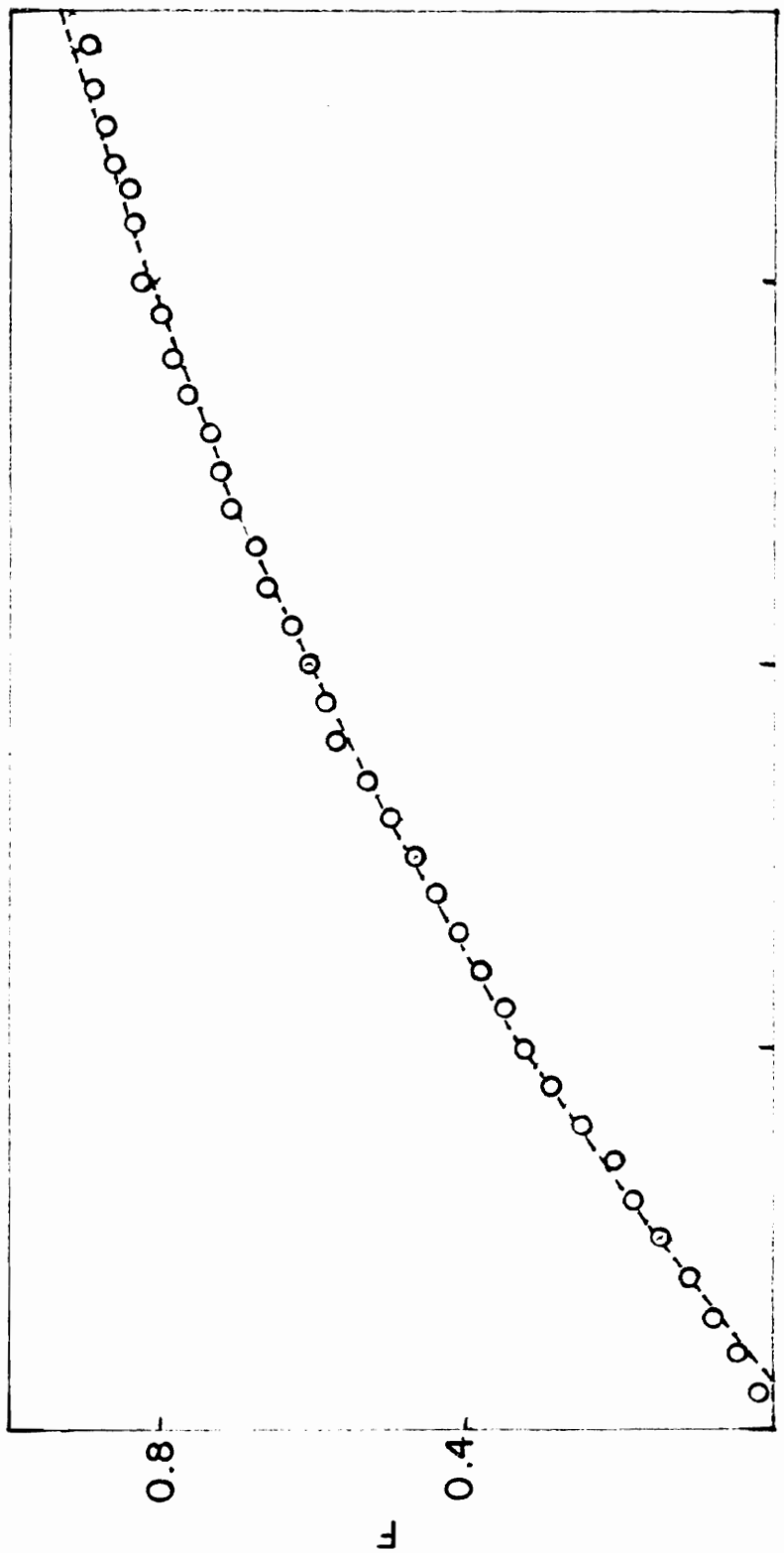

Figure 4.4. Plot of F versus (hours)$^{1/2}$ when b is 0.28. O = experimental; --- = theoretical.

Table 4.1. Permeability and Diffusion Coefficients for Progesterone in Silastic Devices.

System	b	$P^1 \times 10^6 (cm^2/sec)$	$D^1 \times 10^8 (cm^2/sec)$	$P^2 \times 10^6 (cm^2/sec)$	$D^2 \times 10^8 (cm^2/sec)$
A	0.05	2.9	6.9	2.8	6.7
B	0.14	2.9	6.9	3.0	7.1
C	0.28	2.9	6.9	3.3	7.9

[1]Data obtained by Equation 4-12.

[2]Data obtained by Equation 4-4.

full range of release. This is shown by the dashed line in Figures 4.2 to 4.4. Therefore, it is concluded that Equation 4-12 accurately reflects the release behavior of solutes from cylindrical monolithic devices for all values of b.

For comparison, the permeability and diffusion coefficients for progesterone in these devices were calculated by means of Equation 4-4. This was done by plotting $[(1 - F)\ln (1 - F) + F]^{\frac{1}{2}}$ versus $t^{\frac{1}{2}}$. P is obtained from the slope of this plot. The values obtained are shown in Table 4.1. It is apparent that as b increases, the calculated P (and D) values increase with successively increasing deviations from the value obtained via Equation 4-12.

In the practical application of these equations, a compromise between time spent in data analysis and accuracy may be required. Fron the data given in Table 4.1, it may be concluded that if b is less than about 0.10, calculated values of P will be approximately the same with both Equations 4-12 and 4-4. However, if b is more than 0.1, Equation 4-12 will provide a more accurate estimate of P and the time spent in data analysis may be justified.

4.2.3 Progesterone Release from Monolithic Hydrogel Devices

Drug release kinetics from monolithic devices containing drugs dispersed within the polymer matrix has been extensively investigated (102). Most of this work has dealt with the release of solutes from polymers, such as polydimethylsiloxane, which do not swell in the presence of solvent. In contrast, very little work has

been done on the release of drugs from polymers, such as the hydrogels, which swell in the presence of water. Recently, Good (103) presented an in-depth study of the release of a water soluble drug from hydrogels with slab geometry. In this study, the total drug present was soluble in the polymer matrix at equilibrium swelling. Graham (104) has also studied the release of drug from hydrogels of slab geometry in which the drug was present below its saturation solubility at equilibrium swelling.

In this section, data on the release of progesterone from cylindrical hydrogel devices which are initially dry are presented. The release rates are evaluated with respect to the effects of water uptake, initial drug load, and the equilibrium water content of the devices.

Based upon the study presented in Section 4.2.2, it was concluded that drug release from cylindrical devices, which have a ratio of the radius to length of less than 0.10, can be adequately described by the equation of Roseman and Higuchi (97). The devices prepared for the present study have dimensions of 4 cm in length by 0.25 cm in radius ($b = 0.063$). Therefore, the release rates should be consistent with the treatment of Roseman and Higuchi (Equation 4-4).

When F is plotted versus time, according to Equation 4-4. a nonlinear plot is obtained such that negative deviations occur with time. However, at early times, F is linear with time. The rationale as to why this occurs can be developed from a comparison of the initial release rates from devices of any geometry with the

initial release rates from slabs. Using the hypothesis, Roseman (105) has shown that the initial release rate from cylinders can be described by

$$F = \sqrt{2Kt} \tag{4-19}$$

where

$$K = \frac{4C_s D}{C_o r_o^2} \tag{4-19a}$$

The validity of Equation 4-19 was tested by Roseman (105). By comparing plots of F versus $t^{1/2}$ for both Equations 4-4 and 4-19, where K was arbitrarily set at 1.0 day^{-1}, Roseman concluded that Equation 4-19 provides a good approximation of the initial release rate from cylinders. Significant deviations (greater than 10%) do not occur until F is greater than about 0.50.

For several of the systems investigated in the present study, (Figures 4.5 to 4.10, plots of F versus $t^{\frac{1}{2}}$ follow the pattern suggested by Equations 4-4 and 4-19. During the early stages of drug release, these plots are linear. When t becomes large, the plots show the expected negative deviations from linearity. Based on this, it may be concluded that, in general, drug release rate from hydrogels follows the trend predicted based on theories developed for polymers which do not swell in the eluting solvent.

Such behavior was not universally observed. Figures 4.11 and 4.12 are plots of F versus $t^{1/2}$ for the release of progesterone from devices prepared from pHEMA (Figure 4.11), and a copolymer of

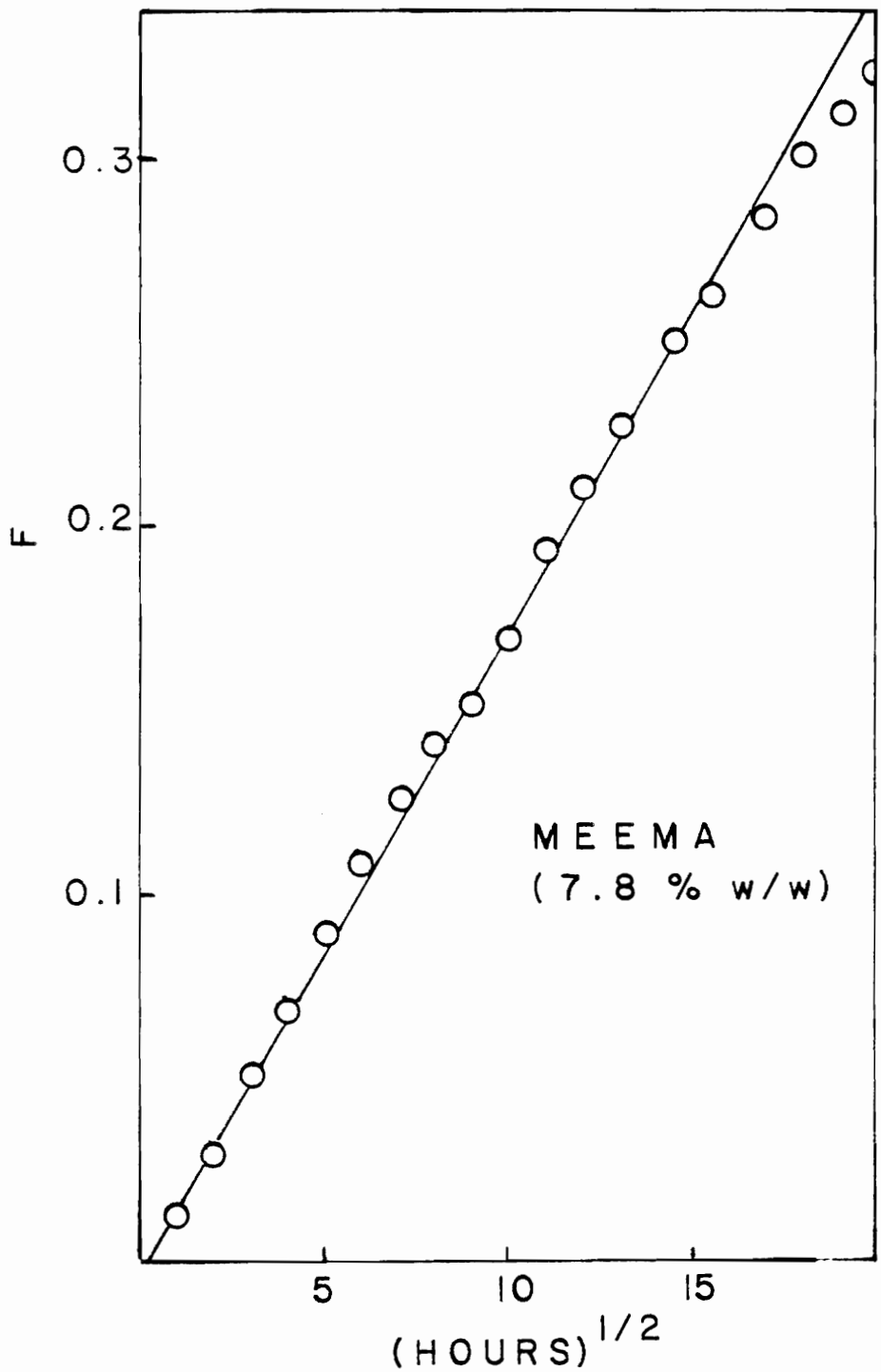

Figure 4.5. A plot of F versus (hours)$^{1/2}$. Open circles are experimental points; solid line used to determine slope and the permeation coefficient.

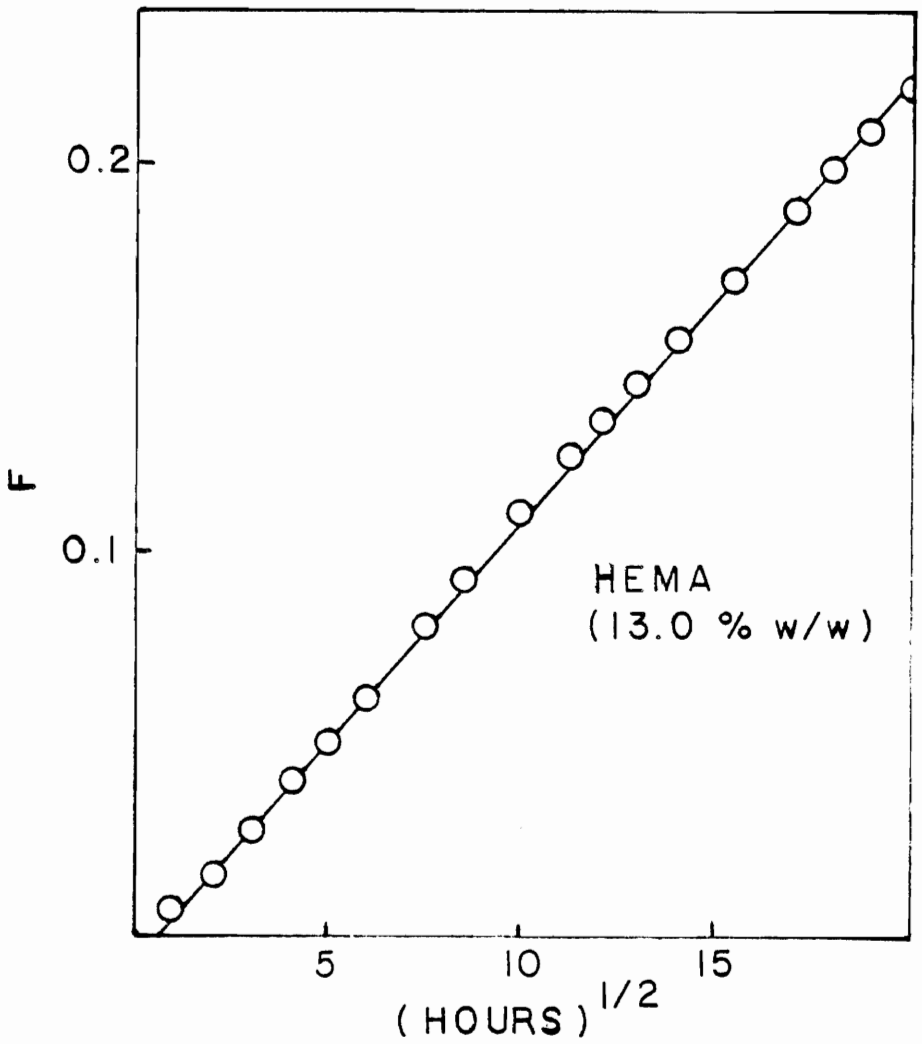

Figure 4.6. A plot of F versus $(\text{hours})^{1/2}$. Open circles are experimental points; solid line used to determine slope and the permeability coefficient.

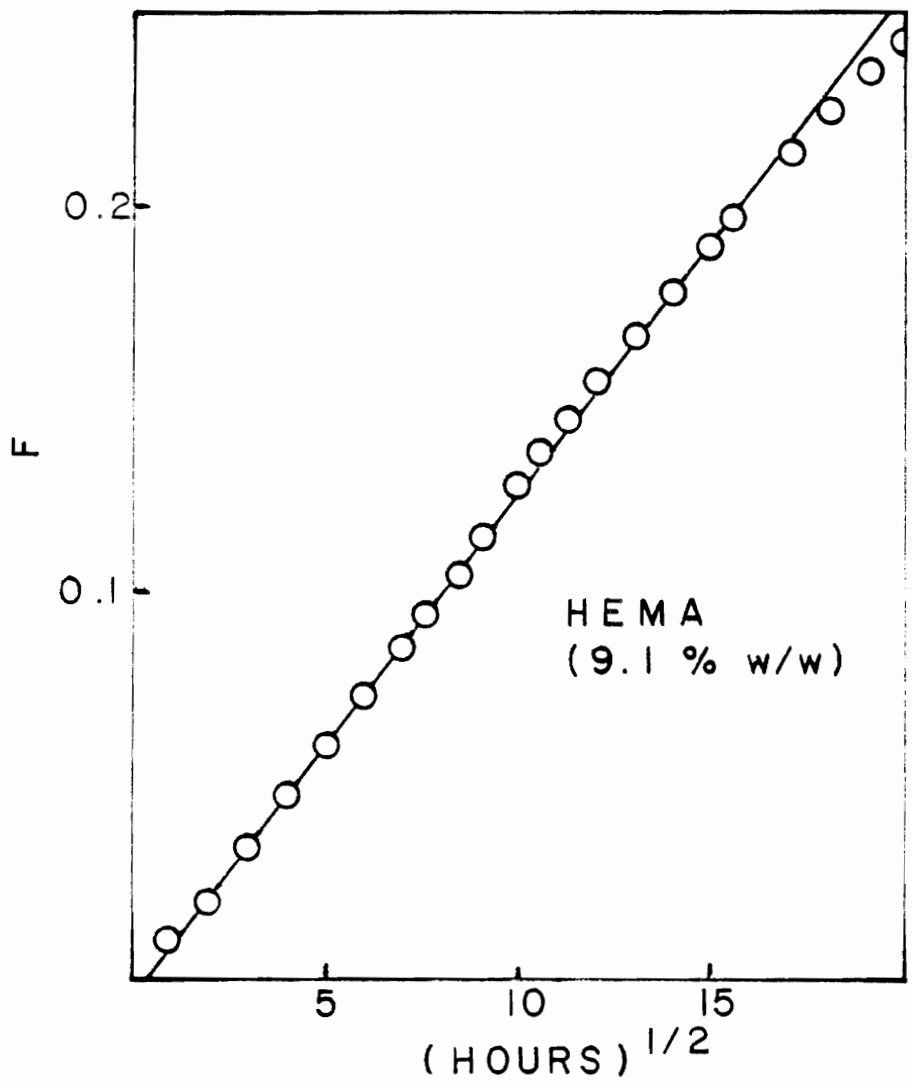

Figure 4.7. A plot of F versus $(\text{hours})^{1/2}$. Open circles are experimental points; solid line used to determine slope and the permeability coefficient.

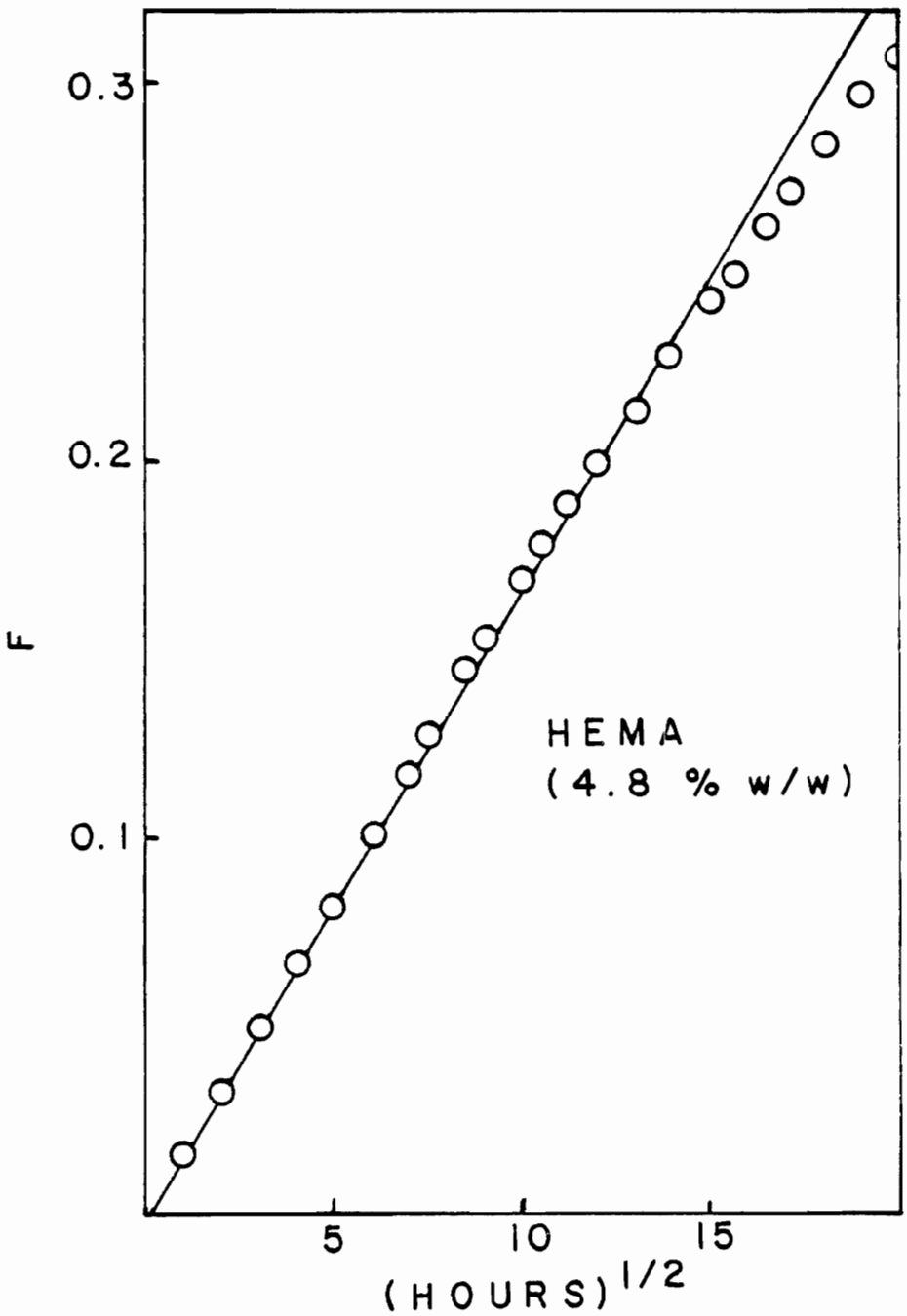

Figure 4.8. A plot of F versus $(\text{hours})^{1/2}$. Open circles are experimental points; solid line used to determine slope and the permeability coefficient.

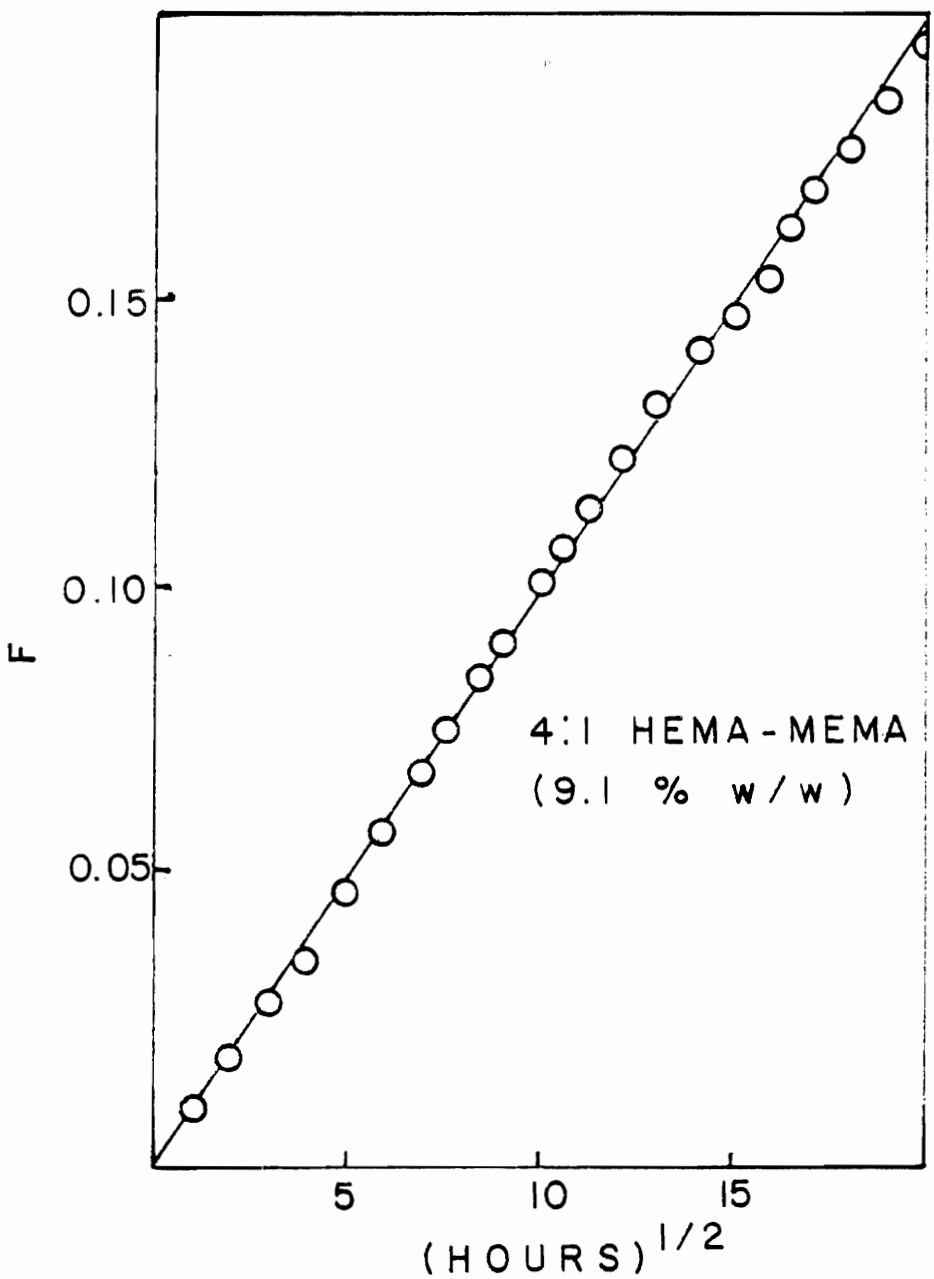

Figure 4.9. A plot of F versus $(\text{hours})^{1/2}$. Open circles are experimental points; solid line used to determine slope and the permeability coefficient.

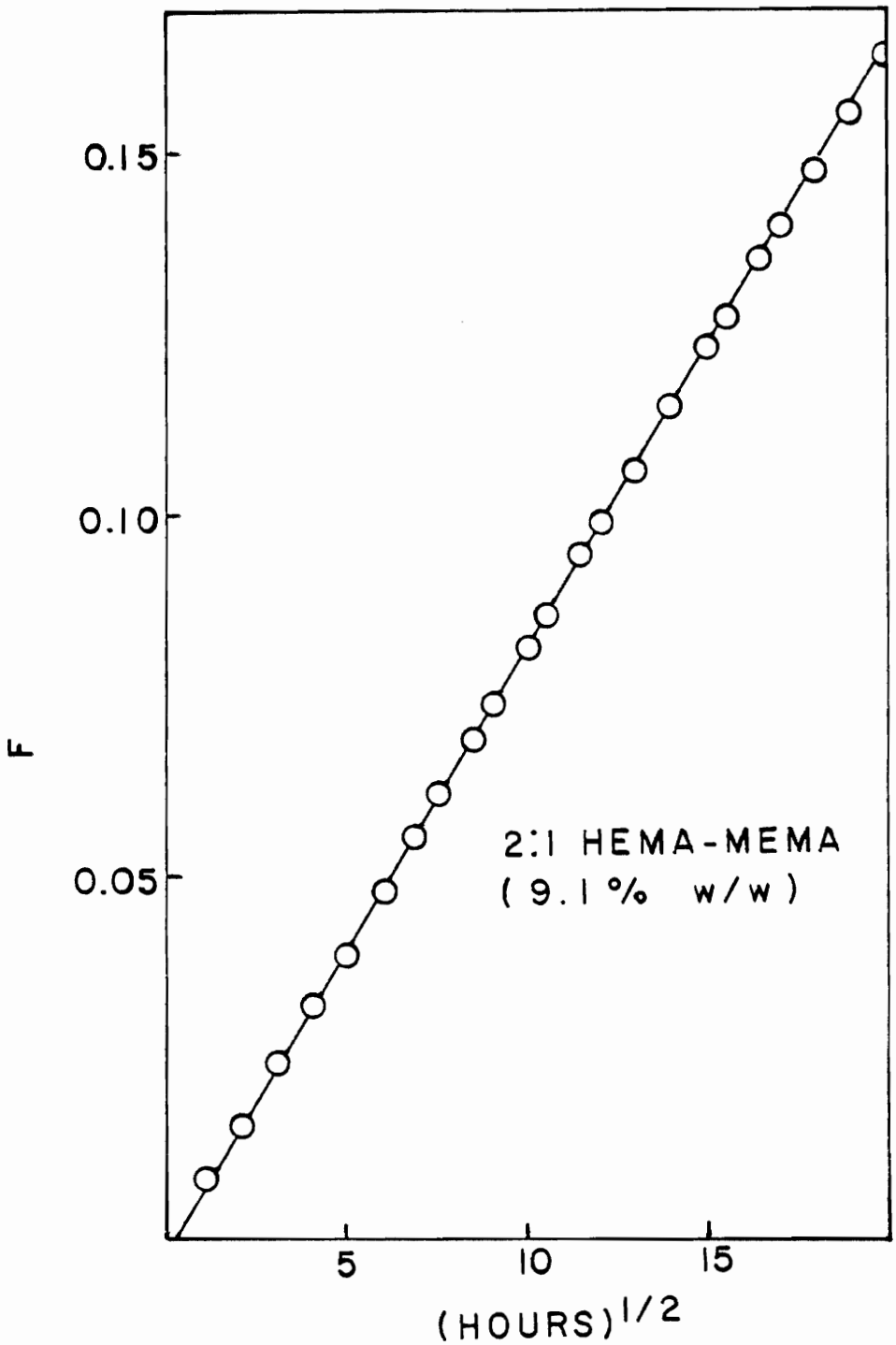

Figure 4.10. A plot of F versus $(\text{hours})^{1/2}$. Open circles are experimental points; solid lines used to determine slope and the permeability coefficient.

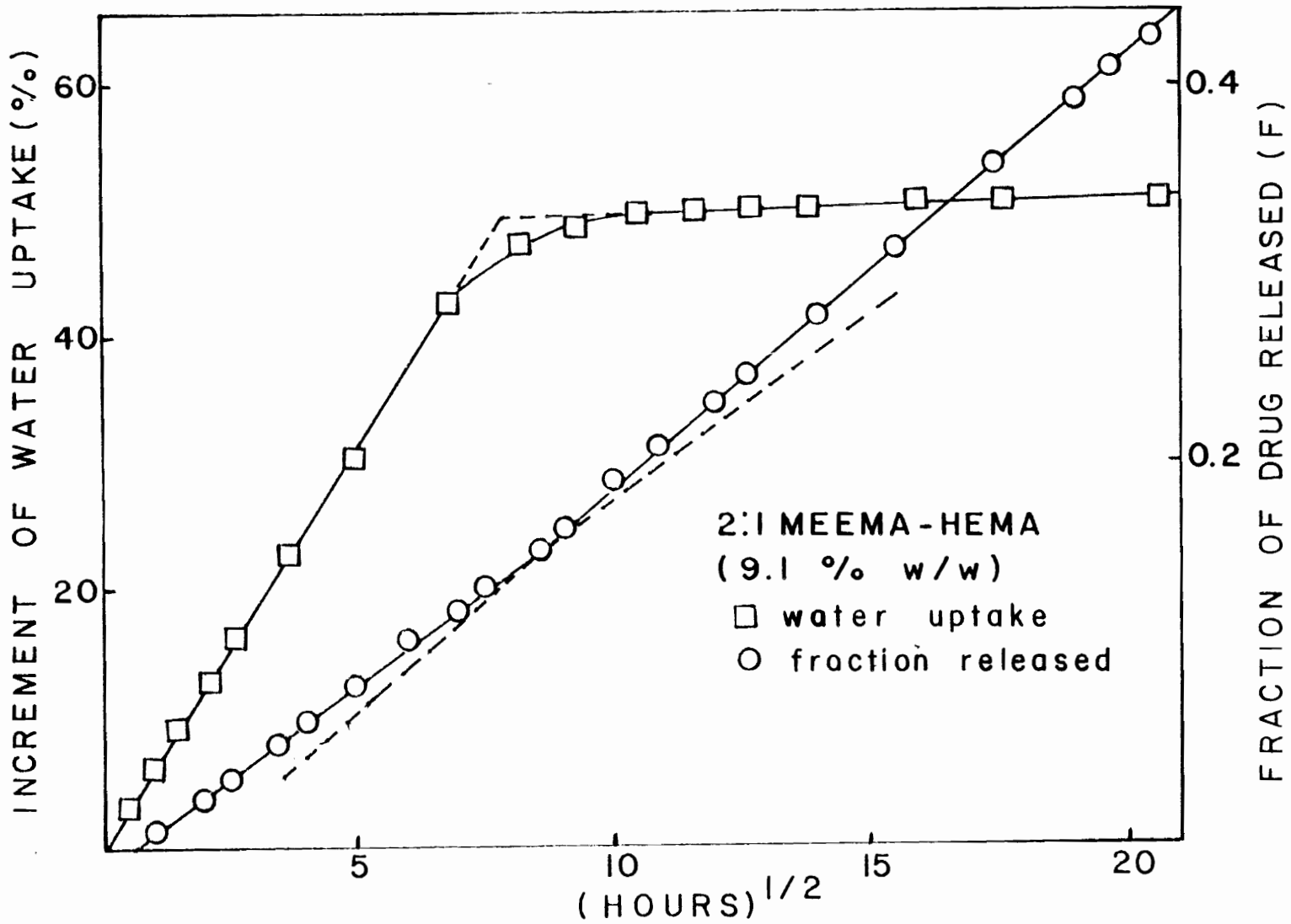

Figure 4.11. Plots of F and increment of water uptake (% w/w) versus (hours)$^{1/2}$.

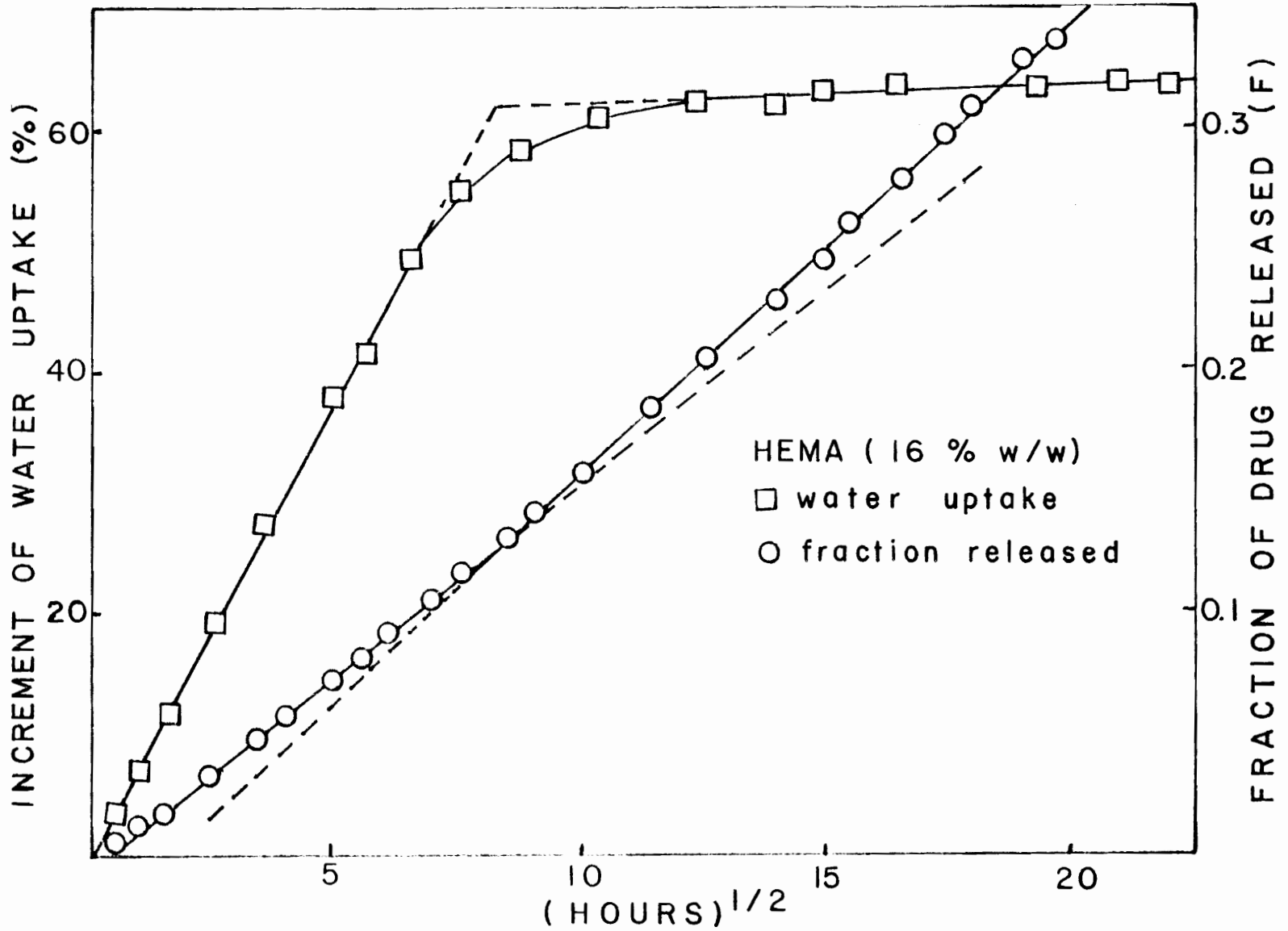

Figure 4.12. Plots of F and increment of water uptake (% w/w) versus $(\text{hours})^{1/2}$.

MEEMA and HEMA (monomer mole ratio 2:1) (Figure 4.12). The initial drug loading of these devices were 16.0 and 9.1 weight percent, respectively. Both plots appear to be best represented by two straight lines with a discernable breakpoint during the early stages of release. The existence of these breakpoints was confirmed from plots of $\Delta Mt/\Delta t$ versus t. This function is constant in each case until about eight hours in root time. At times greater than this, $Mt/\Delta t$ is again constant but its value is somewhat greater.

Also given in Figures 4.11 and 4.12, are plots of the water uptake of these devices (defined as the increased weight of hydrated polymer/initial weight of the nonhydrated device) versus the square root of time. The breakpoints in these curves correspond with those in the drug release curves. Based on this, it is suggested that the influx of water into the device may influence the release rate of drug from the device. From the observed smaller slope in the drug release curve before the breakpoint, it can be concluded that drug release is slower during the early stages of release. The slower rate of drug release may arise due to the interaction between the influxing water and effluxing drug. If progesterone transport occurs mainly through the water filled pores of the hydrogel, the frictional force between the solute and the water present in pores will contribute an energy barrier for solute diffusion through the hydrogel membrane (106). Work (84, 86) from this laboratory has shown that both water transport and the permeation of steroids occurs predominately through the water filled pores of the hydrogels. This indicates

that before the breakpoint is reached, a counter flow of the solute and water occurs in these pores. This counter flow is thought to provide an additional resistance to solute diffusion. The duration of this effect is dependent on the water saturation time.

In the following, an empirical parameter, Q, will be developed which will serve as a semiquantitative measure of the magnitudes of these crossflows. The magnitude of Q will be compared with the experimental results obtained from the drug release curves.

The rate of drug release is dependent upon the permeability of drug in the device. These values were determined from the slope of drug release curves. According to Equation 4-4, a function f (F) may be defined as follows:

$$f(F) = [(1 - F) \ln (1 - F) + F]^{1/2} = K^{1/2} t^{1/2} \qquad (4\text{-}20)$$

where

$$K = \frac{4C_s Dt}{C_o r_o^2} \qquad (4\text{-}20a)$$

When f (F) is plotted versus $t^{1/2}$, a linear plot should be obtained which has a slope of $K^{1/2}$. For cases in which a breakpoint is observed, $K^{1/2}$ was obtained from the slope of tne plot above the breakpoint. The permeability coefficient, P, can be obtained from K and Equation 4-20a as follows:

$$K = \frac{4C_s D}{C_o r_o^2} = \frac{4K_d DC_w}{C_o r_o^2} = \frac{4PC_w}{C_o r_o^2} \qquad (4\text{-}21)$$

where $P = DK_d$, $K_d = C_s/C_w$, and C_w is the satuaration solubility of progesterone in water.

It is hypothesized that the effect of water influx on the drug release rate is proportional to both the rate of water influx and the rate of drug efflux. According to this hypothesis, the product of the two rates should give a value which provides a measure of the effect of water uptake on drug release.

The rate of drug release is dependent on many factors as shown in Equation 4-19. In order to obtain the main factors which affect the release rate, the equation is further treated. From Equation 4-19, it can be shown by substitution of $\pi r_o^2 h_o C_o$ for M_∞ that Mt is given by

$$Mt = (8 \pi^2 h_o^2 D C_o C_s r_o^2 t)^{1/2} \qquad (4\text{-}22)$$

or by substituting P for DK_d

$$Mt = (8 \pi^2 h_o^2 r_o^2 C_o C_w P t)^{1/2} \qquad (4\text{-}23)$$

where h_o is the height of the device. For this experiment, nearly identical devices were used so r_o and h_o can be assumed constant for all devices studied. It is apparent from Equation 4-23 that Mt is proportional to the square root of both the initial drug load and the permeability of the solute.

From Equation 4-25, it may be concluded that P and C_o are the parameters which should control the relative release rate of

progesterone from the various devices investigated. The rate of water influx is dependent upon the permeability coefficient of water in each device. This value cannot be determined directly, however, the rate should be proportional to the slope, β, of the water influx curve. Accordingly, the empirical parameter, Q, can be defined as:

$$Q = \beta \sqrt{P C_o} \qquad (4\text{-}24)$$

This semi-empirical parameter should give a relative measure of the interaction arising from the counter-flows of the solute and water at the early stage of drug release. Values of Q, the water saturation time, and the presence of the breaking point are shown in Table 4.2.

A breakpoint in the drug release curve is observed when the value of Q is greater than about 5×10^{-6} cm/sec. Thus, as the magnitude of the solute and water crossflow increases (as measured by the parameter Q), breakpoints occur in the drug release curve. The absence of a breakpoint in the drug release curve for the matrix prepared from MEEMA can be explained by this method. This device has the highest equilibrium water content and is expected to be affected the most by water uptake. However, the value of β, slope of water influx, is rather small compared with that for HEMA devices. Therefore, the magnitude of the counterflow of solute and solvent is too small to show the presence of a breakpoint.

In order to calculate the permeability coefficients listed in Table 4.2, Equation 4-21 was used. In this case, it is

Table 4.2. Release Characteristics for Progesterone from Monolithic Hydrogel Devices.

Monomers	Initial Drug Load (% w/w)	Permeability $P \times 10^6$ cm^2/sec	Slope of H_2O Influx Plot ($hr^{-1/2}$)	Water Sat. Time ($hr^{-1/2}$)	$Q \times 10^5$ (cm/sec)	Appearance of Breaking Point
MEEMA[a]	7.8	3.64	0.44	14	3.9	No
67% MEEMA 33% HEMA[b]	9.1	2.01	0.78	8.2	5.56	Yes
HEMA	16.7	1.55	0.60	8	5.09	Yes
HEMA	13.0	1.22	0.63	9.5	4.18	No
HEMA	9.1	1.05	0.65	7.5	3.35	No
HEMA	4.8	0.88	0.67	7.5	2.30	No
80% HEMA 20% MEMA[c]	9.1	0.61	0.34	8.0	1.34	No
67% HEMA 33% MEMA	9.1	0.44	0.46	8.5	1.53	No

[a]Methoxyethoxyethyl methacrylate

[b]Hydroxyethyl methacrylate

[c]Methoxyethyl methacrylate

necessary to know the aqueous solubility of the solute in water. In case of hydrophilic solutes, aqueous solubilites are usually easy to obtain. However, it is relatively difficult to obtain accurate aqueous solubility data for hydrophobic solutes like progesterone (107). In this study, a value of 38 μgm/ml was used based on the average value obtained from three methods described in Section 2.2.2.1 This value is about three times higher than that of 11.4 μgm/ml given by Roseman (105). Considering the fact that Roseman's data was obtained at 37°C while the value presented here was obtained at 23°C, present data is much higher.

Such differences in the aqueous solubility will strongly affect the measured values of the permeability coefficient obtained by using Equation 4-21. Because of this, a second method was developed to determine progesterone permeability in the monolithic devices. When permeability coefficients are calculated from studies of the rate of transfer of a solute across a thin film using a diffusion cell, the P values can be obtained directly from plots of concentration variation versus time using Equation 3-14 derived in Section 3.2.1.

Table 4.3 shows the values of P and D obtained from progesterone transport study through hydrogel films together with those from progesterone release study from cylindrical monolithic devices. The films used in this study were prepared with the initial drug loadings listed in Table 4.3, and then depleted of drug before the permeation experiments were performed. This table shows that there is good agreement between the two sets of P values obtained by

Table 4.3. Comparison of Permeation Parameters from Monolithic Devices and Drug Depleted Films.

Monomers	Initial Drug Load (T w/w)	P (From Matrix) p x 10^6	P (From Cross-Memb.) p x 10^6	W_f (With Drug)	W_f After Drug Depletion)	K_d	D^a D x 10^8 cm^2/sec	D^b D x 10^8 cm^2/sec
MEEMA[d]	7.8	3.64	--	--	--	130[c]	2.80	--
67% MEEMA 335 HEMA[e]	9.1	2.01	1.84	.36	.540	141	1.43	1.30
HEMA	16.7	1.55	1.50	.34	.434	130	1.19	1.15
HEMA	13.0	1.22	--	.35	--	129[c]	0.95	--
HEMA	9.1	1.05	1.05	.35	.426	143	0.73	0.73
HEMA	4.8	0.88	0.88	.35	.426	127	0.69	0.69
80% HEMA 20% MEMA[f]	9.1	0.61	0.57	.24	.371	212	0.29	0.27
67% HEMA 33% MEMA	9.1	0.44	--	.25	--	192[c]	0.23	--

[a]From matrix release studies

[b]From cross-membrane studies

[c]For polymer with 0 percent initial drug load

[d]Methoxyethoxyethyl methacrylate

[e]Hydroxyethyl methacrylate

[f]Methoxyethyl methacrylate

separate methods. This agreement between P values provides further evidence that the aqueous solubility of progesterone is close to 38 μgm/ml. In fact, these two methods of obtaining permeability may be used to determine the solubility of slightly soluble solutes in aqueous solution.

Further support for this hypothesis can be generated from the paper of Roseman (105). In this paper (105), Roseman obtained two different values of diffusion coefficients of progesterone in silastic rubber. One value, obtained from lag time method, was 4.50×10^{-7} cm^2/sec. A second value, obtained from matrix release studies, was 16.5×10^{-7} cm^2/sec. These values together with the reported aqueous solubility value (11.4 μgm/ml) can be used to predict the aqueous solubility of progesterone. When the data were treated with the proper manipulation of Equation 4-21, 41.8 μgm/ml was obtained. This value is in good agreement with that obtained in the present study.

In order to study the effect of initial drug load on the transport properties of the matrix, permeability parameters of the monolithic devices were compared with that of the polymer system which has the same polymer composition though there is no initial drug load. Table 4.4 shows literature values of P, W_f, and K_d of the polymer system without initial drug load (85), together with the permeability coefficient obtained in this study. Table 4.4 shows that the permeability of the initially drug-filled polymer is greater than that of the same polymer without initial drugs. This

Table 4.4. Comparison of Permeation Parameters Between Drug Depleted Film and Film Prepared Without Drug.

Monomers	Initial Drug Load (% w/w)	$P^a \times 10^6$ (cm^2/sec)	$P^b \times 10^6$ (cm^2/sec)	W_f [b]	K_d [b]
MEEMA[d]	7.8	3.64	2.5	0.723	180
67% MEEMA 33% MEMA[c]	9.1	2.01	1.53	0.504	129
HEMA	16.7	1.55	0.84	0.423	129
HEMA	13.0	1.22	0.84	0.423	129
HEMA	9.1	1.05	0.84	0.423	129
HEMA	4.8	0.88	0.84	0.423	129
80% HEMA 20% MEMA[f]	9.1	0.61	0.29	0.340	156
67% HEMA 33% HEMA	9.1	0.44	0.30	0.308	192

[a] From drug depleted film

[b] From film prepared without drug (85)

increase is proportional to the initial drug loads as shown by the data with pHEMA. This may be interpreted that the presence of drug during polymerization affects the average pore size of the resulting polymer.

The effect of initial drug loading on the equilibrium water content was also studied. The equilibrium water contents of the monolithic devices after drug depletion were greater than those of same polymer systems without initial drug load. However, the equilibrium water contents of the drug depleted devices agree with those obtained in pHEMA films prepared without drug (85).

Table 4.3 shows that the progesterone permeability in monolithic devices increases as the equilibrium water content of drug depleted polymer increases. Same phenomena is observed in the drug permeation through polymer membrane without any initial drug load as shown in Table 4.4. The partition coefficients shown in Table 4.3 obtained on the drug depleted films are, in general, quite close to those obtained on the same polymer systems without initial drug load. This indicates that the introduction of drug into matrix device does not affect the equilibrium solubility of progesterone in the polymer matrix. The independence of drug solubility and dependence of drug permeability on the drug incorporation may be interpreted that the pore mechanism is predominant in progesterone permeation through hydrogel membrane. If progesterone permeates mainly by the partition mechanism, it is expected that increased value of permeation coefficient is accompanied by the change of drug solubility in polymer (78).

From the study of progesterone release from monolithic devices it can be concluded that release rate of drug is affected by: (i) water content of swollen devices, (ii) initial drug load, (iii) rate of water uptake, and (iv) that progesterone permeates through hydrogel membranes mainly via pore mechanism.

Chapter 5

PROGESTERONE RELEASE FROM RESERVOIR AND COMBINED DEVICES

5.1. Introduction

5.1.1 Progesterone Release from Reservoir Devices

Since the pioneering work of Folkman and Long (108), who used silastic capsules to prolong drug therapy for heart blockage, many investigators have used reservoir type devices for sustained release drug delivery systems.

Dziuk and Cook (109) observed that when silastic tubes were filled with steroids and placed in a saline solution, the steroids were released from the tubes at a constant rate for several days. Similarly, Croxatto (110) found that when silastic capsules containing a progestin were subdermally implanted in rates, pregnancy rates decreased.

This early work (108) with silastic reservoir devices utilized dry drug powder inside the core. Such devices do not provide a constant release rate of drug. This can be explained by the decreased surface contact of the drug with the polymer as the drug is depleted. Under the conditions of a constant effective surface area and a constant chemical activity of the drug, zero-order kinetics can be achieved.

Most of the early work was performed using silastic rubber

since it can be easily molded into devices of various shapes and is nontoxic. Other polymers also have been tried. Alza developed the Progestasert^{TM} 65 system which is made of an ethylene-vinyl acetate copolymer and delivers progesterone at a constant rate in utero for more than one year (111). Recently, Abraham and Ronel (112) used a hydrogel reservoir system for sustained zero-order release of narcotic antagonists.

In this chapter progesterone release is described from hydrogel reservoir devices of cylindrical geometry in order to obtain additional input for contraceptive drug delivery systems. Zero-order release is possible with reservoir devices when the chemical activity of the drug and the diffusional surface area are maintained constant. For this purpose, the core of the device is filled with a biologically active agent suspended in a liquid which solubilizes the drug to some extent but does not penetrate the membrane composing the walls surrounding the drug reservoir core. Silicone oil usually is used for this purpose.

The release rate varies with geometry. For cylindrical geometry the release rate of the drug from such devices is given as follows (113, 114).

$$\frac{dM_t}{dt} = \frac{2\pi h_o D C_s}{\ln (r_o/r_i)} \qquad (5\text{-}1)$$

or

$$\frac{dM_t}{dt} = \frac{2\pi h_o P C_w}{\ln (r_o/r_i)} \qquad (5\text{-}1\text{-}a)$$

where h_o is the length of the drug reservoir within the cylinder and r_o and r_i are the outer and inner radii of the cylinder, respectively. Diffusion coefficients can be calculated using Equation 5-1.

The total amount of drug released over time can be expressed as,

$$M_t = \frac{2\pi h D_o C_s t}{\ln (r_o/r_i)} \qquad (5\text{-}2)$$

Once diffusion coefficients are obtained, release rates and the amount of drug released can be predicted from Equations 5-1 and 5-2, respectively. However, for devices stored for a long time before use, a "burst effect," in which the release rate is initially higher than the steady state rate, is expected. For devices freshly prepared, a "time lag" effect, in which the release rate is initially less than the steady state value, is expected.

Because the diffusion coefficient for a given membrane is constant regardless of geometry, diffusion coefficients obtained by any method can be used for the prediction of the steady state release rate. Once the diffusion coefficient is obtained, a desired amount of drug can be delivered by proper fabrication of devices where length, inner radius, and outer radius can be controlled.

5.1.2 Release of Drug from Combined Type Devices

Most of the recent designs of polymeric drug delivery systems belong to one of two types, namely the monolithic device type or the

reservoir device type. Each type of device has its own advantages and disadvantages.

The reservoir type device is preferred for most applications because it can provide a zero-order release rate which is an important factor for controlled release drug delivery systems. However, this type of device has problems related to the mechanical properties of the polymer. Depending on the polymer material and wall thickness of the devices, there is the possibility of the rupture of the device. In the study of drug release from reservoir type devices composed of estriol core and polyurethane polymer, Baker et al. (115) pointed out that the device is too fragile below a certain thickness. Same problem of weak mechanical property is expected in case of hydrogel devices. If the device ruptures inside the body, too much drug will be released and the suspending agent will contact the biological tissues at the implant site, causing unexpected side effects. Usually, a highly potent drug is used for sustained release drug delivery systems so the tissues or the organ of the body where the device is implanted should be protected from exposure to large amounts of the drug.

In the case of the monolithic device type, there is no danger of exposing too much drug or other agents to the implantation site of the body in the event of the device rupturing. But, as previous work (work in Chapter 4) has shown, the release rate of a drug from monolithic device follows a square root of time law and, therefore, the amount of drug released will decrease continuously with time. For this reason, monolithic devices cannot be used for long-term drug

delivery systems, especially when the difference between the toxic level and the therapeutic level, or therapeutic and nonactive level is small.

However, if the major resistance to release of drug from a monolithic device occurs in the boundary diffusion layer, a zero-order release rate can be obtained. Chien et al. (116,117) found that drug release from monolithic device followed a square root of time relationship when high drug solubility was maintained. As they decreased the drug solubility in the elution medium, zero-order release of drug was observed showing that the higher energy barrier outside of the device can be used to give zero-order release kinetics. In the same manner, other polymers which are less permeable to the drug can be used to give major resistance to the release of the drug.

For these reasons, combined type devices were tried in this study. A combined type device is defined here as reservoir type device whose core is a dispersed monolithic device. Instead of a suspending medium, the drug was dispersed in a polymer which constitutes the core of a plymer reservoir device. This combined type device is expected to give zero-order drug release and to cause no serious side effects in case of device rupture inside the body where the device is implanted.

Equations which describe the release of drug from combined type devices were developed by Roseman and Higuchi (97). Initially, these equations were derived to explain aqueous boundary diffusion layers but should be applicable to the release of drug from combined type devices where aqueous boundary layer effects are neglected.

For the cylindrical geometry, the following equation can be obtained:

$$(1 - F) \ln (1 - F) + (1 + K') F = Kt \qquad (5\text{-}3)$$

where

$$K = \frac{4C_{s1}D_1}{C_o r_o^2} \qquad (5\text{-}3\text{-}a)$$

and

$$K' = \frac{2D_1 l_2 C_{s2}}{D_2 r_o C_{s2}} \qquad (5\text{-}3\text{-}b)$$

and

$$F = \frac{M_t}{M_\infty} = \frac{r_o^2 - r'^2}{r_o^2} \qquad (5\text{-}3\text{-}c)$$

where

r_o = radius of core cylinder (cm)

r' = distance from center of cylinder to receding drug boundary (cm)

C_{s1} = drug solubility in core membrane

C_{s2} = drug solubility in outside membrane

D_1 = diffusion coefficient of drug in core membrane

D_2 = Diffusion coefficient of drug in outside membrane

l_2 = Thickness of outside membrane

Equation (5-2) defines the fraction of drug release. The following equation describes the release rate:

$$\frac{dM_t}{dt} = \frac{4\pi h_o r_o C_{s1} C_{s2} D_1 D_2}{2D_1 l_2 C_{s1} - D_2 C_{s2} r_o \ln (1-F)} \qquad (5\text{-}4)$$

where h_o is height of cylinder (cm).

Equation 5-3 shows that in a strict sense, the release rate from a combined system cannot be constant (zero-order) because it will decrease as the F value increases. However, the combined type device is usually designed such that the decrease in release rate during several months is so small that it can be assumed constant.

5.2. Results and Discussion

5.2.1 Drug Release from Reservoir Devices

Figure 5-1 shows the progesterone release rate per day and total amount of drug released plotted versus time for a reservoir type device prepared from pHEMA. The release rate decreased continuously for 20 days and then became constant for the last experimental period. Similar type of "burst effect" was found for the release of progesterone from reservoir devices containing various polymer compositions. In every case, the constant value of release rate was observed after certain time.

Table 5.1 provides the permeability coefficients of progesterone from reservoir devices whose polymer capsules are composed of pHEMA, of pHEMA crosslinked with 2.3 mole percent EGDMA, and of copolymers of HEMA and MEMA. These values were obtained from the constant release rate of each device, together with Equation 5-5. Equation 5-5 is obtained from Equation 5-1a by rearrangement.

$$P = \frac{\ln (r_o/r_i)}{2\pi h C_w} \times \frac{dM_t}{dt} \qquad (5\text{-}5)$$

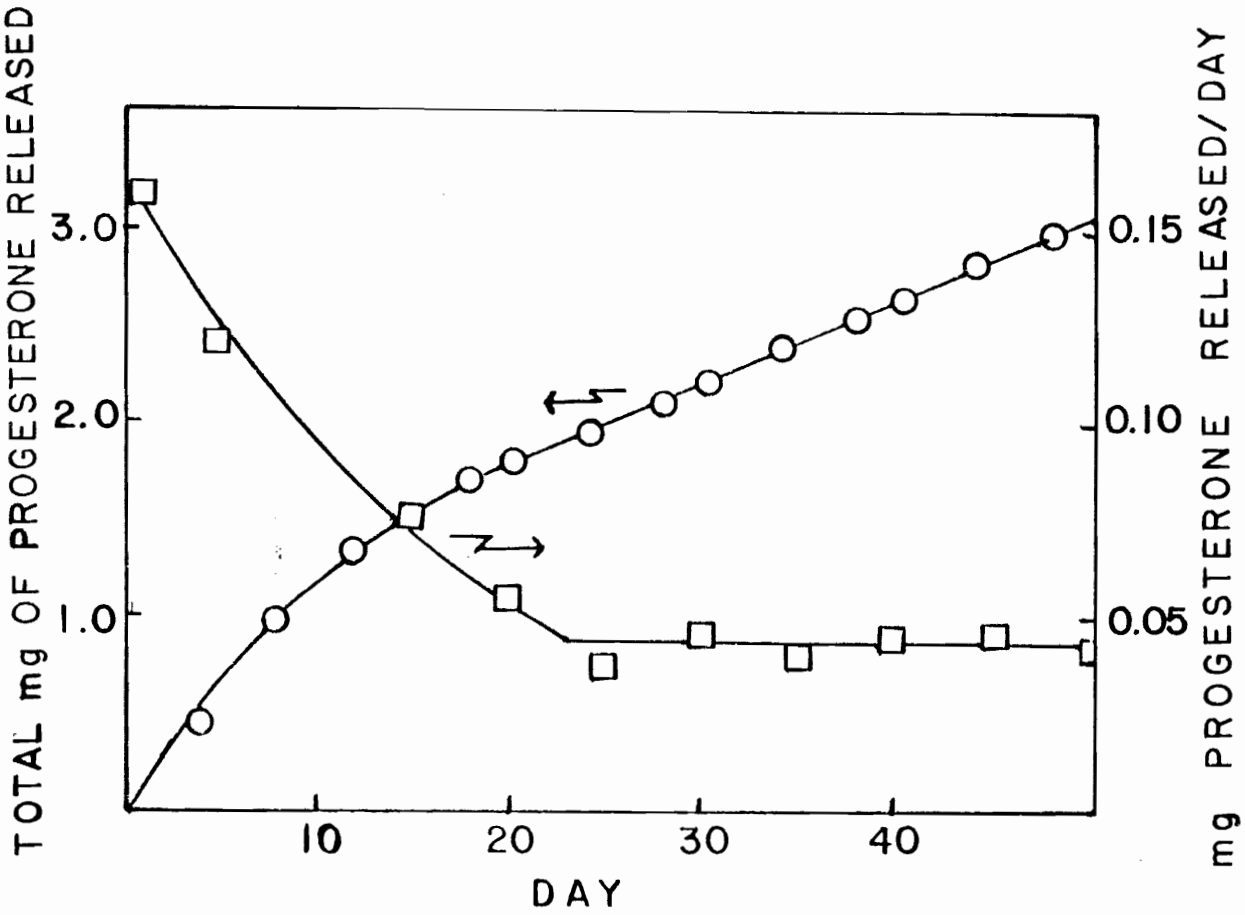

Figure 5.1. Plots of total progesterone released and progesterone released per day versus time for a reservoir type device.

Table 5.1. Release Characteristics for Progesterone from Reservoir-Type Hydrogel Devices.

Polymer	Length (cm)	Thickness (mm)	Permeability* $\times 10^{-7}$ cm^2/sec	Permeability+ $\times 10^{-7}$ cm^2/sec
HEMA	2.85	1.18 ± .01	10.7	10.3++
HEMA + 2.3% EGDMA	1.80	0.93 ± 0.1	2.32	2.35
MEMA-HEMA (1:2)	3.20	0.16 ± 0.1	2.76	2.97
MEMA-HEMA (1:4)	2.70	1.02 ± 0.1	3.08	2.69

*Obtained from release studies.

+Obtained from membrane permeation studies (85).

++Data taken from Table 3.1.

Because r_o, r_i, and h_o can be obtained by measuring the dimensions of the reservoir device, the permeability can be calculated from the release rate provided that the drug solubility in water, C_w, is known. A value of 38 ugm/ml was utilized based upon the average value obtained from the three methods described in Section 2.2.2.1.

The permeability coefficients obtained from the release studies of progesterone from reservoir devices were in good agreement with those obtained from membrane permeation studies where the hydrogel is in contact only with water. From these results, the following may be concluded.

1. The presence of silicone oil in the reservoir does not affect the steroid permeability in the membrane and, therefore, does not significantly affect the equilibrium water content of the hydrogel membrane.

2. The silicone oil maintains the chemical activity of progesterone in the core constant.

3. The solubility of progesterone in water is close to 38 ugm/ml and the solubility measurement methods used in this study (2.2.2.1) can be used for other sparingly soluble steroids.

4. The solubility of slightly soluble solutes in aqueous solution can be calculated by the combination of permeation data from reservoir device with that from cross membrane experiment (2.2.1) using the same polymer.

Permeation parameters for progesterone transport through polymers in reservoir devices are shown in Table 5.2. From the diffusion coefficients and water fraction data, it can be concluded that the diffusion coefficient increases as the equilibrium water content of polymer increases for these polymers. Data in Table 5.2 shows that other factors besides the equilibrium water content affect the diffusion coefficient. If water content is the only factor, the diffusion coefficient of progesterone in a HEMA-MEMA (4:1) copolymer should less than that in pHEMA with 2.3 mole percent of EGDMA since the water content of the former is less than that of later. According to the data given in Table 5.2, the permeabilities of hydrogels depend upon the water content and/or the nature and concentration of the crosslinker. It can be concluded that desired constant release rate can be obtained by choosing proper polymer composition.

5.2.2 Drug Release from Combined Devices

Progesterone release from combined devices prepared with an outer membrane prepared from pHEMA were studied. An inner core matrix was made from either MEEMA or a HEMA-MEEMA copolymer in which progesterone is dispersed or dissolved. Figure 5.2 is a plot of the fraction of drug released from the combined devices as a function of time, comparing experimentally determined data (solid lines) to the theoretically expected values (dashed line) as determined by Equation 5-3, together with necessary data obtained through the literature.

Table 5.2. Permeation Parmaters of Progesterone Transport in Reservoir Devices.

	$P \times 10^7 (cm^2/sec)$	K_d	$D \times 10^9 (cm^2/sec)$	W_f
HEMA	10.7	139	7.70	0.41
HEMA + 2.3% EGDMA	2.32	151	1.54	0.38
MEMA-HEMA (1:2)	2.76	192	1.44	0.31
MEMA-HEMA (1:4)	3.08	156	1.97	0.34

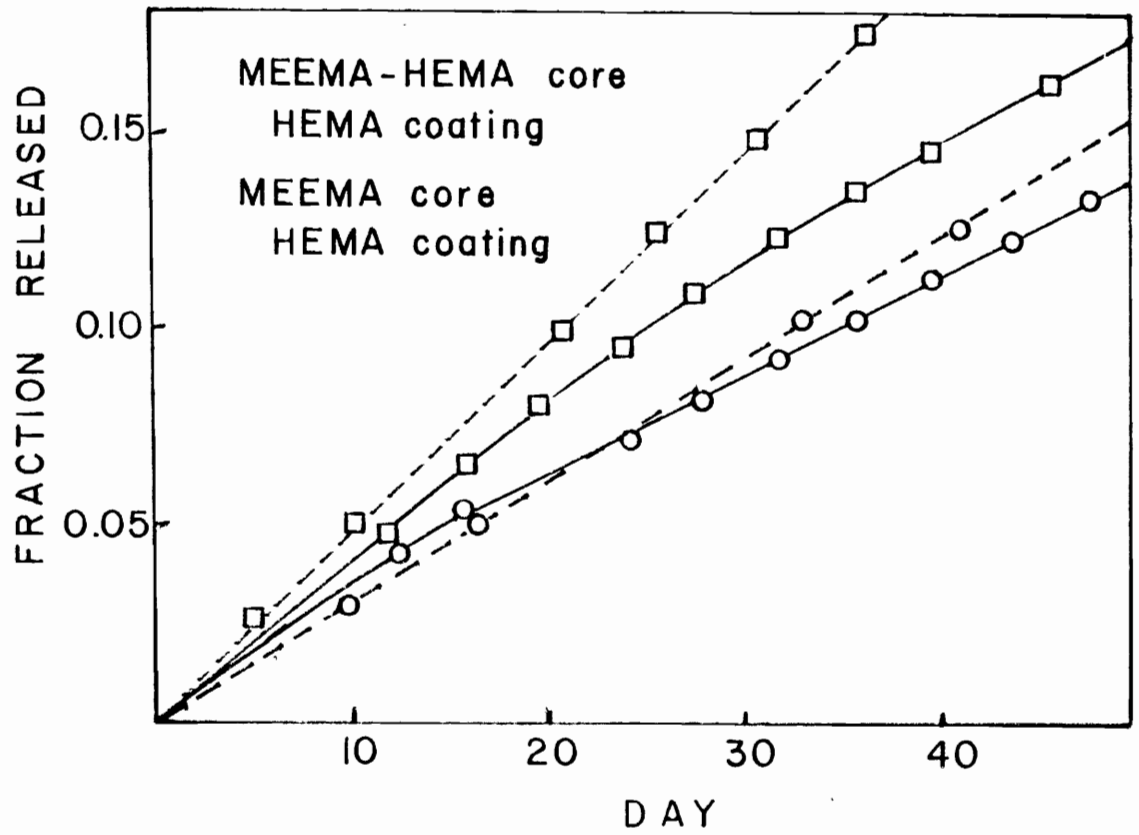

Figure 5.2. Plot of fraction of progesterone released from combined type devices versus time. The ratio of MEEMA to HEMA is 2:1 (w/w).

In both experimental cases, the release rate of progesterone per day becomes constant after 20 days. For the device prepared with HEMA-MEEMA copolymer core and pHEMA coating, the positive deviation of early time from the calculated value is probably due to the "burst" effect. However, the early time negative deviation in device with pMEEMA core cannot be explained clearly. The observed and predicted release rate together with the dimensions of the devices are given in Table 5.3. The predicted release rates were obtained by using Equation 5-4. Because less than 15% of the drug was released during the experiment, a value of 0.1 was used for F (fraction of drug released). The change in the predicted release rate arising from the change of F value from 0 to 0.1 was less than 5%.

In both cases, experimental values were smaller than predicted values. Rather small difference between the observed and predicted release rate was obtained for the device with a HEMA-MEEMA copolymer core. Large differences were obtained with the device having pMEEMA core. This may be explained by a "restricted water swelling" of core polymer due to the outer coating polymer. The swelling capacity of outer coating material (pHEMA) is less than that of core material (pMEEMA or copolymer of HEMA and MEEMA). Because of the less effective swelling of outside polymer, the core polymer will receive pressure resisting the expansion of core polymer which is the result of swelling. Thus, restricted water swelling will result in reduced water uptake which in turn will decrease progesterone permeability in the polymer. This "restricted water swelling" effect is more predominant in polymer which has high equilibrium water content. The

Table 5.3. Release Characteristics for Progesterone from Combined Type Hydrogel Devices.

Monolithic Core	Coating	Coating Thickness (cm)	Core Radius (cm)	Length (cm)	Release Rate (µgm/day)
67 percent MEEMA + 33 percent HEMA	HEMA	0.103 ± 0.01	.160	3.37	74.7* 88.1+
MEEMA	HEMA	0.103 ± 0.01	.205	3.13	67.7* 106.0+

*Experimental

+Predicted

larger negative deviation of the experimental value in combined device with pMEEMA whose equilibrium water content is greater than that of copolymer of HEMA and MEEMA can be explained by this "restrict water swelling."

From this study of drug release from the combined device, it can be concluded:

1. Pseudo zero-order release rate can be achieved for months from combined devices.

2. In case of combined device whose core is composed of a hydrogel, experimental release rates are smaller than predicted due to 'restricted water swelling effect.'

3. For combined devices whose core is composed of hydrogel, further refinements in the preparation method is required, for practical application.

Chapter 6

SOLUTE PERMEATION IN HYDROGEL FILMS: AN IRREVERSIBLE THERMODYNAMIC APPROACH

6.1. Introduction

In classical transport studies solute permeation through membranes is described by two coefficients, namely the diffusion coefficient and the partition coefficient. It has already been mentioned that diffusion in a membrane comes from molecular motion which is a function of the kinetic energy of the molecule as well as of the frictional forces exerted on the molecules by the medium through which the dissolved molecules are moving. Thus, solute passage through a membrane involves three factors, namely, the friction between solute and membrane, the friction between solute and solvent, and the friction between solvent and membrane. A full description should be able to take account of these coefficients whose value will depend upon the nature of the three processes involved. As mentioned by Kedem and Katchalsky (118), the two coefficients obtained by classical methods are not sufficient for a complete description of the permeation phenomena through a membrane.

In case of phenomenological theories based on irreversible thermodynamics, which were developed by Staverman (119-121) and extended by Kedem and Katchalsky (118, 122, 123) a membrane system where solute and solvent are present is described by means of three

characteristic quantities. These are the filtration coefficient Lp, the reflection coefficient σ of Staverman and the solute permeability coefficient ω of Kedem and Katchalsky (118). The quantities ω and σ provide information about the relative selectivity of the membrane for a particular solute.

For an ideal semipermeable membrane in which only the solvent permeates, $\sigma = 1.0$ and $\omega = 0$. For membrances permeable to the solute $\sigma < 1$ and $\omega > 0$ and σ decrease as the selectivity of the membrane decreases. The quantity Lp provides a measure of the total flow of solute and solvent. The only drawback of these three coefficients is the fact that these coefficients refer to the system as a whole. Specific interactions are not taken into account by the analysis.

Such specific information can be obtained from the frictional coefficients. These coefficients result from the frictional model (124-127). In this model, it is assumed that at steady state, the driving force for diffusion is counterbalanced by the retarding frictional forces generated between molecules. These coefficients are fsw, fsm, and fwm. The coefficient fsw refers to the interaction between one mole of solute with the water found in the membrane; the coefficient fsm refers to the interaction of one mole of solute with the membrane matrix; and the coefficient fwm describes the interaction of one mole of water and the membrane matrix. These frictional coefficients can be evaluated from the three experimental quantities σ, Lp, and ω. When the membrane is chemically inert,

information is gained about its geometry by comparing the friction between solute and solvent in free solution to the friction between the same components in the membrane.

If for a given membrane, with regard to a number of different solutes but always with the same solvent, these frictional coefficients are equal except for a constant factor, then this is a strong indication that only geometrical effects are involved (128). In this case, a purely geometrical character can be ascribed to the coefficients, such as the porosity and the tortuosity of the membrane. It is also possible to make a clearer distinction between the "pore mechanism," and the "partition mechanism" models by comparing frictional coefficients.

It is apparent, therefore, that the irreversible thermodynamic approach provides information which reflects both the selectivity of the membrane as well as the nature of the interaction between the solute, solvent, and membrane. This information is difficult to develop from the more classical approach based upon measurements of diffusion coefficients.

In this chapter, the permeation of a solute is examined based upon the irreversible thermodynamic approach. The polymer films examined were prepared from hydroxyethyl methacrylate, both with and without the crosslinker, ethyleneglycol dimethacrylate. Because of the low water solubility of the hydrophobic steroids, which makes the experiment quite difficult, water soluble solutes such as urea and sucrose were used. These results provide valuable information about the nature of the permeation process and can be useful in the

development of these membranes for applications in controlled release drug delivery systems and in the artificial kidney.

The permeation parameters, Lp, σ, and ω can be obtained experimentally from measurements of the volume flow, Jv, and from the solute flow, Js, under differing pressures. The pressure difference is produced either via a hydrostatic pressure (ΔP) or via osmotic pressure ($\Delta \pi$). Under a condition in which a hydrostatic pressure is applied to the compartment lower in concentration, the volume flow across a semi-permeable membrane is defined by:

$$Jv = Lp\ (\Delta P + \Delta \pi_o) = Lp\ (\Delta P + \sigma\ \Delta \pi) \qquad (6\text{-}1)$$

Where the effective osmotic pressure ($\Delta \pi_o$) is given by $\sigma \Delta \pi$, and $\Delta \pi_o$ is the ideal (van't Hoff) value. The total solute flow under the condition in which the volume flow is zero is given by:

$$Js = \omega \Delta \pi \qquad (6\text{-}2)$$

Based on these quantities, the permeation parameters are defined as follows:

$$Lp = \left(\frac{Jv}{\Delta P}\right) \Delta \pi = 0 \qquad (6\text{-}3)$$

$$\sigma = \left(\frac{Jv - Lp\ \Delta P}{Lp\ \Delta \pi}\right) \qquad (6\text{-}4)$$

$$\omega = \left(J_s/\Delta \pi\right)_{Jv} = 0$$

$$= \left(\frac{DKd}{lRT}\right) Jv = 0 \qquad (6\text{-}5)$$

where l is the thickness of the membrane.

In general, the total frictional coefficient of one mole of given molecule with a system (f_t) can be expressed as:

$$f_t = \frac{RT}{D} \tag{6-6}$$

The three frictional coefficients, fsw, fsm, fwm, necessary to describe solute-water-membrane system can be defined in terms of the phenomenological coefficients as follows:

$$fsw = (1 - \sigma - \frac{\omega \bar{V}_s}{Lp}) \frac{\phi v}{l\omega} \tag{6-7}$$

$$fsm = \frac{\phi v}{l\omega} [(\frac{Kd}{\phi v} - (1 - \sigma - \frac{\omega \bar{V}_s}{Lp})] \tag{6-8}$$

$$fwm = \frac{\phi v \bar{V}w}{lLp} - \bar{V}w\ Cs\ (1 - \sigma)\ fsm \tag{6-9}$$

where

ϕv = Water content of membrane in terms of volume fractions

$\bar{V}w$ = Partial molar volume of water

$\bar{V}s$ = Partial molar volume of solute

Cs = Average solute concentration in the membrane.

6.2. Results and Discussion

Table 6.1 shows the results obtained for the phenomenological coefficients for the hydrophilic solutes in a hydrogel membrane. Urea, glucose, and sucrose are used as solutes while pHEMA and pHEMA crosslinked with one mole percent EGDMA are used as membranes. Since

Table 6.1. Phenomenological Coefficients, Water Contents, and Partition Coefficients for Urea, Glucose, and Sucrose in Various Membranes.

Membrane	Solute	ϕ_v	$L_p \times d$ $cm^4/dyne\text{-}sec$	σ	$\omega \times d$ $\frac{mole\text{-}cm}{dyne\text{-}sec}$	K_d
pHEMA[a]	Urea	.526	8.56×10^{-15}	0.0718	3.08×10^{-17}	0.53
	Glucose	.475	6.75×10^{-15}	0.752	2.43×10^{-18}	0.23
	Sucrose	.470	5.95×10^{-15}	0.940	4.64×10^{-19}	0.23
pHEMA + 1 mole % EGDMA[a]	Urea	.525	6.34×10^{-15}	0.0632	2.50×10^{-17}	0.48
	Glucose		3.05×10^{-15}		1.52×10^{-18}	0.24
	Sucrose				3.58×10^{-19}	0.25
Cupraphane[b]	Urea	.676	1.084×10^{-13}	0.026	1.07×10^{-16}	0.54
	Glucose	.676	9.09×10^{-14}	0.088	2.41×10^{-17}	0.29
	Sucrose	.676	7.74×10^{-14}	0.174	1.72×10^{-17}	0.30
Cellophane[c]	Urea					
	Glucose	.694	1.70×10^{-13}	0.0885	3.39×10^{-17}	0.704
	Sucrose	.694	1.62×10^{-13}	0.105	2.12×10^{-17}	0.734
Wet Gel[d]	Urea	.77	8.21×10^{-13}	0.0016	2.66×10^{-16}	
	Glucose	.77	8.21×10^{-13}	0.024	9.51×10^{-17}	
	Sucrose	.77	8.21×10^{-13}	0.036	6.44×10^{-17}	

[a] $\Delta c = 0.15$ M [b] data from Ref. (76) $\Delta c = 0.05$ M

[c] data from Ref. (129) $\Delta c = 0.05$ M [d] data from Ref. (128) $\Delta c = 1.0$ M

Lp and ω are both dependent upon the membrane thickness, the normalized values, Lp x l and ω x l, are used in Table 6.1. The reflection coefficient, σ, is independent of the membrane thickness.

The filtration coefficient (normalized for thickness) is a measure of the total volume flow per unit thickness in a membrane. From Table 6.1, we see that the filtration coefficient for a given membrane decreases as the solute size increases. This result is consistent with a blockage or clogging of some of the pores or channels through which solvent and solute molecules pass in a hydrogel membrane. Based upon this interpretation, it is expected that Lp x l should be dependent upon solute concentration. Furthermore, Lp x l should reach a limiting value, independent of solute size, in very dilute solution. These expectations, have been experimentally verified for cellophane membranes by Kaufmann and Leonard (129).

Table 6.1 also shows literature data of the phenomenological coefficients for urea, glucose, and sucrose in cellulosic based hydrogel membrances. From this table, it can be seen that the filtration coefficient increases as the water content of the membrane increases for a given solute. The magnitude of change in Lp x l with water content is much greater than the solute size effect discussed above. For example, Lp x l in pHEMA changes by a factor of about 1.5 (5.95×10^{-15} cm^4/dyne-sec to 8.56×10^{-15} cm^4/dyne-sec) when the solute is changed from sucrose to urea. In contrast, Lp x l increases by more than a factor of 100 when the water content is increased from about 0.47 (pHEMA) to 0.77 (wet gel). Lp x l for cuprophane and cellophane are intermediate between these extremes.

Nonetheless, it is apparent that pHEMA is a much less permeable membrane than any of the cellulosic based films. The restrictive nature of pHEMA is enhanced by the incorporation of one mole percent EGDMA (Table 6.1).

The solute permeability coefficient, ω, of Kedem and Katchalsky is directly related to the classical diffusion coefficient, D, obtained from Fick's Law. From Equation 6-5, it can be seen that ω is inversely proportional to membrane thickness and directly proportional to the diffusion coefficient. In a sense, ω, normalized for thickness ($\omega \times l$) can be viewed in the same way as the classical diffusion coefficient D. Data in Table 6.1 shows that $\omega \times l$ for a given solute in the various membranes increases as the water content of a membrane increases. Table 6.1 also shows that for a given membrane $\omega \times l$ decreases with an increase in solute size. In general, the scale of the decrease in the solute permeability ($\omega \times l$), with solute size is larger with a hydrogel having a relatively small water content. These findings from solute permeability data are consistent with the hypothesis that hydrophilic solutes such as urea, glucose, and sucrose transport a hydrogel membrane primarily by a pore mechanism (59).

The reflection coefficient σ is a measure of the relative degree of selectivity of the membrane between solute and solvent. If a hydrophilic solute permeates via pores or micro channels present in the hydrogel membrane, selectivity for a given solute should decrease as the water content or pore size increases. The reflection coefficient data in Table 6.1 demonstrate this trend. The low

selectivity for a solute in a cellulosic membrane indicates relatively large pore size compared with the solute size. The large value of this coefficient for glucose or sucrose in a pHEMA membrane shows that the pore size of pHEMA hydrogels is approximately equal to or slightly larger than the size of the solute. It can be said that sucrose is almost totally reflected relative to water while urea and water permeate pHEMA membrane at very similar rates.

From Table 6.1, it can be seen that the σ value for urea in pHEMA is greater than that of pHEMA which has been crosslinked with EGDMA. This can be interpreted to imply that a crosslinked pHEMA membrane is less selective toward urea. An opposite result is expected if the solute is thought to permeate in the hydrogel by a pore mechanism. The selectivity of a crosslinked pHEMA should increase since a crosslinked pHEMA is thought to have a smaller pore size than noncrosslinked pHEMA. Considering the fact that the total permeability of both solute and solvent decrease as the pHEMA membrane is crosslinked, it can be concluded that the contribution of a partition mechanism in urea permeation through hydrogel membrane cannot be neglected. Further comment about this point will be provided from frictional coefficient data.

In very dilute solution, fwm for a single membrane should be the same as that of a pure water-membrane system regardless of the nature of solute. This limiting value, (fwm^b) may be defined as follows:

$$fwm^b = \frac{\phi_w \bar{V}_w}{1 \times Lp^b} \qquad (6\text{-}10)$$

where Lp^b is the filtration coefficient of a pure water - membrane system. This fact was confirmed by the work of Kaufmann and Leonard (129).

From the relationship between Lp x l and the water content, together with Equation 6-9, it is expected that fwm should increase with decreases in water content. Table 6.2 shows that the dependence of fwm on the water content is as predicted. The data for the pHEMA and pHEMA crosslinked with EGDMA indicates that the pore size of the crosslinked pHEMA is smaller than that of noncrosslinked pHEMA. The smaller pore size causes a larger clogging effect for the same solute resulting in a greater interaction between the solvent and the membrane. The dependence of the solute clogging effect on the pore size of a membrane is expected to be greater for a larger solute molecule. This point can be verified by the fwm values of solutes on pHEMA and crosslinked pHEMA. Table 6.2 shows that fwm for urea increases 1.2 times as the membrane changes from pHEMA to crosslinked pHEMA while fwm for glucose increases 2.2 times for the same membrane change.

As mentioned earlier, fsw provides a measure of collisional interactions between solute and water in a membrane. It is expected that fsw would be closely related to fsw° which is the frictional coefficient between solute and water in an aqueous solution. fsw° is defined by Einstein as follows:

$$fsw^\circ = \frac{RT}{D^\circ} \qquad (6\text{-}11)$$

where D° is the diffusion coefficient of a solute in water. For an ideal porous-type membrane, like a glass filter, as the pore size of the membrane increases, both σ and ω/Lp approach 0. This trend can be demonstrated by the data in Table 6.1. Namely σ for urea changes from 0.713 for pHEMA to 0.0016 for wet gel and ω/Lp for the same solute changes from 3.6×10^{-3} mole/cm^3 for pHEMA to 3.2×10^{-4} mole/cm^3 for wet gel. Therefore, Equation 6-7 can be approximated as follows:

$$fsw = \frac{\phi w}{1\omega} \tag{6-12}$$

In order to relate fsw to the diffusion coefficient, Equation 6-5 can be combined with Equation 6-12 to yield

$$fsw = \frac{\phi w\ RT}{Dkd} \tag{6-13}$$

Equation 6-14 and Equation 6-11 are very similar. In the extreme case of a large pore size membrane, such as a glass filter, Kd becomes ϕw and D approaches D°. In this case, fsw approaches fsw°. As shown in Table 6.2, the values of fsw of wet gel are quite close to the fsw° for the same solute. Thus, fsw also demonstrates that the wet gel behaves as a membrane with large pores and that the interaction between the solute and water is not very different from that obtained in pure water. As the pore size of the membrane decreases or as water content decreases, a considerable increase in the solute-water interaction occurs. As noted, fwm also increases

Table 6.2. Frictional Coefficients for Urea, Glucose, and Sucrose in pHEMA and Cellulosic Membranes.

Coefficient	Membrane	Urea	Glucose	Sucrose
f_{sw} $\frac{\text{dyne-sec x } 10^{-16}}{\text{mole-cm}}$	pHEMA	1.31	4.06	4.42
	pHEMA + EGDMA	1.60	--	--
	Cupraphane	0.60	2.47	3.06
	Cellophane	--	1.81	2.82
	Wet Gel	0.282	0.78	1.13
f_{sm} $\frac{\text{dyne/sec x } 10^{-16}}{\text{mole/cm}}$	pHEMA	0.408	5.41	45.2
	pHEMA + EGDMA	0.319	--	--
	Cupraphane	-0.086	-1.25	-1.30
	Cellophane	--	0.250	0.617
	Wet Gel	0.0046	0.030	0.067
f_{wm} $\frac{\text{dyne-sec x } 10^{-13}}{\text{mole/cm}}$	pHEMA	111	127	142
	pHEMA + EGDMA	129	281	--
	Cupraphane	11.4	14.5	16.4
	Cellophane	--	8.30	8.55
	Wet Gel	1.68	1.71	1.74
f_{ws}/f_{sm}	pHEMA	3.22	0.750	0.0976
	pHEMA + EGDMA	5.03	--	--
	Cupraphane	-6.8	-2.0	-2.4
	Cellophane	--	7.24	4.6
	Wet Gel	61.0	26.0	16.8
f_{sw}^{o} (a) $\frac{\text{dyne-sec x } 10^{-16}}{\text{mole/cm}}$		0.177	0.385	0.600

a) Values calculated using Equation 6-12 and the diffusion coefficient data obtained from reference (59).

under the same conditions. Thus, frictional interactions between water and membrane appear to be translated into an increased frictional interaction between the solute and water.

As mentioned earlier, fsw provides a measure of interaction between the solute and the membrane. The role of this interaction on solute permeation in a hydrogel membrane can be understood by the modification of Equation 6-9. This equation can be changed as follows:

$$fsm = \frac{\phi v}{l\omega}\left[\frac{Kd}{\phi v} - \left(1 - \sigma - \frac{\omega \bar{V}s}{Lp}\right)\right]$$

$$= \frac{Kd}{l\omega} - \frac{\phi v}{lw}\left(1 - \sigma - \frac{\omega \bar{V}s}{Lp}\right) \qquad (6\text{-}14)$$

Incorporation of Equations 6-5 and 6-7 to Equation 6-15 gives

$$fsm = \frac{RT}{D} - fsw \qquad (6\text{-}15)$$

The first term on the right side of Equation 6-16 can be termed, the total frictional coefficient (ftss) of a solute in a membrane-water-solute system so that Equation 6-16 can be rewritten as:

$$fsm + fsw = \frac{RT}{D} = ftss \qquad (6\text{-}16)$$

Equation 6-17 shows that it is the summation of fsm and fsw rather than fsm which is inversely proportional to the diffusion coefficient. However, data in Table 6.2 shows that fsm changes more

dramatically than fsw with a change of the diffusion coefficient. For example, fsw for pHEMA increases by four times as the solute changes from urea to glucose while fsm for pHEMA increases by 17 times for the same change of solute.

For a porous-type membrane whose pore size is much greater than the size of the solute, the solute will interact primarily with the water molecules present in the pores. The interaction of the solute with the membrane, which acts as the wall of a water-filled pore, is negligibly small when compared to the interaction between the solute and the water molecules. For a given solute, as the pore size of the membrane decreases the contribution of fsm to the total interaction between the solute and the system increases. This is particularly evident from the ratio fsw/fsm (Table 6.2). This ratio decreases both with solute size in given membrane and with the same solute in the various membranes.

It was noted from the analysis of the values that there should be some contribution of the partition mechanism to the total transport of urea in the pHEMA membranes. A similar conclusion is evident also from an analysis of fsm. For example, if porous transport dominates the flow of this solute, then fsm should increase with crosslinking due to the decrease in pore size. In fact, the opposite trend is observed (Table 6.2).

In order to rationalize this result, the following model for urea transport in pHEMA is proposed. This model is presented in Figure 6.1. In this model, it is assumed that transport of urea occurs via both the pore mechanism and the partition mechanism in

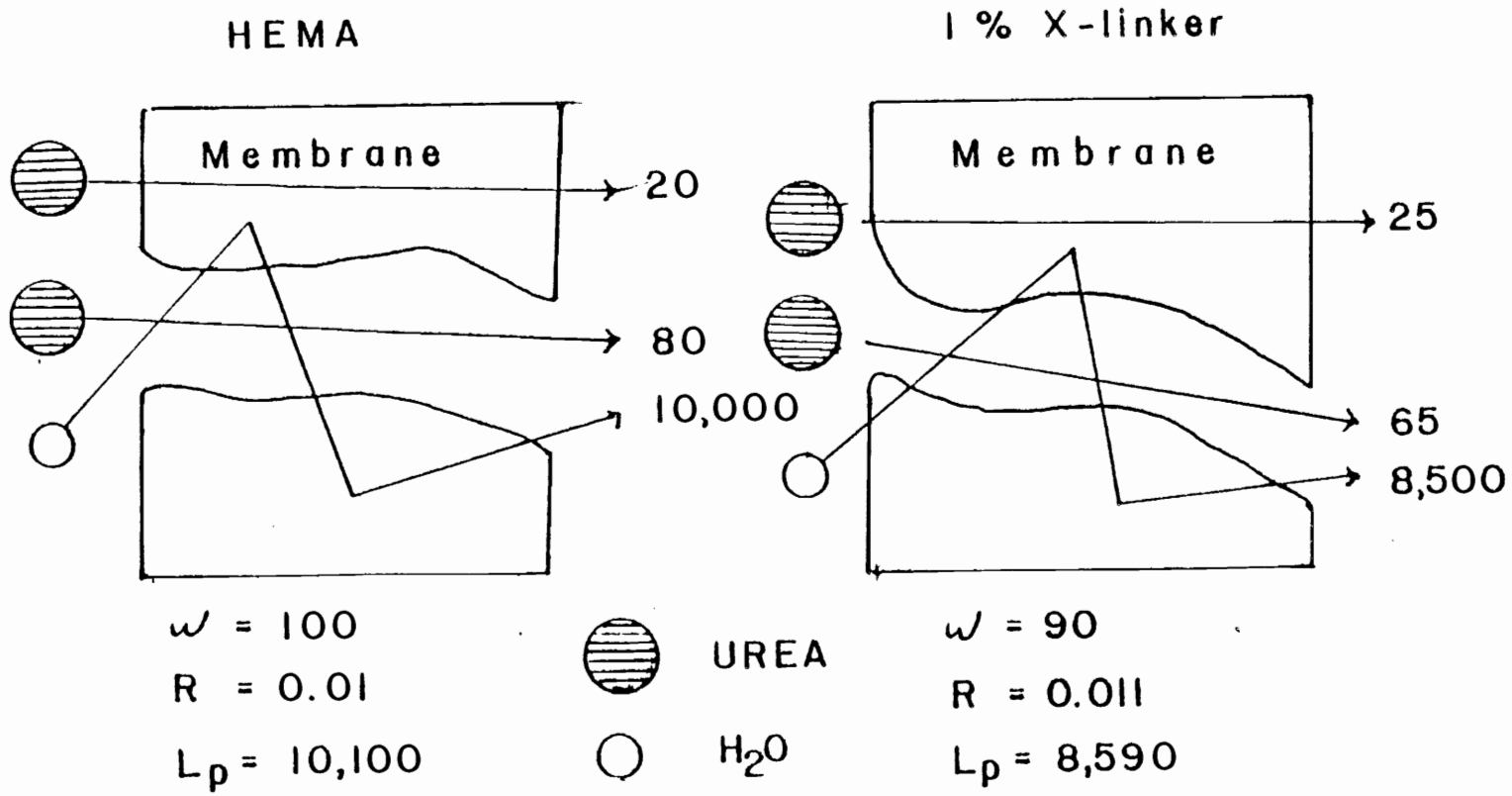

Figure 6.1. Model for urea transport through pHEMA and pHEMA crosslinked with one mole percent EGDMA.

both membranes. Water transport is assumed to occur mainly by a pore mechanism based on the fact that the fwm increases as the membrane changes from a pHEMA to a crosslinked pHEMA system.

In this model, it was assumed that 20 percent and 28 percent of the total urea transport occurs via the partition mechanism in pHEMA and in crosslinked pHEMA, respectively. The numbers of solute molecules permeating by the partition mechanism and by the pore mechanism, together with the number of permeating solvent molecules in both membranes, were arbitrarily assumed as shown in Figure 6.1. The solute permeability (ω), is proportional to the diffusion coefficient and should be proportional to the total number of solute molecules permeating the membrane. Therefore, an arbitrary number of 100 and of 90 was assigned for pHEMA and crosslinked pHEMA, respectively. The filtration coefficient Lp should be directly related to the total volume flow across the membrane. Since the contribution of the solute flow to the total volume flow is very small, the numbers of both molecules were arbitrarily used as the Lp value as shown in Figure 6.1. The relative rate of solute transport (R) is defined as:

$$R = \frac{Ns}{Nw} \qquad (6\text{-}19)$$

Where Ns is the number of solute molecules permeating the membrane and Nw is the number of solvent molecules permeating the same membrane. According to this definition, 0.010 and 0.011 can be assigned for each membrane. It is obvious that R should increase as the selectivity of the membrane or σ decreases.

In order for the model to be valid, the results of the calculations made using the described model should be consistant with the experimental values. This consistancy is tested by the following facts:

1. The Lp x l and ω x l values for a pHEMA membrane are greater than those of a crosslinked pHEMA membrane, both in experimental and model cases.

2. In the experimental case the σ value decreases as the membrane changes from pHEMA to crosslinked pHEMA, while in the model case, the R value increases with the same membrane changes. Considering the fact that R should increase as σ decreases, the same trend is observed both experimentally and in the model case.

3. Experimentally, fwm increases as the membrane changes from pHEMA to crosslinked pHEMA. This indicates that the number of solvent molecules permeating through the membrane will decreases, which is consistent with the model.

4. Experimentally fsm decreases as the membrane changes from pHEMA to crosslinked pHEMA. This predicts that the number of solute molecules permeating by a partition mechanism will increase, which is also consistant with the model.

5. Experimentally fsw increases as the membrane is changed from pHEMA to a crosslinked pHEMA, indicating that the number of solute molecules permeating the membrane

by the pore mechanism will decrease consistent with the model theory.

6. Experimentally, fsw/fsm increases as the membrane is crosslinked indicating that partition character in a solute permeation mechanism will increase. The increase of partition mechanism from 20 percent to 28 percent at the membrane change of the model is constant with the experimental results.

All these agreements between the experimental values and those obtained in the model treatment show that this model can be used to describe this system.

Chapter 7

SUMMARY AND CONCLUSIONS

This dissertation describes investigations of factors which affect permeation of progesterone through hydrogel polymers. The investigations were performed to provide data necessary for the design of a controlled release drug delivery systems. Such systems are designed to deliver an optimum amount of drug at a constant rate for extended periods. Progesterone was used as a model drug. Hydrogels made from momomers such as HEMA, MEEMA, MEMA, and MMA were used as the polymers for the system. The rationale for the use of these hydrogels was discussed in Chapter 1.

In general, the permeation rate of drug in a membrane follows Fick's law: the rate of drug diffusion depends on six factors. These are surface area (A), thickness of the membrane (l), the equilibrium solubility of drug in the polymer (C_s), the partition coefficient (Kd), the diffusivity of a drug in a polymer (D), and the permeability of a drug in a polymer (P).

The values of C_S,K_d,D and P of the drug can be varied by the combination of monomers and methods of preparation. The release kinetics can be varied by changing the thickness and area of the devices over time.

In Chapter 3 permeation parameters such as Cs, Kd, and P of several solutes in various hydrogels were discussed. The effects of

equilibrium water content, initiator, crosslinker, and functional groups were studied. A new equation for transport studies in polymeric films, where partition coefficients are large, was derived and compared with results obtained from previous equations. From these studies the following conclusions were made:

1. The permeability coefficients of progesterone in pHEMA membrane decrease as the initiator concentration increases, however, this effect is rather small.

2. The permeability coefficient of estriol in pHEMA crosslinked with EGDMA, decreases as the amount of crosslinker increase. This may be due to the decreased pore size.

3. In general, solute transport in hydrogel membrane occurs through fluctuating pores present in the gel, and the permeability coefficients increase as the equilibrium water content increases.

In Chapter 4, progesterone releases from monolithic devices was studied. A new equation was developed in order to describe drug release from cylindrical devices which have various ratios of radius to height. In this equation, it is assumed that drug release from the edges and lateral surfaces follows that of planar and long cylinder geometry respectively. Excellent agreement was observed between calculated data using this equation and experimental data obtained on progesterone release from silastic rubber devices.

The progesterone release from monolithic hydrogel devices was investigated using homopolymers and copolymers of MEMA, MEEMA, and HEMA. The following is a summary of the results.

1. Progesterone release from monolithic devices follows first order kinetics.

2. In the case of progesterone release from initially dry devices, water influx into the device affects the release rate of the drug from the device.

3. Initial drug loading affects the permeability of the drug in the polymer.

4. By comparing permeability data obtained from cross-membrane studies and from matrix release studies, aqueous solubility of sparingly soluble solute can be obtained.

In Chapter 5, progesterone release from reservoir and combined type devices with cylindrical geometry was investigated. Zero-order release rates were observed in both reservoir and combined type devices. The observed release rates were compared with the values calculated from data in the literature. Excellent agreement is found in the case of the reservoir devices. The results discussed in Chapter 5 indicate:

1. Silicone oil acts as a suspending medium and maintains the activity of progesterone constant in reservoir devices.

2. In the case of combined type devices the outer membrane, which swells less than the core polymer, restricted the swelling of the inner polymer. The restricted swelling reduces the drug release rate from these devices compared with the predicted values.

In Chapter 6, an irreversible thermodynamic approach to solute permeation through membranes has been used in order to perform an in depth study of solute transport phenomena in hydrogels.

The permeation of sucrose, glucose, and urea through pHEMA membranes both with and without EGDMA crosslinker was studied. The results indicate that, in general, permeation of water soluble solutes in these films is dominated by a pore mechanism. However, in the case of urea, solute-membrane interactions contribute to the total permeability of this solute.

REFERENCES

1. M. L. Parkes, Arch. Otolargyngal., 72, 429 (1962).

2. M. F. Armaly, Arch. Opth., 68, 390 (1962).

3. G. M. Macnab, Med. Press, 245, 120 (1961).

4. Medical Tribune, April 18, 19, 1965, P 11.

5. S. C. Woodward, J. B. Herrmann, and F. Leonard, Federal Proceedings, 23, 495 (1962).

6. C. E. Phillips, Jr., J. A. DeWeese, and F. C. Campeti, Arch. Surg., 92, 38 (1961).

7. H. S. Withan, M. M. Nachlas, R. D. Solomon, B. D. Helpern, and A. M. Seligman, Ann. Surg., 152, 648 (1960).

8. W. S. Edwards, Surgery, 45, 298 (1959).

9. S. A. Wesolowski, Evaluation of Tissue and Prosthetic Vascular Grafts, C. C. Thomas, Springfield, Ill. (1962).

10. E. Nylias, E. L. Kupski, P. Burnett, and R. M. Haag, J. Biomed. Mater. Res., 4, 371 (1970).

11. J. D. Andrade, Med. Inst., 7, 110 (1973).

12. A. S. Hoffman, J. Biomed. Mater. Res. Symposium, No. 5; 77 (1974).

13. J. D. Andrade, R. N. King, D. E. Gregons, and D. L. Coleman, J. Poly. Sci. Symposium C (in press).

14. B. D. Ratner, A. S. Hoffman, S. R. Hanson, L. A. Harken, and J. B. Whitton, J. Poly. Sci. Symp. C (in press).

15. O. Wichterle, and D. Lim, U. S. Patent 2976576 (1961).

16. O. Wichterle and D. Lim, Nature, 185, 117 (1960).

17. M. Barvic, K. Kliment, and M. Zavadil, J. Biomed. Mater. Res., 1, 313 (1969).

18. G. Cermy, R. Chromecek, A. Opletal, F. Parousek, and J. Otoupelova, Scripta Medica, 43, 63 (1970).

19. L. Sprinel, J. Kopecek, and D. Lim, J. Biomed. Mater. Res., 5, 447 (1971).

20. M. Barvic, J. Vacik, D. Lim, and M. Zavadil, J. Biomed. Mater. Res., 5, 225 (1961).

21. L. Sprinel, J. Kopeck, and D. Lim, Calc. Tissue Res., 13, 63 (1973).

22. L. Sprinel, J. Vacik, and J. Kopeck, J. Biomed. Mater. Res., 7, 123 (1973).

23. C. D. Winter and B. J. Simpson, Nature, 223, 88 (1969).

24. B. S. Levowite, J. N. LaGuerre, W. S. Calem, F. E. Gould, J. Scherrer and H. Schoenfeld, Trans. Amer. Soc. Artif. Int. Organs, 14, 82 (1968).

25. M. Tollar, M. Stol, and K. Kliment, J. Biomed. Mater. Res., 3, 305 (1968).

26. J. N. LaGuerre, H. Kay, S. M. Lararus, W. S Calem, S. R. Weinberg, and B. S. Levowitz, Surg. Forum, 9, 522 (1968).

27. S. M. Lazarus, J. N. LaGuerre, H. Kay, S. Weinberg, and B. S. Levowitz, J. Biomed. Mater. Res., 5, 129 (1971).

28. V. Majkus, Z. Horakova, F. Vymola, and M. Stol, J. Biomed. Mater. Res., 3, 443 (1969).

29. J. Drobnik, P. Spacek, and P. Wichterle, J. Biomed. Mater. Res., 8, 45 (1974).

30. M. Scott, P. L. Kronick, R. C. May, R. H. Davis, and H. Balin, Biomat. Med. Dev. Art. Org., 1, 691 (1973).

31. I. Michnevic and K. Kliment, J. Biomed. Mater. Res., 5, 17 (1973).

32. A. Warren, F. G. Gould, R. Capulong, E. Gloffelty, S. J. Baley, W. S. Calen, and B. S. Levowitz, Surgical Forum, 18, 183 (1967).

33. M. P. Singh and D. G. Melrose, Biomedical Eng., 6, 157 (1971).

34. M. P. Singh, Biomedical Eng., 4, 68 (1969).

35. B. D. Halpern, H. Cheng, S. Kue, and H. Greenberg, in Artificial Heart Program Conference Proceedings; ed. by R. J. Heggeli, U. S. Gover. Printing Office, Wash. D.C., 87 (1969).

36. M. F. Refojo, J. Biomed. Med. Res., 3, 333 (1969).

37. M. F. Refojo, Survey of Opthalmology, 16, 233 (1972).

38. L. Krejc, and H. Krejcova, Brit. J. Ophthal., 57, 675 (1973).

39. S. Kocvara, K. Climent, J. Kubat, M. Stol, Z. Ott, and J. Dvorak, J. Biomed. Mater. Res., 1, 325 (1967).

40. K. Kliment, M. Stol, K. Fahoun, and B. Stockar, J. Biomed. Mater. Res., 2, 237 (1968).

41. R. S. Molday, W. J. Dreyer, A. Rembaum, and S. P. Yen, J. Cell. Biol., 64, 75 (1975).

42. M. F. Refojo, Preprints - Division of Organic Coatings and Plastics Chemistry, A. C. S., 27(2), 136 (1962).

43. J. D. Andrade, K. Kunitomo, R. Van Wagenen, B. Kastizis, D. Grough, and W. J. Kolff, Trans. Amer. Soc. Artif. Int. Organs, 17, 222 (1971).

44. P. Spacek and M. Kubin, J. Biomed. Mater. Res., 7, 201 (1973).

45. B. D. Ratner and I. F. Miller, J. Biomed. Mater. Res., 7, 353 (1973).

46. R. W. Rubin and J. L. Marshal, J. Biomed. Mater. Res., 9, 375 (1975).

47. G. D. Winter, Proc. Roy Soc. Med., 63, 1111 (1970).

48. J. Kopeck, L. Princl, H. Bazilova and J. Vacik, J. Biomed. Mater. Res., 17, 111 (1973).

49. L. L. Markley, H. J. Bixler, and R. A. Cross, J. Biomed. Mater. Res., 2, 145 (1968).

50. D. W. Marshall, R. A. Cross, and H. J. Bixler, J. Biomed. Mater. Res., 4, 247 (1970).

51. H. J. Bixler, R. A. Cross and D. W. Marshall, in Artificial Heart Program Conference Proceedings, ed. by R. J. Heggeli, U.S. Gov. Printing Off., Washington, D.C. 79 (1968).

52. R. H. Alder and C. Darby, U.S. Armed Forces Medical J., 11, 139 (1960).

53. E. W. Merrill, E. W. Salzman, P. S. L. Wong, T. P. Ashford, A. D. Brown and W. G. Austen, J. Appl. Physiol., 29, 723 (1970).

54. E. W. Merrill, G. W. Salzman, P. S. L. Wong, and J. Silliman, ACS Polymer Preprints, 13 (1), 511 (1972).

55. J. C. Bray and E. W. Merrill, J. Biomed. Mater. Res., 7, 431 (1973).

56. H. Lee, D. G. Soffey, and F. Abronson, in Artificial Heart Program Conference Proceedings, ed. by R. J. Heggel, U.S. Gov. Printing Off., Wash., D.C., 143 (1969).

57. J. C. Bray and E. W. Merrill, J. Appl. Polymer Sci., 17, 3779 (1973).

58. J. C. Bray and E. W. Merrill, J. Biomed. Mater. Res., 7, 431 (1973).

59. S. J. Wisemewski, Ph.D. Dissertation, The University of Utah, Salt Lake City, Utah (1979).

60. M. F. Refojo, Contact Lenses, in Encyclopedia of Polymer Science and Technology; John Wiley and Sons, Inc.; New York, 1976, Supplement Vol. 1, P 195.

61. H. Yasuda, C. E. Lamaze, and L. D. Ikenberry, Die Makromolekulare Chemie, 118, (1968).

62. L. D. Ikenberry, H. Yasuda, and H. G. Clerk, Chem. Eng. Prog. Symp. Ser., 69 (1968).

63. J. Vacik, M. Czakova, J. Exner, T. Kalal, and J. Kopecek, Collection Czechoslov Chem. Comm., 42, 2786 (1977).

64. B. D. Ratner, I. F. Miller, J. Poly. Sci. Part A-1, 10, 245 (1972).

65. J. Kopecek, J. Vacik, and D. Lim, J. Poly. Sci., Part A-1, 9, 2801 (1971).

66. T. A. Jadwin, A. S. Hoffman, and W. R. Vieth, J. Appl. Poly. Sci., 14, 1239-59 (1976).

67. J. Kopecek and J. Vacik, Collection Chzechoslov. Chem. Commun., 38, 854 (1973).

68. M. F. Refojo, J. Appl. Poly. Sci., 10, 183 (1966).

69. A. S. Hoffman, M. Modell, and P. Pan, J. Appl. Poly. Sci., 14, 285 (1970).

70. Marketed by Alza Corp.

71. R. Gale, S. K. Chandrasekaran, D. Swanson, and J. Wright, Abstracts presented in 179th ACS National Meeting, INDE 40.

72. G. A. Mortimer, J. Org. Chem., 30, 1632 (1965).

73. P. Broussignac, Chitosan, A Natural Polymer Not Well Known By the Industry. Chim. Ing. Genie Chim., 91, 1241 (1968).

74. T. J. Roseman, J. Pharm. Sci., 61, 46 (1972).

75. F. T. Gicker, F. W. Gage, and C. E. Moser, J. Am. Chem. Soc., 60, 2582 (1938).

76. B. K. Fritzinger, S. K. Brauman, and D. J. Lyman, J. Biomed. Mater. Res., 5, 3 (1971).

77. G. M. Zentner, Ph.D. Dissertation, The University of Utah, Salt Lake City, Utah 1979, P 17.

78. G. L. Flynn, S. H. Yalkowsky, and T. J. Roseman, J. Pharm. Sci., 63, 481 (1974).

79. D. J. Lyman, Trans. Amer. Soc. Artif. Int. Organs, 10, 17 (1964).

80. L. C. Craig and W. Konigesberg. J. Phys. Chem., 65, 116 (1961).

81. H. Yasuda, A. Peterlin, C. K. Colton, K. A. Smith and G. W. Merrill, Die Makromolekulare Chemie, 126, 177 (1969).

82. H. Yasuda, C. G. Lamaze, and A. Peterlin, J. Poly. Sci., Part A-2, 9, 1117 (1971).

83. H. Yasuda and C. G. Lamaze. J. Macromol. Sci., Phys., B5(1), 111 (1971).

84. S. J. Wisniewski and S. W. Kim, J. Memb. Science (in press).

85. G. M. Zenter, J. R. Cardinal, and S. W. Kim, J. Pharm. Sci., 67, 1352 (1978).

86. G. M. Zenter, J. R. Cardinal, J. Fiejen, and S. Z. Song, J. Pharm. Sci., 68, 970 (1979).

87. R. B. Seymour, Introduction to Polymer Chemistry, P 151, International Student Edition.

88. S. Kapur and C. E. Roger, J. Polym. Sci., A-2, 10, 2107 (1972).

89. G. M. Zentner, J. R. Cardinal, and D. E. Gregonis, J. Pharm. Sci., 68, 794 (1979).

90. G. M. Zentner, J. R. Cardinal, and S. W. Kim, J. Pharm. Sci., 67, 1347 (1978).

91. R. W. Baker, M. E. Tuttle, H. K. Lonsdale, and J. W. Ayres, J. Pharm. Sci., 68, 20 (1979).

92. D. R. Kreger, Biochem. Biophys. Acta, 13, 1 (1954).

93. Bartnicki-Garcia and W. Y. Nickerson, Biochem. Biophys. Acta, 58, 102 (1962).

94. B. D. Ratner and A. S. Hoffman, in "Hydrogels for Medical and Related Applications," ed. by J. D. Andrade, A. C. S. Symposium Series 31, 1978, P 1.

95. T. Higuchi, J. Soc. Cosmetic Chemists, 11, 85 (1960).

96. T. Higuchi, J. Pharm. Sci., 52, 1145 (1963).

97. T. J. Roseman and W. I. Higuchi, J. Pharm. Sci., 59, 353 (1970).

98. J. Cobby, M. Mayersohm, and G. C. Walker, J. Pharm. Sci., 63, 725 (1974).

99. J. Cobby, M. Mayersohm, and G. C. Walker, J. Pharm. Sci., 63, 732 (1974).

100. J. Cobby, J. Biomed. Mat. Res., 12, 627 (1978).

101. J. C. Fu, C. Majemeir and D. L. Mayer, J. Biomed. Mat. Res., 10, 743 (1976).

102. M. K. Akkapedd, B. D. Halpert, R. H. Davis, and H. Balin. in "Controlled Release of Biologically Active Agents," A. C. Tanguary and R. E. Lacey, Plenum Press, New York, P 165 (1974).

103. W. R. Good, Proceedings of the Midland Macromolecular Institute Symposium "Polymeric Delivery Systems" (1976).

104. N. B. Graham, Abstracts presented in 179th ACS National Meeting, POLY. 92.

105. T. J. Roseman, J. Pharm. Sci., 61, 46 (1972).

106. S. Z. Song, J. R. Cardinal, S. J. Wisniewski and S. W. Kim, AIChE Symposium on "Controlled and Tropical Release" (1980) (in press).

107. T. Higuchi, F. L. Shim, T. Kimura, and J. H. Rytting, J. Pharm. Sci., 68, 1267 (1979).

108. J. Folkman and D. M. Long, J. Surg. Res., 4, 139 (1964).

109. P. M. Dziuk and J. B. Cook, Endocrinology, 78, 208 (1966).

110. H. B. Croxatto, S. Diaz, P. Atria, S. Cheviakoff, S. Rosati, and H. Odde, Contraception, 4, 155 (1971).

111. V. A. Place and B. B. Pherriss, J. Reprod. Med., 13, 66 (1974).

112. R. A. Abrahams and S. H. Ronel, J. Biomed. Mater. Res., 9, 355 (1975).

113. J. Crank, The Mathematics of Diffusion, Oxford Univ. Press, London (1956).

114. H. S. Carslaw and J. C. Jaeger, Conduction of Heat in Solids, Oxford University Press, London (1959).

115. R. W. Baker, H. K. Lansdale, M. E. Tuttle, and J. W. Ayres, Proceedings of Drug Delivery Systems, DHEW, Publication No. (NIH)77-1348 P49 (1976).

116. Y. W. Chien, M. J. Lambert and D. E. Grant, J. Pharm. Sci., 63, 365 (1974).

117. Y. W. Chien and H. J. Lambert, J. Pharm. Sci., 63, 515 (1974).

118. O. Kedem and A. Katchalasky, Biochim. Biophys. Acta, 27, 229 (1958).

119. A. J. Staverman, Rec. Trav. Chim., 70, 344 (1951).

120. A. J. Staverman, Trans. Farad. Soc., 48, 623 (1952).

121. A. J. Staverman, Rec. Trav. Chim., 71, 176 (1952).

122. O. Kedem and A. Katchalasky, J. Gen. Physiol., 45, 143 (1961).

123. O. Kedem and A. Katchalasky, Trans. Farad. Soc., 59, 1918, 1931, 1941, (1961).

124. R. Bearman, J. Phys. Chem., 65, 1961 (1961).

125. P. J. Dunlop, J. Phys. Chem., 68, 26 (1964).

126. R. W. Laity, J. Phys. Chem., 68, 80 (1959).

127. L. Onsager, Ann. N.Y. Acad. Sci., 46, 241 (1945).

128. B. Z. Ginzburg and A. Katchalasky, J. Gen. Physiol., 47, 403 (1963).

129. T. G. Kauffmann and E. F. Leonard, AICHE J., 14, 110 (1968).